

# Dualfunktional polymer brushes and dual- funktional polymer nanoreactors

**Inauguraldissertation**

zur

Erlangung der Würde eines Doktors der Philosophie

vorgelegt der

Philosophisch-Naturwissenschaftlichen Fakultät

der Universität Basel



von

Dominik Dobrunz

aus

Deutschland

Basel, 2013

Genehmigt von der Philosophisch-Naturwissenschaftlichen Fakultät auf Antrag von

Prof. Dr. Wolfgang Meier

und

Prof. Dr. Andreas Taubert

Basel, den 26. Februar 2013

Prof. Dr. Jörg Schibler

Dekan

**Für meine Eltern, Bernd und Hanna Dobrunz**

*„Jedes Naturgesetz, das sich dem Beobachter offenbart,  
lässt auf ein höheres, noch unerkanntes schließen.“*

*Alexander von Humboldt*

## **Danksagung/Aknowlegements**

Ich möchte Prof. Dr. Wolfgang Meier herzlich danken für die Möglichkeit ein spannendes und interdisziplinär ausgerichtetes Projekt in seiner Arbeitsgruppe bearbeiten können, in einer freundschaftlichen Atmosphäre und einem Freiraum, der mir die Möglichkeit zur wissenschaftlichen und persönlichen Entfaltung gab.

I want to thank Cornelia Palivan for supervising me during the vital stages of writing my paper.

Ich danke Prof. Dr. Andreas Taubert für die funktion als Koreferent und seine konstruktive Begutachtung der Arbeit.

Besten Dank auch an Prof. Dr. Thomas Pfohl für die bereitwillige Übernahme des Prüfungsvorsitzes.

Ich danke Pascal Tanner für die gute Zusammenarbeit und für die FCS Messungen.

I thank Karolina Langowska for the good atmosphere in the Lab and for her great support.

I thank Adriana-Cristina Toma for the Raman measurements.

I am also grateful to Janne Hyötylä and Dr. Larisa Kapinos-Schneider for conducting the SPR measurements.

Gabriele Persy für die TEM Messungen, Justina for the QCM measurements.

Ebenso danke ich Dr. Daniela Vasquez für die Auswertung der LS Messungen.

Ich danke Dr. Jörg Braun für die interessanten wissenschaftlichen und weniger wissenschaftlichen Diskussionen.

I thank Mark Inglin for the correction of my thesis paper.

Ich danke Sven Kasper für die Unterstützung im Labor.

I want to thank the former and present members of “Gruppe Meier” for the great time we had!

Dem Schweizerischen Nationalfond und der Universität Basel danke ich für die finanzielle Unterstützung.

Ich danke meiner Familie für ihre Unterstützung.



## **Abstract**

The design of new systems featuring multi-functionalities represents a key strategy in meeting complex challenges in various domains including chemistry, medicine, environmental sciences, and technology. The present thesis describes the synthesis and characterization of new nanoreactors and polymeric brushes.

Polymer brushes were used to improve the surface properties of interfaces by attachment to a solid supported surface. For that purpose, PEG polymers were synthesized by atom transfer radical polymerization (ATRP). The polymeric brush was assembled on a gold surface using the grafting method. In this way the polymeric brush provides dual functionality as it is involved both in surface passivation and provides selective binding sites.

In a second project, nanoreactors, we described protein-containing polymer nanoreactors with dual functionality designed for peroxynitrite degradation and oxygen transport. The vesicles were successfully prepared using PMOXA- PDMS- PMOXA tri blockpolymers. Hemoglobin (Hb) was encapsulated in the nanoreactors. It was used as a model protein because of its ability to provide the dual function of oxygen transport and peroxynitrite degradation. We proved that Hb keeps its functionality following encapsulation. The insertion of channel proteins into the polymeric membrane of the vesicle allowed the passage of various compounds that served for the assessment of *in situ* Hb activity.

# Table of Contents

1 Introduction.....	1
1.1.1 Solid supported polymer brush.....	2
1.1.2 Non-covalent methods:.....	3
1.1.3 Covalent methods:.....	4
1.1.3.1 “Grafting to” method.....	4
1.1.3.2 “Grafting from” method.....	4
1.1.4 Responsive brushes.....	6
1.2 Self assembly.....	7
1.3 Nanocarriers.....	9
1.4 Nanoreactors.....	11
1.5 Peroxynitrite degradation.....	11
1.6 Blood substitutes.....	13
2 Materials and methods.....	15
2.1 Materials and methods for creating and analyzing the responsive polymer brush.....	15
2.1.1 Chemicals.....	15
2.1.2 SPR .....	15
2.1.3 <sup>1</sup> H NMR .....	15
2.1.4 QCM .....	15
2.1.5 ATR-IR .....	16
2.1.6 ATRP synthesis.....	16
2.2 Materials and methods for creating and analyzing the polymer nanoreactors.....	17
2.2.1 Chemicals.....	17
2.2.2 Hemoglobin labeling.....	17
2.2.3 Polymer vesicle and nanoreactor preparation.....	18
2.2.4 Characterization of polymer vesicles and nanoreactors.....	19

2.2.4.1 Light Scattering .....	19
2.2.4.2 Transmission Electron Microscopy .....	19
2.2.4.3 Hemoglobin encapsulation efficiency.....	19
2.2.5 Activity assays for peroxynitrite degradation and oxygen binding of Hb.....	20
2.2.6 Raman spectroscopic characterization:.....	21
2.2.7 Stopped flow spectroscopy.....	22
3 Results and discussion .....	23
3.1 Responsive polymer brush.....	23
3.1.1 PEG .....	23
3.1.2 PEG-binding.....	24
3.1.3 Initiator.....	25
3.1.4 PEGA Polymer.....	25
3.1.5 ARGET ATRP.....	30
3.1.6 Polymer Brush .....	31
3.1.7 Conclusion: Polymer brush.....	37
3.2 Hemoglobin nanoreactors .....	38
3.2.1 Polymers used for nanoreactor preparation.....	38
3.2.2 Protein encapsulation efficiency.....	47
3.2.3 Conclusion: Nanoreactors.....	50
3.2.4 Activity studies.....	51
3.2.5 Free Hemoglobin.....	53
3.2.6 Hemoglobin in nanoreactors.....	54
3.2.7 Characterisation of nanoreactors reactivity.....	55
3.2.8 Reducing agents.....	55
3.2.9 Reduction of free Hb.....	56
3.2.9.1 Reduction of metHb to HbCO.....	56



3.2.9.2 Reduction of metHb to deoxyHb.....	57
3.2.9.3 Reduction of metHb to HbO <sub>2</sub> .....	57
3.2.9.4 Reduction from HbO <sub>2</sub> to deoxyHb.....	58
3.2.9.5 Conversion of HbO <sub>2</sub> to HbCO.....	58
3.2.9.6 Raman spectra.....	58
3.2.10 Reduction of Hb in Nanoreactors.....	61
3.2.10.1 Reduction of metHb to HbCO.....	61
3.2.10.2 Reduction of metHb to deoxyHb.....	62
3.2.10.3 Conversion of metHb to HbO <sub>2</sub> .....	62
3.2.10.4 Conversion of HbO <sub>2</sub> to HbCO.....	63
3.2.10.5 Reduction from HbO <sub>2</sub> to deoxyHb.....	64
3.2.11 Conclusion: metHb Reduction.....	64
3.2.12 Peroxynitrite degradation .....	65
3.2.13 Oxidation of deoxyHb, HbO <sub>2</sub> and HbCO.....	66
3.2.14 Hb extracted from fresh blood.....	68
3.2.15 Conclusion: Peroxynitrite degradation.....	68
3.2.16 Kinetics of peroxynitrite degradation.....	69
3.2.17 Oxygen transport.....	72
4 General Conclusion.....	75
5 References.....	i
6 Abbreviations and symbols.....	viii
7 Curriculum vitae .....	x
8 Impact of the work .....	xii



# 1 Introduction

In Nature, polymers play a variety of different and important roles. The most famous biological polymer is deoxyribonucleic acid (DNA).<sup>1</sup> It contains the information needed to create proteins. In addition, there is a wide variety of other polymers such as proteins or cellulose. Proteins are the basic building blocks of life; they feature a diverse variety of specific functions including transport of molecules, selective receptivity, signal transduction, and cell recognition. They provide anchoring sites to which cytoskeletal filaments or components of the extracellular matrix can connect. Furthermore, proteins can act as enzymes, structural components, or have hormonal activities.

Besides their natural variety of properties and functions, they also allow for a wide variety of different applications that help to improve our everyday live.

The first studies related to polymers were done by Henri Braconnot, who did his pioneering work on derivatives of cellulose compounds.<sup>2</sup> The first completely synthetic polymer was created by Leo Baekeland (Bakelit) hundred years later, in 1907.<sup>3</sup>

Since then, many different polymers have been synthesized and used for different applications.

Examples for polymers that we come in contact with every day:

- poly(vinyl chloride), poly(styrene), poly(ethylene), poly(propylene), poly(acrylonitrile)

Because of their chemical nature, polymers offer a unique opportunity to create nano-sized objects such as nanoreactors and nanocarriers, which can be used in bio- and pharmaceutical sciences.

Polymers can also be used to modify the properties of various surfaces.

The simplest polymer architecture is a linear chain of repeating single units, or monomers – a single backbone with no branches – also referred to as a homopolymer<sup>4</sup>

In contrast to homopolymers that consist only of a single monomer, copolymers are made up of different kinds of monomers. Copolymers can be further divided into different subgroups.

The category to which a polymer belongs depends on the positioning of the different monomers in

the polymer.

Copolymers that consist of two different monomers can be divided into the following types:

- Statistical copolymers, where the sequence of the different monomers, A and B, follows a statistical rule (ABBAABBBA).
- Alternating copolymers, where the sequence of monomers consists of alternating A and B monomers (ABABABABAB).
- Block copolymers, where the different monomers are arranged as blocks (AAAAABBBBB).

The different blocks are linked together by covalent bonds.

The use of different monomers also allows the creation of polymer architectures with different features. When polymers comprise a main chain with one or more branches, they are referred to, for example, as star polymers, comb polymers<sup>7</sup>, brush polymers, hyper branched polymers, and dendrimers.<sup>10</sup>

### **1.1.1 Solid supported polymer brush**

One area in which polymers are used is surface modification. Polymer films are thereby deposited on a surface. Solid supported polymer films are used to improve the properties of water/surface- or air/surface interfaces. Engineering such systems allows the formation of many different surface properties, such as adhesion, swelling and wettability, to be optimized.

A polymer brush can be described as tethered, polymer chains that are densely attached to a surface.<sup>11</sup> If the density of the polymer brushes on the surface is high, the polymers are not able to form the same natural random-walk<sup>12</sup> conformation as they would in solution.

In solution, polymer chains form a conformation in order to maximize the free energy of the system. Consequently, a polymer chain on the surface prefers the same conformation as in solution.

However, if the grafting density is very low, there will not be a huge effect because the only steric hindrance to the polymer comes from the surface and by self-avoidance of the polymers. In contrast, if the grafting density of the polymer chain increases, repulsive forces between the

polymer chains also increases, due to the avoidance of overlaps. To minimize overlap, the polymer chains are forced to stretch away from the surface, leading to a lowering of the configurational entropy.<sup>13</sup>

Solid supported polymer films can be formed with different covalent or non-covalent methods.

### **1.1.2 Non-covalent methods:**

There are different methods to create non-covalent bound monolayers, such as the Langmuir-Blodgett or LBL method.

For amphiphilic copolymers, the Langmuir Blodgett method is often used. The principle of this method is that amphiphilic copolymers form a self-assembling monolayer at the water-air interface.

The hydrophilic part enters the aqueous phase and the hydrophobic part is pushed away from the water. The monolayer is transferred to a given surface by immersing that surface through the monolayer into the aqueous phase.

The density of the resulting polymer brush is limited to the density of the self-assembled monolayer.

This method is often used for the preparation of monolayers. However, for the deposition of multilayered structures, the Layer by Layer (LbL) method has also been shown to be suitable. The method is based on the adsorption of polymers from a polymer-containing solution. For the LbL method, anionic and cationic charged polymers are used.

By immersing the surface alternately in an anionic and cationic polymer solution, a well defined multilayer can be achieved.<sup>14</sup>

### **1.1.3 Covalent methods:**

#### **1.1.3.1 “Grafting to” method**

To create covalent bound polymer brushes, two different strategies can be employed. One is the “grafting to” method, by which a polymer is synthesized in solution, and is then attached to the surface with an end functional group. The synthesis of these polymer chains is no different from the synthesis of polymers in solution, except for the end functional group, which is required to attach the polymer to the surface. Different surfaces require different end functionalized groups. To attach polymer brushes to a gold substrate, a disulfide or a thiol group is used, because it forms a covalent bond to the metal surface. Many different surfaces can be used, including flat surfaces such as silicon, or surfaces having a complex shape such as nanoparticles, or cellulose<sup>17</sup>. Synthesis in solution allows the use of a wide variety of polymerisation techniques, such as free radical-, living radical-, ring opening- or anionic polymerisation. These result in a broad range of monomers being polymerizable. Also, oligonucleotide brushes can be formed in this way.<sup>18</sup> The grafting density depends on both the molecular weight of the polymer chain and the surface properties. Additionally, this density is influenced by some other parameters such as the reaction temperature or the grafting time. The grafting density can be controlled by varying these parameters. It is also possible to form a grafting gradient by creating a temperature gradient.<sup>19</sup>

One drawback of the “grafting to” method is that, compared to the “grafting from” method, the grafting density on the surface is lower. That is why the “grafting from” method is often used.<sup>20</sup>

#### **1.1.3.2 “Grafting from” method**

In the “grafting from” method, the polymer is polymerized directly on the surface. The initiator for the polymerisation is placed on the surface prior to the polymerisation. This can be done by immersing the surface in an initiator solution. One of the most commonly used methods is a living

radical polymerisation such as Nitroxide-mediated Radical Polymerization NMP or Atom Transfer Radical Polymerisation (ATRP). ATRP is a robust method and, compared to free radical polymerisation, it is a much more controlled reaction. This effect decreases the problem of polymers created during the same polymerisation process not having the exact same molar mass, thereby leading to a smaller polydispersity. In addition, the functional group for the polymerisation can be in one of two different states: the active and the dormant state. In the active state new monomers add to the polymer chain. And in the dormant state the functional group is not active; therefore, the polymer can be conserved and later reactivated, which offers the opportunity to create diblock or triblock copolymers.<sup>22</sup>

The length of the polymer chain can be controlled by the reaction time. The grafting density depends on the density of the initiator molecules on the surface. It is also possible to create a grafting gradient by generating a gradient in the initiator concentration.<sup>23</sup>

The “grafting from” method is often used because it is possible to obtain a much higher grafting density than with the “grafting to” method. The grafting density that can be achieved with the “grafting to” method is limited, due to steric hindrance and the limited diffusion of the polymer chains to the surface during the grafting process.<sup>24</sup>

The most advanced polymer brushes respond to stimuli such as temperature or pH change. These stimuli cause a change in the conformation of the polymer brush.

In a polymer brush there are interactions between the individual polymer chains as well as between the polymer chains and the solvent-like attractive interactions: van der Waals or H-bond interactions, and repulsive interactions: steric hindrance. In a polymer brush, these interactions are balanced and define the shape of the brush. If the strength of the interactions changes, for example with an increase in temperature, the strength of the H-bond interactions decreases. This will change the conformation of the polymer brush.

### 1.1.4 Responsive brushes

- Temperature responsive brushes

One example that demonstrates this effect is poly(*N*-isopropylacrylamide) (PNIPAM) in an aqueous solution. PNIPAM has a lower critical solution temperature (LCST) of 30 °C. That means that above 30 °C the hydrophobic interactions are stronger than the hydrophilic interactions, causing the polymer to become insoluble in aqueous solution. With increasing or decreasing temperatures close to the  $LCST \pm 5$  °C, PNIPAM bound to a surface changes its shape, as was reported by H. Yim *et al.*<sup>25</sup>

- Salt responsive brushes

There are polymer brushes such as PMAEMA that respond to a high concentration of salt in the solvent. When adding salt, the electrostatic interactions will change and this will alter the conformation of the polymer brush, forcing it to collapse.<sup>26</sup>

- pH responsive brushes

Changing the pH of the solvent is another way to change the structure of the brushes. Some polymers such as poly(acrylic acid) (PAA) are weak acids or bases and they change their ionisation state when the pH varies.<sup>26</sup> This change influences the interactions between the polymer brush and the solvent surrounding the polymer brush.

When the pH is below the  $pK_a$  value of the polymer, the polymer is in the collapsed form. When the pH is above the  $pK_a$  value, the polymer is fully stretched.



## 1.2 Self assembly

### Amphiphilic block copolymers

AB and ABA block copolymers consist of two different blocks made of different monomers. Block copolymers have the ability to form superstructures such as vesicles, micelles or rods.

In order to form vesicles, micelles or rods, the polymer should feature amphiphilic properties, which result from a combination of hydrophilic and hydrophobic blocks (**Figure 1**). Hydrophilic blocks are readily soluble in polar solvents such as water or methanol and are not soluble in non-polar solvents such as hexane or toluene. Hydrophobic blocks are readily soluble in non-polar solvents and are not soluble in polar solvents. In the absence of solvent, block copolymers also form superstructures such as lamellar structures, where they are arranged in layers in order to optimize the interactions between the hydrophobic and the hydrophilic chains. For the formation of ordered superstructures, three key properties are involved: the overall mass of the polymer (MW), the length ratio between the different blocks, and the interaction energy between the monomers in the different blocks.<sup>27</sup> Diblock copolymers contain one hydrophobic block and one hydrophilic block, while triblock copolymers contain one hydrophobic block and two hydrophilic blocks.

The superstructures (Figure 2) are created by optimizing the hydrophilic and hydrophobic interactions to minimize unfavorable contact between polymer blocks and solvent molecules with different polarities.

The driving force behind this optimization is that the system tends toward achieving the lowest energy level; as a consequence, the process is also driven by a low mixing entropy.<sup>28</sup> The formation of vesicles, micelles, and rods is similar because all of these morphologies are solvent-dependent self-assembled superstructures.

However, micelles strictly lack the shell-like character and encapsulated bulk solution phase of a vesicle. Therefore, micelles are not ideal to encapsulate substances.



**Figure 1.** Schematic representation of amphiphilic copolymers **AB (A) and ABA (B) Copolymers**, where the hydrophobic block is represented in blue and hydrophilic block in yellow.

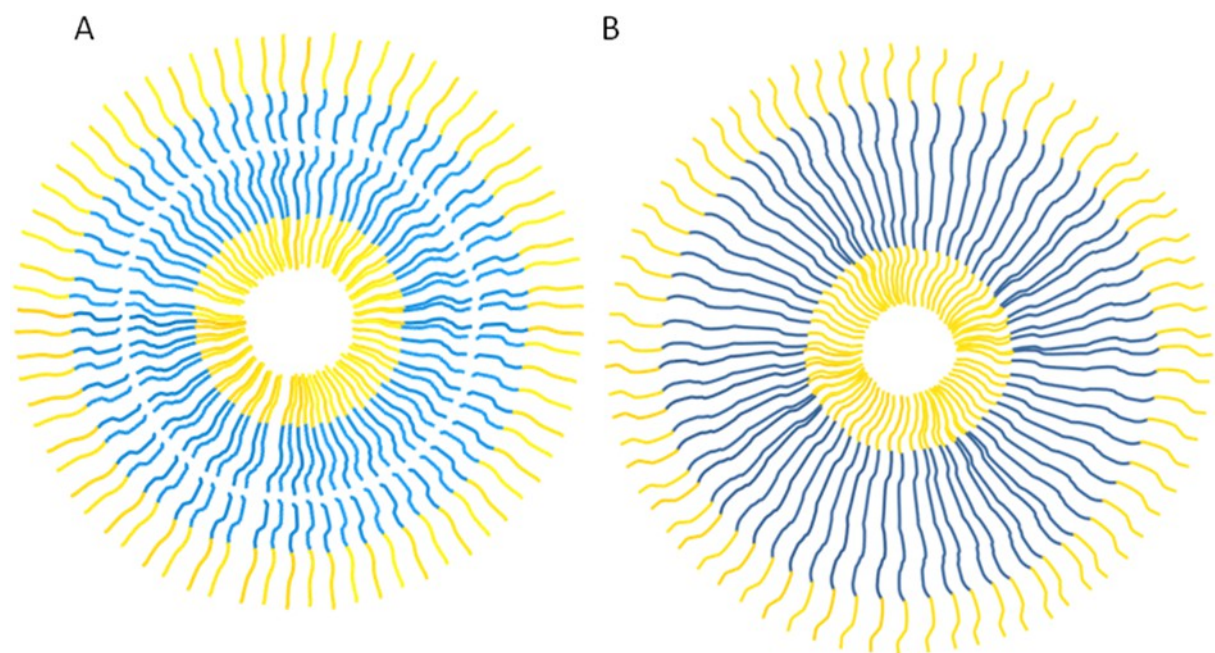


**Figure 2.** Schematic representation of vesicles prepared from **AB (A) and ABA; (B) Copolymers** where the hydrophobic block is represented in blue and the hydrophilic block in yellow.

### 1.3 Nanocarriers

Many substances used in medicine do not remain in the bloodstream for very long. Oral intake of a drug is limited by the stability of the substance under proteolytic attack by the environment of the body. The encapsulated molecules are protected from the environment of the human body and evade the immune system to prolong the *in vivo* therapeutic half-life of the substrate.

Transportation of a substrate can also be limited, due to insolubility of the substance, which can be encapsulated in nanocarriers in order to solve the problem.

Nanocarriers can provide an enhanced dissolution rate of sparingly soluble or hydrophobic drugs because of their amphiphilic structure and can be divided into four main groups of organic nanocarriers<sup>29</sup>: liposomes, micelles, lipidic- or polymer-based micelles or vesicles, and dendrimers. Dendrimers<sup>30</sup> – tree-like structures formed by the ramification of subunits around a core – are very well established for drug delivery.

Many drug delivery studies have been carried out on lipid vesicles, for reasons of their biocompatibility. For this reason, many substances, such as proteins, can be encapsulated in them.

There have been many studies on lipid vesicles in order to mimic Nature. It has been shown that lipids are able to form vesicles and can also encapsulate substances under laboratory conditions. The prepared lipid vesicles can be used as nanoreactors or nanocarriers. They provide high biocompatibility and close interaction with host cells. In addition, liposomes are capable of delivering both water and oil-soluble compounds, because of their amphiphilic structure. These properties have motivated the development of liposomes as drug and protein carriers.

The main drawback to liposomes is that such vesicles have a short lifespan<sup>35</sup> and a tendency to aggregate or precipitate.<sup>36</sup> Their stability can be increased by different methods, including partial polymerization, especially the coating of the lipid vesicles with PEG polymers, which increases the stability<sup>37</sup>; however, stability is not as good as desired. To further increase the stability of the

vesicles, lipids or lipid conjugates have been replaced by polymers. The use of polymeric vesicles constitutes a better approach because of their increased mechanical stability: block copolymer membranes are thicker and far more stable than those of liposomes.<sup>38</sup> The polymers used have molecular weights more typical of a magnitude of 10 kDa), whereas lipids possess molecular weights less than 1 kDa. Polymeric nanoparticles possess high structural integrity afforded by the rigidity of the polymer matrix, and are thus inherently more stable than liposomes. Several different kinds of polymers have been used to produce nanocarriers, including poly (ethylene glycol) (PEG) and poly (lactide acid) (PLA) blocks, poly(butadiene)-poly(ethylene glycol) (PEO/PBD) <sup>34</sup> and poly(ethylene glycol)-*b*-(caprolactone) (PEG/PCL). In addition to higher stability, polymers have tunable properties that allow different applications due to the differing compositions of the hydrophilic and hydrophobic blocks. These tunable properties include the ability to incorporate proteins into the polymeric membrane, e.g. OmpF.<sup>42</sup> Important to the functioning of many nanocarriers is the controlled, sustained release of their cargo. Nanoreactors should be stable in order to protect the encapsulated substance until the point where the release of the encapsulated substrate should occur. The ability to modify the hydrophobic/hydrophilic blocks for drug targeting, with targeting surface functionalization, permits targeted delivery.

## 1.4 Nanoreactors

In addition to nanocarriers, nanoreactors are becoming increasingly important to biological and medical applications, because they offer the possibility for new treatments. The concept of the nanoreactor differs from the concept of the nanocarrier, in that there is no release of the encapsulated substance in the nanoreactor. The encapsulated substance maintains its functionality inside the nanoreactor; therefore, the functionality of the nanoreactor depends on the activity of the encapsulated molecule. A nanoreactor works as follows: molecules from outside enter the nanoreactor via proteins that form tunnels that are incorporated in the copolymer membrane. Such a tunnel can be formed e.g. by OmpF. Simple diffusing through the polymer membrane may also occur. The entering molecules react with the molecules inside the nanoreactor. As a result, a modification or degradation of the entering substrate occurs. The requirements of a polymer membrane in a nanoreactor are: (i) to allow entrance of a substrate, (ii) high stability, which is required for long lifespan; (iii) no leakage of the encapsulated substrate, and (iv) high biocompatibility in order not to trigger an immune response.

## 1.5 Peroxynitrite degradation

Oxidative stress is related to partial reactive oxygen species (PROS) such as peroxynitrite  ${}^1\text{O}_2$ ,  $\text{O}_2^{\cdot-}$ ,  $\text{HOO}\cdot$ ,  $\text{H}_2\text{O}_2$ ,  $\text{HO}\cdot$ , and  $\text{CO}_3^{\cdot-}$

These species are generated as a side reaction to cell metabolism, or are created by radiation, toxic agents, and drugs.<sup>45</sup>

Besides ROS, oxidative stress can also be associated with toxicity from a variety of inorganic nanoparticles or quantum dots.<sup>46-48</sup> Oxidative stress is involved in many diseases and defects. In this respect, peroxynitrite has been reported to be implicated in the development of neurodegenerative disorders, cardiovascular diseases,<sup>51</sup> and cancer.<sup>52</sup> There are efficient biological strategies to regulate

ROS to reduce or prevent the formation of oxidative stress, including cellular antioxidants (glutathione and ascorbate) and enzymes (glutathione peroxidase, glutathione transferases, catalase, and superoxide dismutase), but these mechanisms can be overwhelmed by a high quantity of ROS. The superoxide anion, which is present in every living cell as a result of normal metabolism<sup>53</sup>, is problematic, because it can react with nitrogen monoxide, which plays a critical role in cell regulation and communication. If the superoxide anion reacts with nitrogen monoxide, peroxynitrite is formed by the diffusion-limited reaction (rate constant  $\sim 1 \times 10^{10} \text{ M}^{-1} \text{ s}^{-1}$ ).<sup>54</sup> The superoxide anion has a short half-life of less than milliseconds<sup>55</sup> and permeates membranes only via anion channels.<sup>56</sup> NO is much more stable, having a half-life in the range of seconds, and it readily diffuses across membranes<sup>57</sup>; therefore, peroxynitrite is formed in the area where the superoxide anion is formed. The formation of large quantities of peroxynitrite can occur when a large amount of  $\text{O}_2^-$  is available. Physiological concentrations of peroxynitrite have been reported on the order of  $50 \mu\text{M}$ <sup>58</sup>; however, they have extended as high as  $500 \mu\text{M}$  in some cases.<sup>59</sup> This happens when the combination of  $\cdot\text{NO}$  with  $\text{O}_2^-$  becomes competitive with the dismutation of  $\text{O}_2^-$  by superoxide dismutases, which was shown, for example, in the mitochondrial respiratory complex. Peroxynitrite is not only a strong oxidative species, it also has the ability to diffuse longer distances than the diameter of a typical cell. For this reason, peroxynitrite can cause damage even far from its origin. It has been shown that amino acids, nucleic acids, and membrane lipids can be modified with peroxynitrites.<sup>60</sup>

In order to reduce the amount of peroxynitrite, there are compounds that exhibit high second-order rate constants with peroxynitrite.<sup>61</sup> In this respect, various proteins are capable to detoxify peroxynitrite under natural conditions, including peroxiredoxins, Se-containing proteins (glutathione peroxidase), and heme proteins (hemoglobin, cytochrome c oxidase,  $\text{Fe}^{\text{II}}$  cytochrome c)<sup>15</sup>. The problem is that the concentration of antioxidant enzymes is not high enough to overcome the excess peroxynitrite involved in metabolic dysfunction. Administration of the above antioxidant proteins is

expected to decrease the amount of peroxynitrite involved in pathological situations. A compound that is active in peroxynitrite decomposition and that can be used for medical applications should possess several properties: (i) reacting quickly with peroxynitrite; (ii) present in large amounts in the desired biological compartment (iii) the decomposition reaction should generate products that are not toxic by themselves and, in addition, (iv) its reaction with peroxynitrite should have a relatively high rate constant (human hemoglobin has a rate constant of  $2 \times 10^4 \text{M}^{-1}\text{s}^{-1}$  at  $\text{pH} = 7.4$ , at  $37^\circ\text{C}$ ),<sup>64</sup> which supports a medical application.

## 1.6 Blood substitutes

It is well known that the hemoglobin (Hb) inside red blood cells play an essential role in the transport of oxygen to organs and tissues. The loss of a large amount of red blood cells can be compensated via blood transfusions. Over the course of the last hundred years the demand for blood transfusions has steadily increased. Stemming from short storage times<sup>65</sup> and safety risks associated with cross-matching and viral infections<sup>66</sup>, there have been many attempts to create artificial blood with the use of hemoglobin, as will be seen below.

A limiting factor in the use of hemoglobin in both cases, however, is that, on its own, hemoglobin – a tetramer – tends to separate into dimers. These dimers are rapidly filtered by the kidneys and excreted.<sup>69</sup> The use of purely polymeric vesicles, however, can increase lifespan significantly.

One approach to solving both mentioned problems simultaneously is to either polymerize hemoglobin in order to reduce dimerization<sup>70</sup> or to encapsulate it, as occurs naturally in red blood corpuscles. The problem with polymerized hemoglobin is that the molecule continues to dissociate<sup>39</sup>, thus leading to toxic dimers. Therefore, the encapsulation of hemoglobin in a nanocarrier has been attempted.

In recent years various block co-polymers, including poly(ethylene glycol) (PEG) and poly(lactide acid) (PLA) blocks, poly(butadiene)-poly(ethylene glycol) (PEO/PBD)<sup>71</sup> and poly(ethylene glycol)-

*b*-(caprolactone) (PEG/PCL) have been used to produce nanoobjects such as vesicles that have the ability to encapsulate Hb.

In addition to hemoglobin, other molecules such as perfluorochemicals (PFCs) have been used as a potential oxygen carrier. The PFCs have shown promising results in animal tests

The oxygen carrying capacity of PFCs is a function of the high solubility of oxygen and carbon dioxide in them (20 times higher than in water). The problem is that PFCs are not water soluble. For this reason, PFCs cannot be directly injected into the blood stream and PFCs are used as suspensions with small size droplets of around 0.1  $\mu\text{m}$ . In this way, PFCs can be removed from the vascular space by the reticuloendothelial system and they leave the body through the lungs.<sup>72</sup>



## **2 Materials and methods**

### **2.1 Materials and methods for creating and analyzing the responsive polymer brush.**

#### **2.1.1 Chemicals**

Ascorbic acid, poly(ethylene glycol)methyl ether acrylate (PEOA), 2-hydroxyethyl acrylate (HEA), 5-bromopyridine-2-thio,  $(\text{BrC}(\text{CH}_3)_2\text{COO}(\text{CH}_2)_{11}\text{S})_2$ , PMDETA, CuBr and methemoglobin were purchased from Sigma (Switzerland).

#### **2.1.2 SPR**

SPR measurements were performed using a BIAlite system (Biacore, Sweden) consisting of two flow cells. All reagents used in the measurements were dissolved in PBS pH 7.2. The samples were degassed before use. The incubation time in the flow cells ranged from 25 to 33 min. The flow rate was 3  $\mu\text{l}/\text{min}$ . All SPR measurements were performed at 25 °C

#### **2.1.3 $^1\text{H}$ NMR**

$^1\text{H}$  NMR spectra were recorded on a Bruker DPX-400 spectrometer operated at 400.140 MHz in  $\text{CDCl}_3$  and processed with MestReNova software. Chemical shifts are reported in ppm relative to tetramethylsilane.

#### **2.1.4 QCM**

QCM measurements were performed using a Q-Sense E1 system. The sensors were cleaned using a freshly prepared basic Piranha solution (5:1:1  $\text{H}_2\text{O}:\text{NH}_3:\text{H}_2\text{O}_2$ ), then rinsed with bidistilled water

and afterwards dried under a nitrogen gas stream. The measurements were performed with a flow rate of 200  $\mu\text{L}/\text{min}$  and 25  $^{\circ}\text{C}$

### **2.1.5 ATR-IR**

ATR-IR measurements were acquired using a Bruker Alpha spectrometer. Spectra were recorded with 128 scans and a resolution of 2  $\text{cm}^{-1}$ .

### **2.1.6 ATRP synthesis**

Poly(ethylene glycol)methyl ether acrylate, PMDETA, DMF, ascorbic acid, and the initiator 5-bromopyridine-2-thiol were added to a Schlenk flask and degassed by argon flow. After stirring the mixture at room temperature for 30 min, CuBr was added to start the reaction. The reaction proceeded overnight, the polymerization was stopped by opening the flask and exposing the catalyst to air. The reaction mixture was then passed through to a neutral aluminum oxide column to remove the copper complex. The remaining unreacted poly(ethylene glycol)methyl ether acrylate was removed by ultrafiltration in  $\text{H}_2\text{O}$ , and the pure brush polymer was dried under vacuum.

## **2.2 Materials and methods for creating and analyzing the polymer nanoreactors.**

### **2.2.1 Chemicals**

Fluorescent dye Alexa488 carboxylic acid and succinimidyl ester were purchased from Invitrogen (Switzerland) and phosphate buffered saline (PBS) (pH 7.2) was obtained from Fluka (Switzerland). All chemicals were used without further purification. Outer membrane protein F (OmpF) expression was carried out in *E. coli* (BL21(DE3)omp8)<sup>73</sup> according to a previously optimized protocol<sup>74</sup> and was stored (700 µg/mL) in 3 wt% OPOE stock solution at 4 °C. The procedure for the synthesis of peroxyxynitrite is described in detail elsewhere.<sup>75</sup>

### **2.2.2 Hemoglobin labeling**

A solution of 1 mg Alexa488 in 50 µl DMSO was slowly added to a solution of 15 mg methemoglobin in 850 µL PBS buffer. After 15 min 0.1 mL of a 0.1 M Na<sub>2</sub>CO<sub>3</sub> solution was added. The mixture was stirred for one hour at room temperature. The free dye was removed by size exclusion chromatography (SEC) on Sephadex G25 (300 mm) equilibrated with phosphate buffered saline (PBS). The labeling efficiency was determined by UV spectroscopy, using the Beer-Lambert law. On average, 2.3 Alexa488 dye molecules per Hb were attached.

### 2.2.3 Polymer vesicle and nanoreactor preparation

PMOXA-PDMS-PMOXA was synthesized according to the procedure described in.<sup>74</sup> The copolymer was characterized by NMR and gel permeation chromatography (GPC). Polymer vesicles were prepared by the film rehydration method: 5 mg of triblock copolymer formed a thin film on the walls of a 25 mL round-bottom flask using a rotary evaporator. After the addition of 1 mL PBS buffer to the polymer film and stirring for 2 h, the solution was extruded through polycarbonate membranes (pore  $\varnothing = 400$  nm) in order to generate vesicles with a low size distribution.

The other method that was used was the cosolvent method. In this method the polymer is dissolved in a small amount of ethanol and is then slowly added while stirring to a buffer solution. The problem with this method is that it only produced micelles and small vesicles with a radius of around 25 nm. The vesicles were too small to encapsulate Hb.

Nanoreactors were prepared by addition of 1 mL of labeled methemoglobin (3 mg/mL in PBS buffer) to the polymer film, stirring for 2 h, and extrusion through polycarbonate membranes (pore  $\varnothing = 400$  nm). Vesicles containing both the protein, and the channel protein OmpF were prepared by simultaneous addition to the polymer film of: 0.95 mL of metHb (3.16 mg/mL in PBS buffer), and 50  $\mu$ L of OmpF (8  $\mu$ M in PBS buffer),<sup>74</sup> stirring for 2 h, and extrusion through polycarbonate membranes (pore  $\varnothing = 400$  nm). Hb initial concentration was selected such that a similar value was achieved as in the case of other Hb-encapsulated vesicles.<sup>76</sup> The extrusion process results in a loss of around 50% of the polymer-hemoglobin aggregates, which has been taken into account for the encapsulation efficiency of Hb. In order to purify the un-encapsulated methemoglobin, the extruded mixture was dialyzed with 300 kDa molecular weight cut off dialysis bags in PBS at 2 – 3 °C at a 1:300 v/v, the dialyzed sample to PBS ratio. In addition, the solution was purified by size exclusion chromatography (SEC) on a Sephadex G25 column (300 mm) equilibrated with PBS. The final

solution was analyzed by FCS to determine the fraction of encapsulated hemoglobin.

## **2.2.4 Characterization of polymer vesicles and nanoreactors**

### **2.2.4.1 Light Scattering**

Light Scattering (LS) experiments were performed with a compact goniometer system ALV/DS/SLS 5000/E correlator, from ALV, Langen (Germany), equipped with a helium-neon laser (JDS Uniphase) with  $\lambda = 633 \text{ nm}$  ( $T = 20 \text{ }^\circ\text{C}$ ). The diffusion coefficient ( $D_0$ ) was obtained from a second-order fit of dynamic light scattering (DLS) data from dilute suspensions. From  $D_0$ , the hydrodynamic radius ( $R_h$ ) was calculated using the Stokes- Einstein relation. Scattering angles were varied between  $30^\circ$  and  $150^\circ$ , with each 10 angles measured for 100 seconds. For static light scattering (SLS) measurements, the data, presented in a Guinier plot extrapolated to zero concentration and zero scattering angle, were used to calculate the radius of gyration.<sup>77</sup>

### **2.2.4.2 Transmission Electron Microscopy**

Transmission Electron Microscopy (TEM) micrographs were recorded using a CM 100 Philips microscope operating at 120 kV, and equipped with an USC1000-SSCCD 2 k\_2 k Gatan camera. The solution of vesicles (empty vesicles, and Hb-containing vesicles) was deposited on a carbon-coated copper grid. The excess solution was removed using absorbent paper and the sample was allowed to dry at room temperature for 1 min before the images were recorded. The grids were stained with uranyl acetate.

### **2.2.4.3 Hemoglobin encapsulation efficiency**

The encapsulation efficiency and the percentage of free Hb were measured by fluorescence correlation spectroscopy (FCS). Solutions of Alexa Fluor 488, Alexa Fluor 488-methemoglobin, and Alexa Fluor 488-methemoglobin-containing vesicles were measured at room temperature in

special chambered quartz-glass holders (Lab-Tek; 8-well, NUNC A/S) that provided optimal conditions for the measurement while reducing evaporation of the aqueous solutions. FCS measurements were performed with a Zeiss LSM 510-META/Confocor2 confocal laser scanning microscope (Zeiss AG, Germany) equipped with an argon laser ( $\lambda = 488$  nm) and a 40x water-immersion objective (Zeiss C/Apochromat 40X, NA 1.2), with the pinhole adjusted to a diameter of 70  $\mu\text{m}$ . The excitation power of the Ar laser was  $P_L = 40$  mW, and the excitation transmission at 488 nm was 3%. Fluorescence intensity fluctuations were analyzed in terms of an autocorrelation function with the LSM 510/Confocor software package (Zeiss, AG). Spectra were recorded over 30 s, and each measurement was repeated ten times; results are reported as the average of three independent experiments. Adsorption and bleaching effects were reduced by exchanging the sample droplet after 5 minutes of measurement. To reduce the number of free fitting parameters, the diffusion time of the free dye (Alexa Fluor 488), and of Alexa 488-labeled methemoglobin (Alexa488-metHb) were independently determined and fixed in the fitting procedure.

### **2.2.5 Activity assays for peroxynitrite degradation and oxygen binding of Hb**

The conversion of Hb was similarly established in solution and *in situ* inside nanoreactors by various reactions:

a) **Conversion of** metHb was realized by:

- i. addition of L-ascorbic acid and carbon monoxide, and
- ii. addition of sodium dithionite.

i) A solution of 2  $\mu\text{mol}$  methemoglobin in 1 mL PBS was converted by adding 50  $\mu\text{L}$  of L-ascorbic acid solution (1 mol/L in PBS). After reacting for 10 min, the mixture was flushed with carbon monoxide for 10 min.

ii) Methemoglobin (900  $\mu\text{L}$  of 50  $\mu\text{M}$  metHb solution) was converted by adding 100  $\mu\text{L}$  of sodium dithionite solution (10 mmol/L in PBS) at room temperature. Excess sodium dithionite was

removed by SEC. The SEC column consisted of Sephadex G25 (300 mm) equilibrated with phosphate buffered saline (PBS). Samples were measured both before and after removal of the sodium dithionite excess.

b) ***Peroxynitrite degradation*** was achieved by the addition of 100  $\mu\text{L}$  of 10 mM peroxynitrite solution to 900  $\mu\text{L}$  of a 50  $\mu\text{M}$  HbO<sub>2</sub> or deoxyHb solution (pH 7.4, room temperature). At least 8 – 10 mol ONOO<sup>-</sup> were required to completely convert 1 mol of HbO<sub>2</sub> to metHb.

c) ***Oxygen binding*** was tested by conversion of deoxyHb to HbO<sub>2</sub> and by conversion of HbO<sub>2</sub> to HbCO. DeoxyHb obtained after addition of sodium dithionite was passed through a column of Sephadex G25 (100 mm) to remove the excess sodium dithionite, in the presence of oxygen. To obtain HbCO, an HbO<sub>2</sub> solution was flushed with carbon monoxide for 20 min.

The different oxidation states of hemoglobin were measured by UV-Vis spectroscopy and Raman spectroscopy. UV-Vis measurements were performed at room temperature using a SPECORD 210 Spectrophotometer (Analytic Jena, Germany). The spectra were recorded at room temperature, in a range from 390 nm to 1000 nm. Samples were measured immediately after preparation (within 20 s), to avoid further reaction with nitrate, a ubiquitous contaminant of ONOO<sup>-</sup> solution.

### **2.2.6 Raman spectroscopic characterization:**

Raman spectra were recorded using an *alpha300R* (WITec GmbH, Ulm, Germany) confocal upright microscope spectrometer (UHTS 300, WITec) equipped with epi-illumination. A water immersion objective lens with glass correction (Olympus UAPON 40XW340 NA1.15WD0.25UV) was used to focus the laser beam on the sample and to collect the Raman backscattered light. Raman scattering was excited by a 532 nm Nd:Yag laser. *Sample preparation for Raman experiments:* Hemoglobin samples were analyzed between two 0.15 mm thick glass cover slides separated by a 50  $\mu\text{m}$  thick double sided tape (Tesa, Switzerland). All measurements were performed with the laser beam focused 20  $\mu\text{m}$  below the top cover slide. The Raman signal could not be collected from

encapsulated hemoglobin solutions because the Rayleigh scattering from the 200 nm-size vesicles interfered greatly with spectra acquisition. Moreover, the encapsulated Hb concentration in solution was one order of magnitude lower than what would normally be detected using Raman spectroscopy. We thus decided to work at a bulk concentration between 20 and 50  $\mu\text{M}$ , which is relevant to a local protein concentration within one vesicle when considering between 10 and 20 encapsulated protein molecules per polymeric vesicle. Each Raman spectrum represented the cumulative signal of 100 measurements of 1 s integration time. Spectra were processed to remove cosmic rays (WITec Project Software) and background corrected by subtraction of the signal acquired with the laser off immediately after each series of 100 consecutive measurements.

### **2.2.7 Stopped flow spectroscopy**

The kinetics of the reaction of hemoglobin with peroxynitrite was studied by single-wavelength stopped flow spectroscopy under pseudo-first order conditions (at  $\lambda = 430$  nm). Peroxynitrite was always present at least at 10-fold excess, to maintain pseudo first order conditions. Measurements were performed at room temperature using an SFM-20 instrument equipped with an MOS-200 monochromator. The degradation of peroxynitrite was measured at its absorption maximum  $\lambda = 302$  nm. The traces correspond to the average of at least 10 single traces, and were analyzed with Biokine32 software. The data were fitted with a second order exponential fit. In order to acquire a better signal, the nanoreactor solution was concentrated by centrifugation (10 min at 4500 rpm).



## 3 Results and discussion

### 3.1 Responsive polymer brush

In material science, polymer brushes are important for the protection of surfaces. Brushes can prevent fouling of the surfaces because they hinder the binding of other molecules to the surface.

Another application for polymer brushes that was investigated in this study was the use of responsive brushes to create a selective layer that combines passivation abilities with the supply of binding sites for special molecules. This selectivity of binding lends the brush the ability to detect specific molecules. In these studies we used a polymer with PEG side chains to create the polymer brush. We also used special, commercially available antibodies that are able to bind to the PEG chains (**Figure 3**).

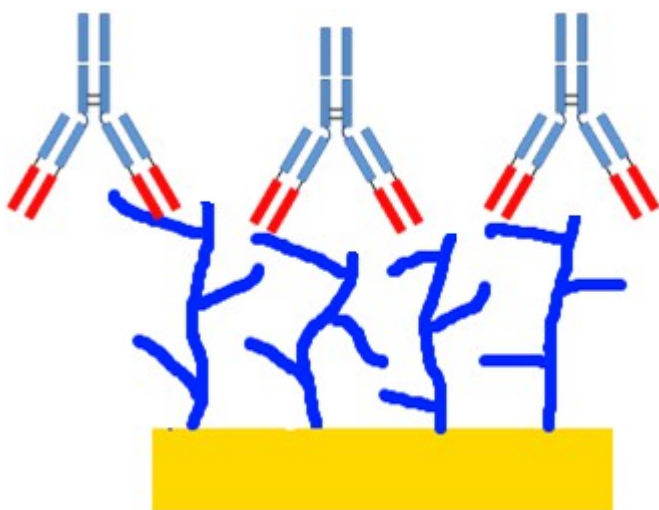


**Figure 3.** Schematic representation of the antibodies bound to the polymer brush.

#### 3.1.1 PEG

PEG has been used for different applications, due to its renowned properties of biocompatibility and protein resistance.<sup>78</sup> PEG polymers have a high capacity to passivate a surface. This has been

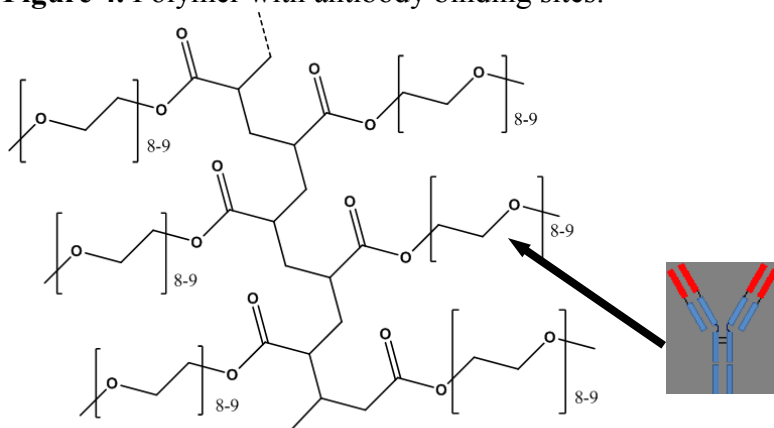
demonstrated for different applications of anti-fouling surface protection, such as protection from protein- and cell adsorption on various kinds of surfaces<sup>78</sup>, and it is also used as a part of a copolymer for the protection of ultrafiltration membranes used in water purification.<sup>79</sup> It can also be used in biomedical applications<sup>80</sup> to reduce immunogenicity and to shield drugs, prolonging their circulation time in the blood stream. PEG reduces the tendency to aggregate and increases resistance to proteolytic cleavage in drug targeting.<sup>80</sup>

### 3.1.2 PEG-binding

In this study, PEG-specific antibodies have been used as a model protein for the selective binding of molecules to the surface and have also been developed for the measurement of PEG-modified molecules *in vivo*, for drug development. These antibodies have the ability to bind to repeating units of PEG. **(Figure 4).**

that passivate the surface; therefore, PEG chains have a dual-function of surface passivation and providing binding sites for the antibodies. Another advantage is that antibodies are huge proteins and therefore the extent of binding of the antibodies shows the degree to which binding sites are accessible for large molecules.

**Figure 4.** Polymer with antibody binding sites.



### 3.1.3 Initiator

The initiator is important because, in addition to the bromide that is required for the polymerization, the initiator also provides the thiol group for “grafting to” the surface. The first used ATRP initiator was  $(\text{BrC}(\text{CH}_3)_2\text{COO}(\text{CH}_2)_{11}\text{S})_2$ . This initiator was not used for further experiments. The problem with this initiator was that the polymerization only leads to oligomers. As a result, therefore, the number of repeating units of PEG chains was very low. The initiator is symmetrical and contains two bromides that can form two radicals and is therefore able to react intermolecularly to form a ring. For this reason, 5-bromopyridine-2-thiol was used as the initiator. The new initiator only forms one radical, so it cannot react intermolecularly, but it has low activity and, for this reason, only a small fraction of the monomer polymerizes. The GPC data show that the polymer only consisted of around 20 repeating units.

### 3.1.4 PEGA Polymer

We selected for testing a polyPEGA polymer with a branched architecture. Instead of a linear PEG homopolymer, in order to introduce specific binding sites for future functionalizations, knowing that the polymer brush has the same passivation abilities no matter if formed from linear or branched polymers (**Figure 5**). The PEGA polymer with desired branched architecture was synthesized by the controlled radical polymerization of poly(ethylene glycol)methyl ether acrylate (PEGA) monomers.

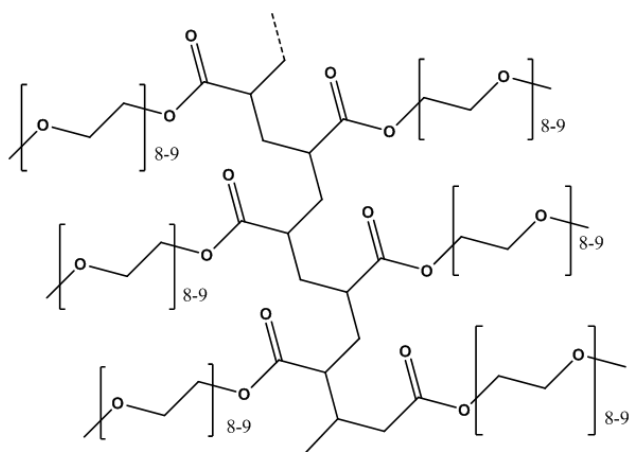


**Figure 5.** Structure of the branched polymer.

The monomer that was used for the polymerization was a poly(ethylene) glycol acrylate with 8 – 9 repeating units of PEG. This number of repeating PEG units is needed in order to provide a binding site for the antibody. Another problem is that the polymer has a carbon backbone that can lead to highly unspecific binding. The carbon backbone is hydrophobic; therefore, unspecific binding of other hydrophobic molecules can occur. The PEG chains that were used are long enough to shield the carbon backbone and prevent the unspecific binding. Polymer formation was confirmed by  $^1\text{H}$  NMR (**Figure 6**). The GPC measurements showed that the polymer has an average  $M_n$  of 12000 and a PDI of 1.3, in average polyPEGA contained 20 repeating units of poly(ethylene glycol)methyl ether acrylate (PEGA) monomer (**Figure 9**).

Other monomers with different numbers of PEG repeating units were tested, for example polymers with shorter side chains with only three PEG repeating units are not adequately water soluble and they can only be dissolved in water at low temperature, while polymers with longer side chains with 18 to 20 repeating units can be prepared, but the polydispersity is higher (**Figure 7**). The poly(ethylene glycol)methyl ether acrylate (PEGA) monomers were also copolymerized with 2-hydroxyethyl acrylate (HEA) monomers (**Figure 8**). The addition of shorter chains may increase the binding of antibodies, because they provide more space for the antibodies to bind. The problem with these copolymers is that they form hydrogels. The copolymerisation is important in order to create a polymer brush that is not specifically prepared for binding PEG-binding antibodies, but

also for binding other molecules. Such as tris-nitrilotriacetic acid that provides binding sites for other molecules.

The PEG monomer can be copolymerized with other molecules that contain an acrylate or methacrylate group that contains binding sites for other molecules. The copolymers may provide binding sites for other molecules and maintain their surface passivation abilities and, as a result, many different monomers can be used, because PEG is soluble in many different solvents. In order to attach the polymer to the surface and create a polymer brush, the polymer should contain a terminal thiol group that can be attached to a gold surface.

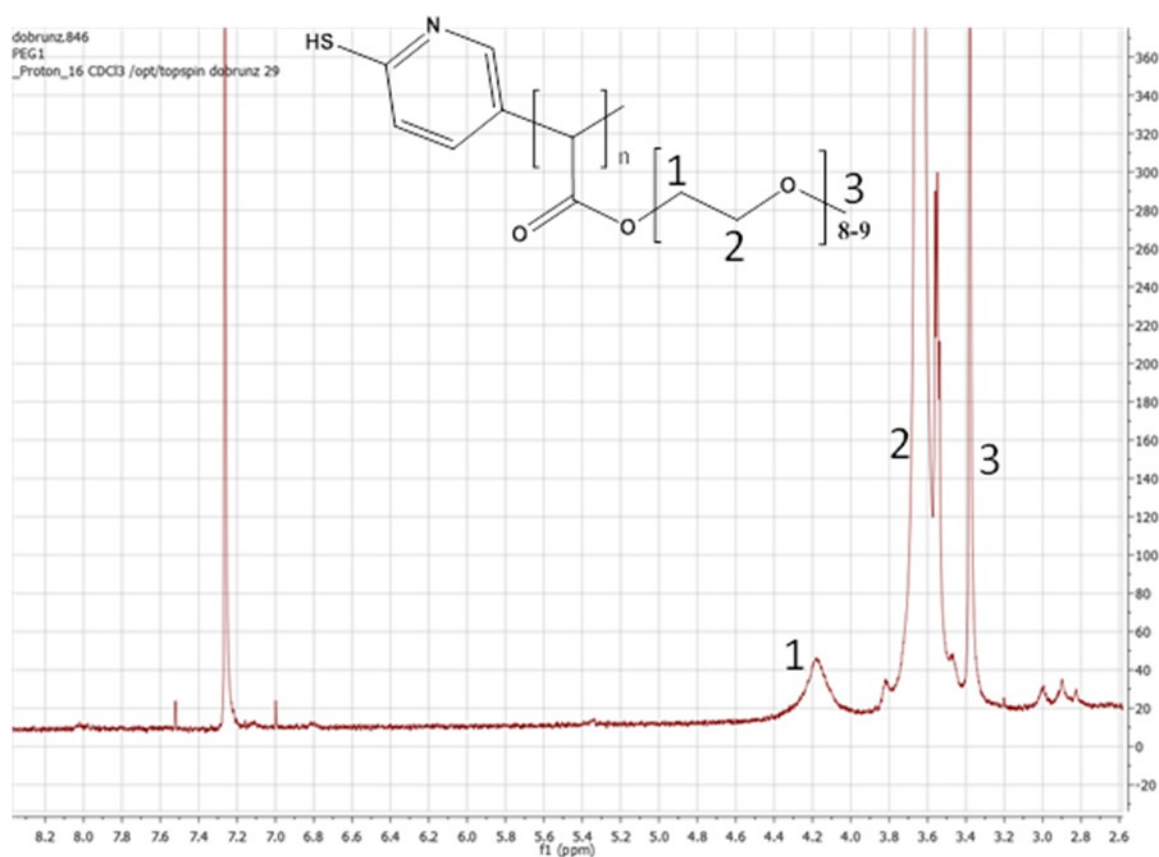


**Figure 7.** <sup>1</sup>H NMR spectrum of the poly(ethylene glycol) methyl ether acrylate polymer with 8 – 9 repeating units of ethylene glycol .

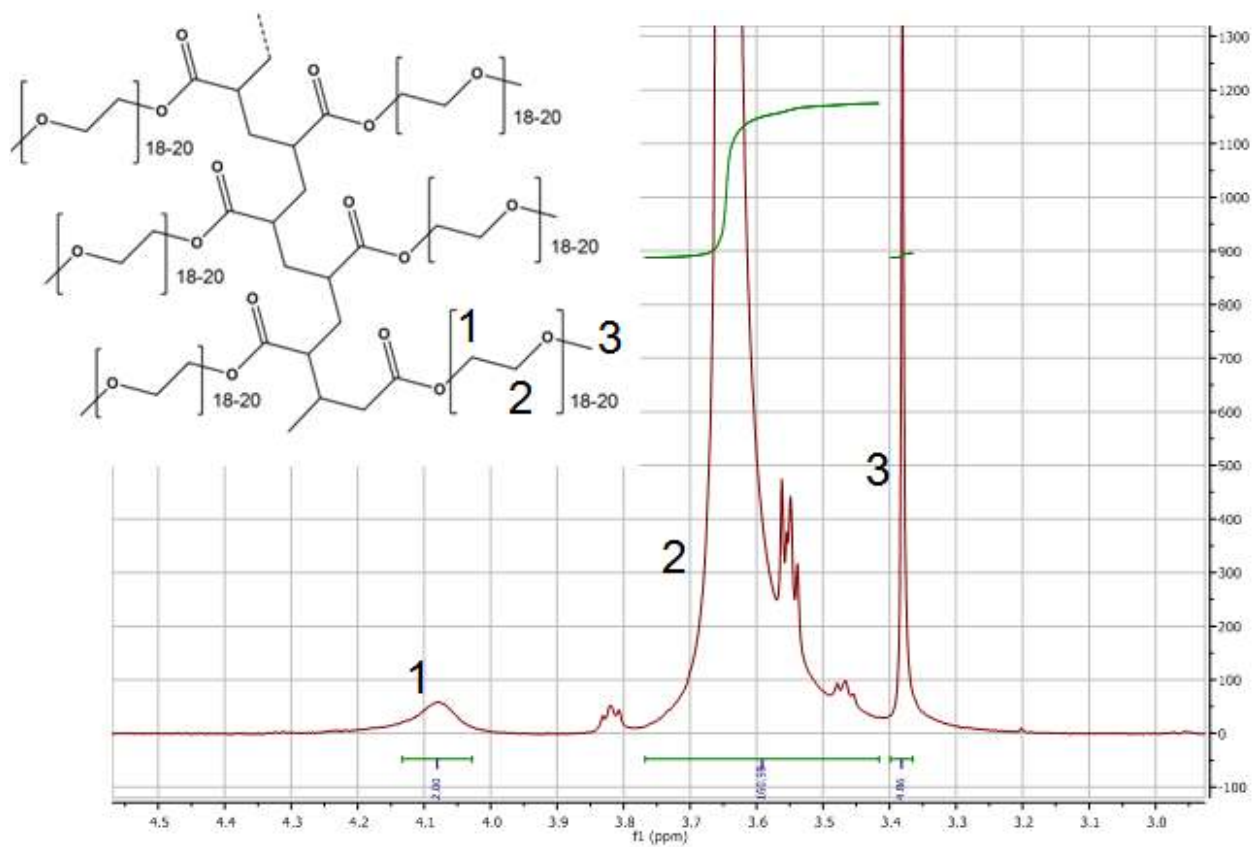


**Figure 7.**  $^1H$  NMR spectrum of the poly(ethylene glycol) methyl ether acrylate polymer with 18 – 20 repeating units of ethylene glycol.

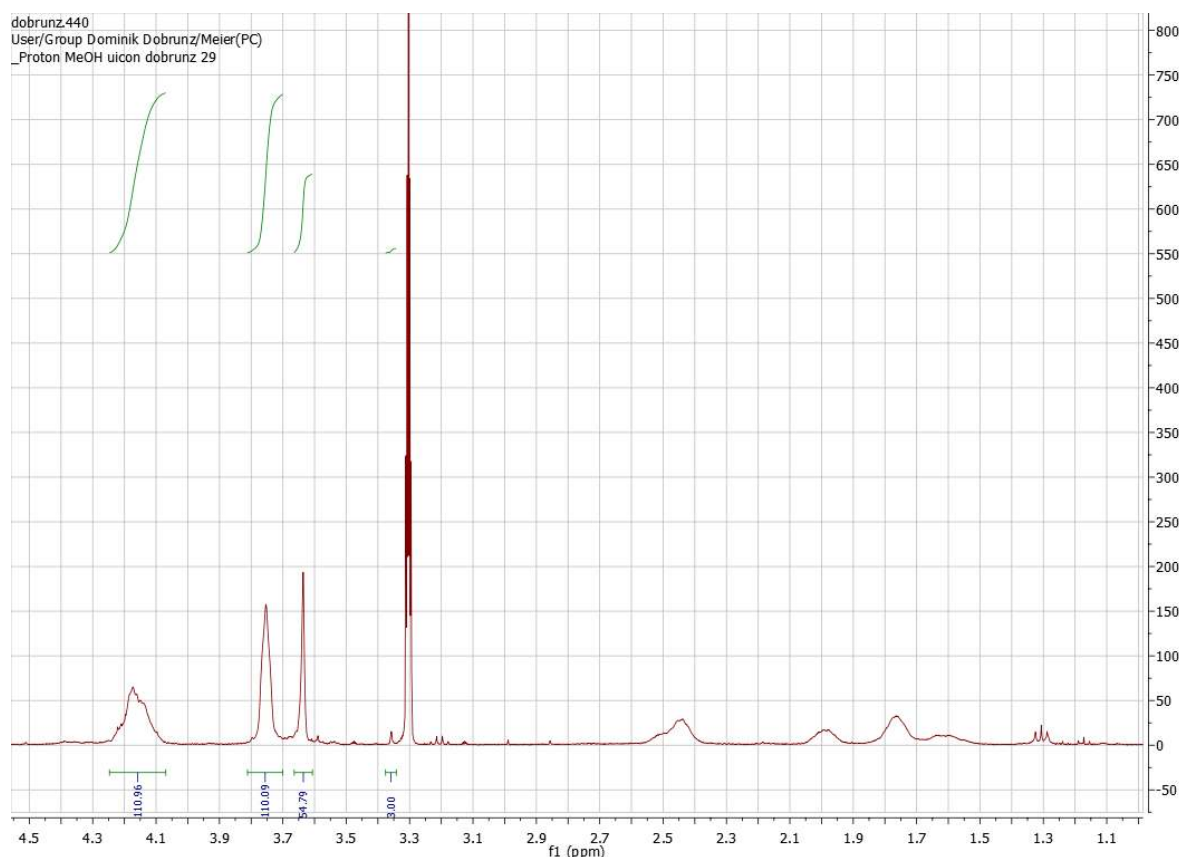


**Figure 8.**  $^1\text{H}$  NMR spectrum of the copolymer of poly(ethylene glycol) methyl ether acrylates and poly-2-hydroxyethyl acrylate.

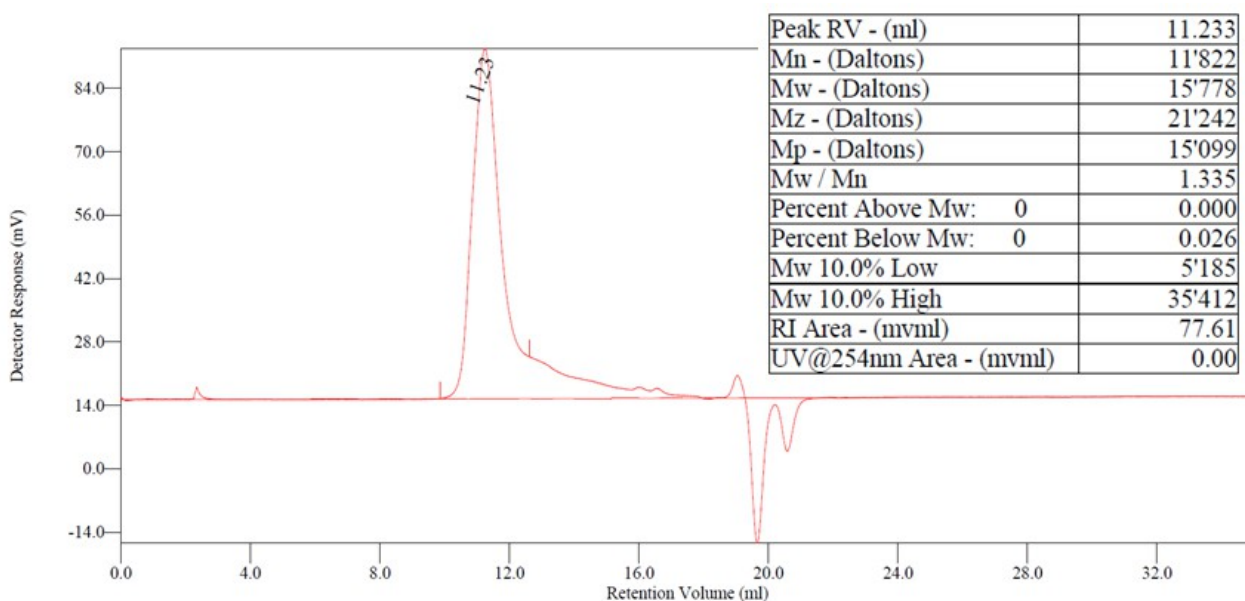
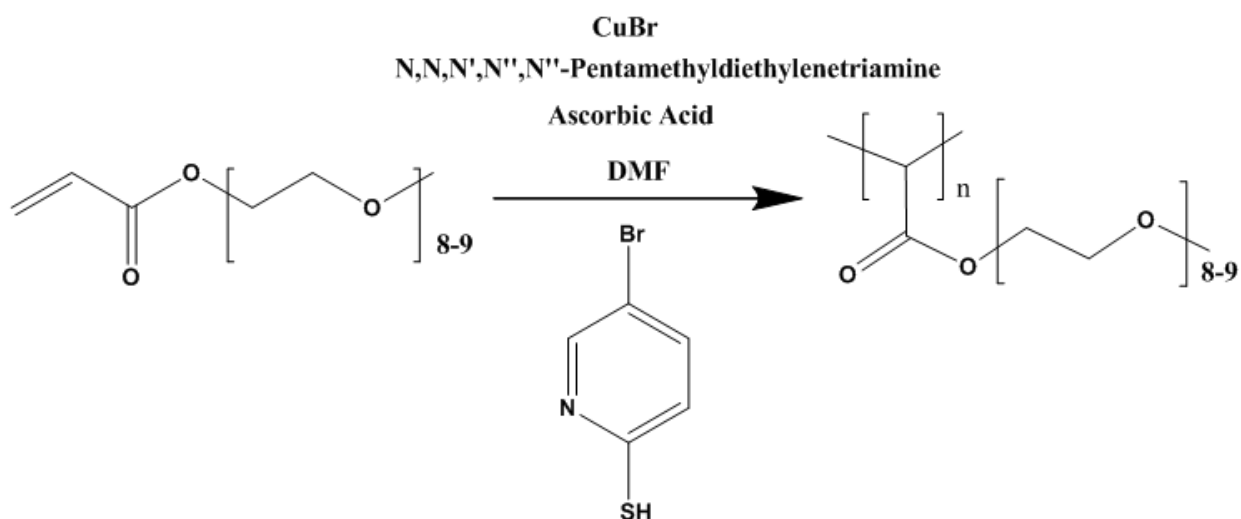


**Figure 9.** GPC spectra of the poly(ethylene glycol) methyl ether acrylate polymer with 8 – 9 repeating units of ethylene glycol.

### 3.1.5 ARGET ATRP

The method used for the polymerization of poly(ethylene glycol)methyl ether acrylate (PEOA) monomers was atom transfer radical polymerization ARGET ATRP (**Scheme 1**). This method is one of the most successfully controlled/living radical polymerizations (CRP),<sup>83</sup> due to its robust nature and to the possibility of controlling molecular weight and providing a narrow molecular weight distribution  $M_w/M_n, < 1.5$ . It enables synthesis of a wide spectrum of polymers and allows the controlled synthesis of polymers with a branched structure with different chains, leading to different architectures such as block-, random-, gradient-, comb-shaped-, brush-, multiarmed-, end-functional-, and star copolymers, increasing in this way the number of multiple applications.

In addition to the wide variety of monomers that can be polymerized with ATRP it is also possible to use a wide variety of non-organic and organic solvents.<sup>90</sup> ATRP has been successfully used for the polymerization of PEG-containing copolymers<sup>91-93</sup>



**Scheme 1.** Polymerization reaction of the monomers.



### 3.1.6 Polymer Brush

The brushes were formed on a gold surface (**Figure 9**). A gold surface was used because it can bind strongly to thiols and disulfides. The polymer brush can be produced with two different methods: the “grafting from” and the “grafting to” method. The method that was used was the “grafting to” method because it allows the synthesis of the polymer in solution and the final polymer can then be easily grafted onto the surface by simply deposition. The “grafting from” method was not used because it is more complicated, due to the polymerization all being done on the surface. The advantage of the “grafting from” method is that it allows a higher density of the polymer brush. The experiments have shown that the grafting density with the “grafting to” method is high enough. The brush density is an important point when it comes to the surface passivation and the binding of the PEG-binding antibodies. The surface has to be covered with a brush that is dense enough so that no other molecule can bind to the surface. For the binding of the antibodies on the other side, a low grafting density is favorable because the antibodies need space to bind to the binding sites of the polymer. The polymer that was used has a different structure than other polymers that have previously been grafted on the surface. The influence of the different structure also has an influence on the brush formation.

In order to confirm that deposition of the polymer on the surface, the sample was analyzed with attenuated total reflection infrared spectroscopy (ATR-IR), a blank gold slide was measured as a reference, for which no adsorption bands could be detected. The spectra of the polymer monolayers on gold were recorded. ATR-IR measurements can yield information on the structure of the polymer that is attached to the surface. The ATR-IR measurements confirmed that the polymer is attached to the surface. The peak at  $1117\text{ cm}^{-1}$  shows the ether bonds of the PEG side chains and the bonds at  $1570\text{ cm}^{-1}$  show the ester group (**Figure 10**).

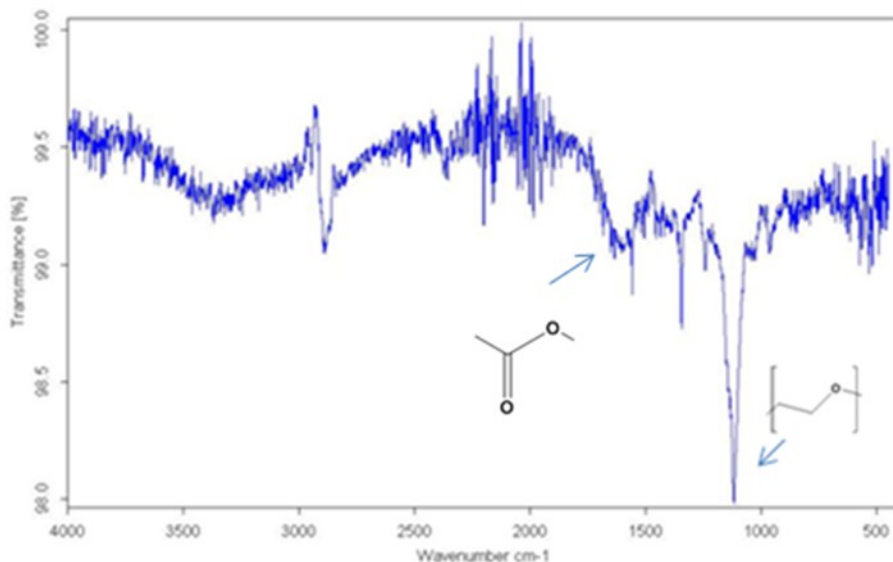


**Figure 10.** ATR-IR spectra of the polymer brush-coated gold surface with the bonds from the ester group at  $1570\text{ cm}^{-1}$  and ether bonds at  $1117\text{ cm}^{-1}$

The monolayer formation was also characterized by surface plasmon resonance spectroscopy (SPR). This optical method allows for non-invasive thin film characterization and is very sensitive to small changes in adsorbed mass. In order to form a polymer brush on the surface, the polymer was dissolved in PBS buffer and then deposited on the gold surface. After washing, a film remained on the surface. The same procedure was repeated and the amount that was deposited after the second cycle was low. This showed that the surface was already covered with the polymer film. No further polymer was able to attach to the surface (**Figure 11**). The thickness of the polymer brush was calculated to be  $10.2\text{ nm} \pm 2.5\text{ nm}$ . In a second step, BSA was added to the polymer film. BSA is a protein with high, unspecific binding and it attaches to nearly any surface. The measurements showed that BSA was not able to attach to the surface. All of the deposited BSA on the surface was removed by flushing the surface with buffer (**Figure 12**). This result showed that the BSA cannot attach to a polymer coated surface. From this, we conclude that the polymer brush has high passivation ability. The passivation indicates that there is no free surface to which the BSA can bind.

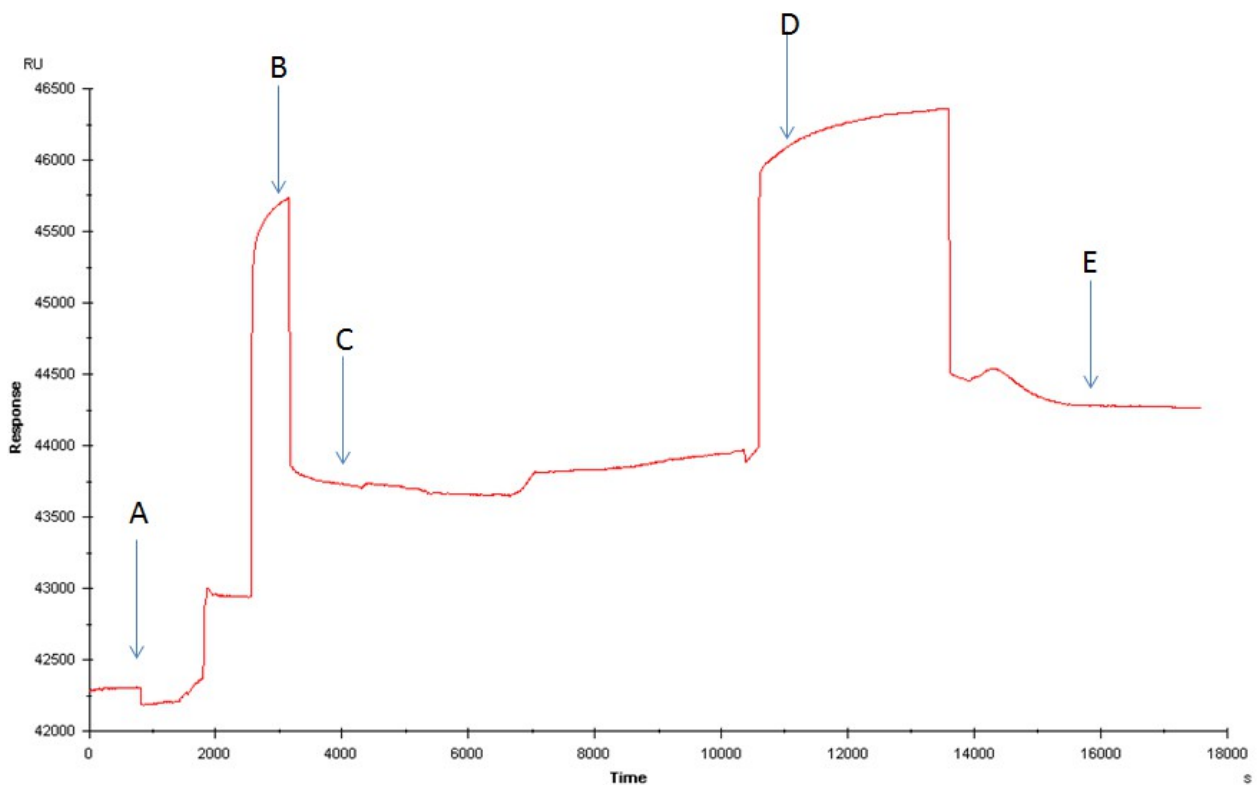


**Figure 11.** SPR spectrum of the adsorption of the polymer to a gold surface. The polymer solution was deposited on the sensor (B), which changes the frequency compared to the baseline (A). Then, the polymer was able to graft onto the surface for 5 min. The sensors were then flushed again with water to remove the free polymer that could not graft to the surface (C). In a second step the polymer solution was added again to the sensor, then the polymer was able to graft onto the surface for another 30 min (D). The sensors were then flushed again with water to remove the free polymer that was not attached to the surface (E).

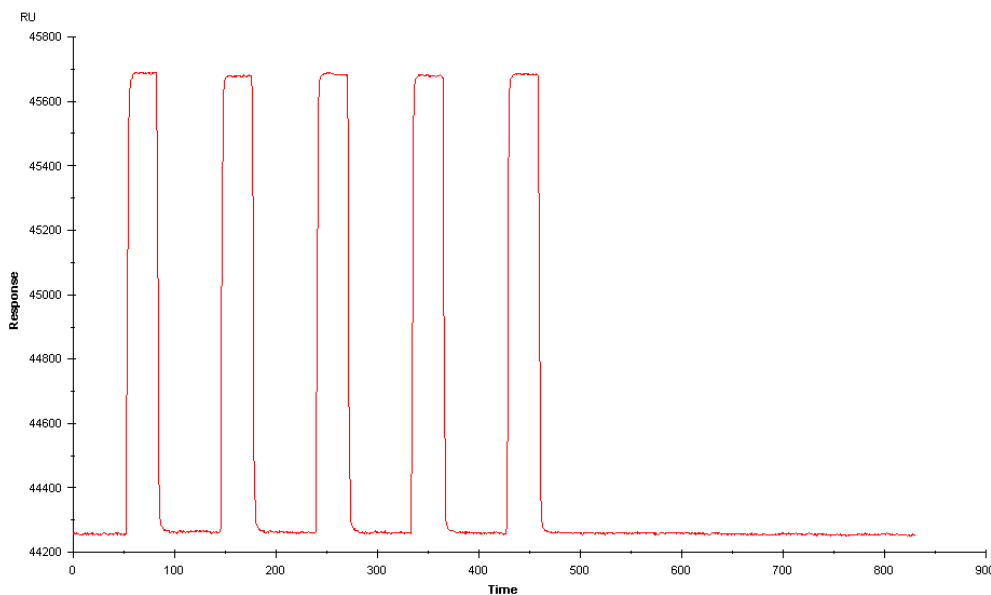


**Figure 12.** BSA adsorption to a polymer-coated gold surface

A commercially available PEG 20k was used as a reference to compare brush formation. It has been reported that PEG 20k is able to passivate a gold surface and it is also able to bind PEG antibodies.<sup>24</sup> PEG 20k is known to form dense brushes on the surface. Our polymer showed similar results to PEG 20k. The antibodies were placed on the polymer coated surface. The PEG side chains provide binding points for the antibody surface. With SPR, an antibody binding curve was observed. The SPR data shows that the antibodies can bind to the polymer coated surface (**Figure 13**). The equilibrium dissociation constant  $K_D$  of the antibody binding was calculated by fitting Req to the Langmuir adsorption isotherm<sup>25</sup> giving  $K_D = 0.77 \pm 0.93$  nM (**Figure 14**). The calculation does not provide good results because the amount of data from the antibody binding curve that could be used was small.

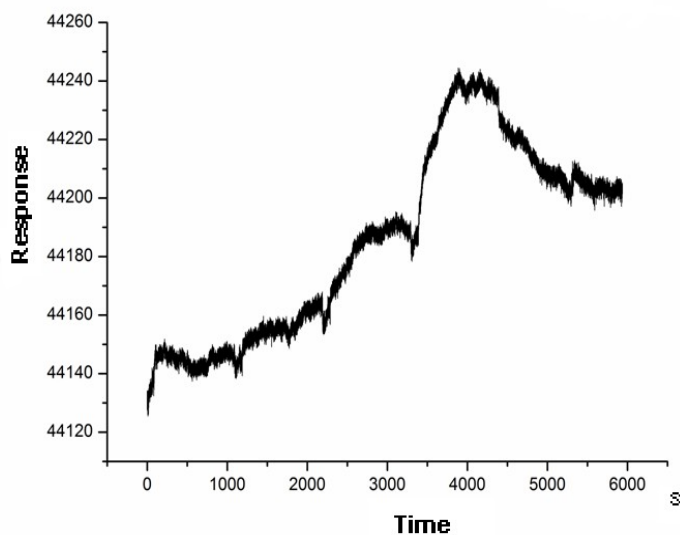


**Figure 13.** Antipeg binding curve for a polymer-coated surface.

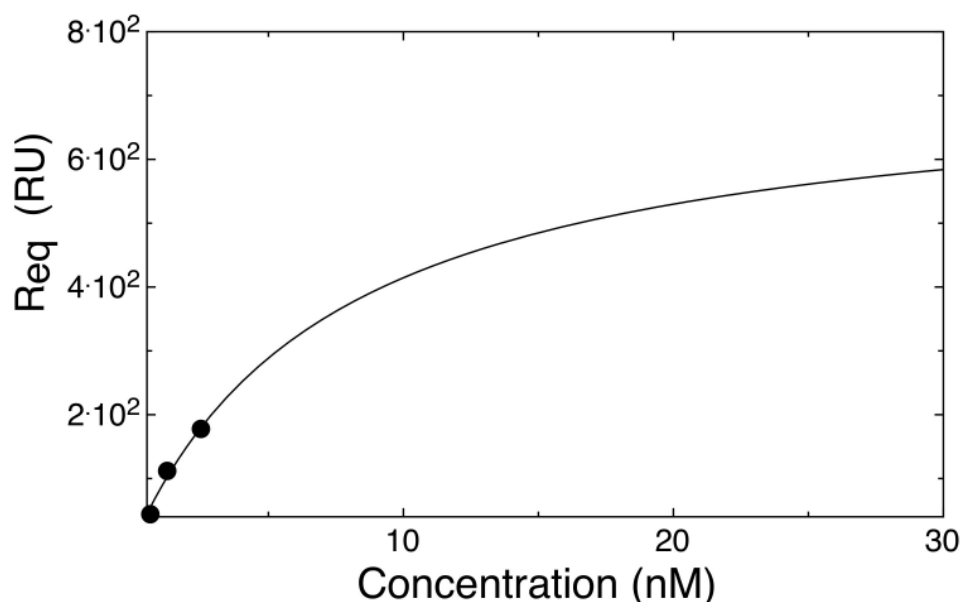


**Figure 14.** Antipeg binding curve fitted to the Langmuir adsorption isotherm.

In addition to the SPR measurements, QCM measurements have also been done to analyze brush formation and surface passivation. QCM measures mass per unit area by detecting the change in frequency of a quartz crystal resonator. The resonance is disturbed by the addition of molecules that bind to the surface. As a mass is deposited on the surface of the crystal, the thickness increases and the frequency of oscillation decreases from the initial value. This frequency change can be quantified and correlated to the mass change using Sauerbrey's equation.<sup>96</sup> In this experiment, a sensor with a gold surface was used. The polymer was dissolved in water at a concentration of 1 mg/mL and deposited on the sensor.

The polymer was then able to graft onto the surface for 30 min. The sensors were then flushed again with water to remove the free polymer that wasn't grafted to the surface. The change in the frequency shows the amount of polymer that was attached to the surface. By comparing the frequencies before the addition of the polymer solution and after the flushing of the sensor with water, the mass that was attached to the surface can be obtained. The change in mass on the sensor shows that a brush with a thickness of  $6.2 \text{ nm} \pm 2.5 \text{ nm}$  was created. The QCM measurements show that the polymer was bound to the surface. In a second step, BSA was added to the polymer film. The measurements showed that BSA was not able to attach to the surface. All of the deposited BSA on the surface was removed by flushing the surface with water (**Figure 15**)

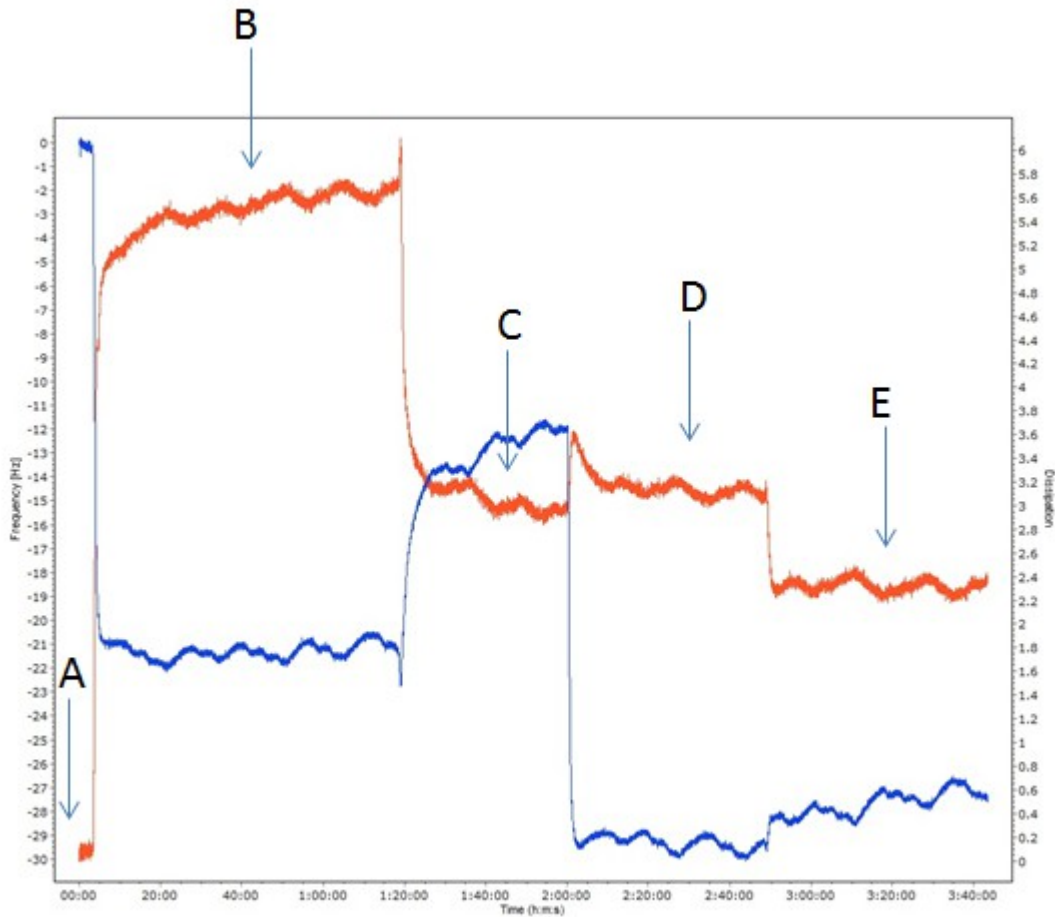


**Figure 15.** QCM spectra of the adsorption of the polymer and BSA to the gold surface. The polymer solution was deposited on the sensor (B), which changed its frequency compared with the baseline (A). The polymer was then able to graft to the surface for 30 min. The sensors were then flushed again with water to remove the free polymer that wasn't grafted to the surface (C). The BSA solution was deposited on the polymer coated sensor (D).

Then, the BSA was able to graft onto the surface for 30 min. The sensors were then flushed again with water to remove the free BSA that wasn't attached to the surface (E).

### **3.1.7 Conclusion: Polymer brush**

Here, we have synthesized and characterized a responsive polymer brush with dual-functionality: surface passivation and with selective binding sites for specific molecules. We selected a polymer with branched architecture because of its ability for further modification and copolymerization. The polymer was successfully synthesized by ARGET ATRP. The polymer structure was confirmed by <sup>1</sup>HNMR. The GPC measurements showed that the polymer on average has 20 repeating units of the poly(ethylene glycol)methyl ether acrylate (PEGA) monomer. The polymer was able to be deposited on the surface via the grafting to method, while the QCM and SPR measurements showed that a 6.2 – 10.2 nm thick polymer brush was deposited on the gold surface.

The polymer has been shown to be efficient at passivation. Surface passivation abilities were proven by SPR and QCM. In addition to the passivation, the system also provides many possible binding sites. An antibody binding curve was recorded by SPR, indicating clearly that the antibody was able to bind to the polymer brush. This new system was able to achieve higher selectivity, which means low unspecific binding and high specific binding.

## 3.2 Hemoglobin nanoreactors

The aim of the project was to generate a nanoreactor with the dual functionality of oxygen transport and peroxynitrite reduction. Therefore, a substance that had the ability to transport oxygen and to degrade peroxynitrite was needed. Hb was used as a model protein because Hb has the ability to transport oxygen and reduce peroxynitrite. The advantage of Hb is that it is commercially available, has a good stability, and its activity can be detected by UV- absorption measurements. That allows the study of the protein inside the nanoreactor.

### 3.2.1 Polymers used for nanoreactor preparation

All nanoreactors used for this study were obtained from PMOXA-*b*-PDMS-*b*-PMOXA triblock copolymer self-assembly (**Figure 16**). PMOXA-*b*-PDMS-*b*-PMOXA triblock copolymers were previously reported in the literature as suitable for drug delivery, due to their increased stability and non-toxicity. The triblock copolymer nanoreactors were proven to be impermeable to hydrophilic cargo<sup>99</sup> and prevented it from leaking into in the reaction medium.<sup>100</sup> With a proven record of good biocompatibility,<sup>101</sup> the membrane of PMOXA-*b*-PDMS-*b*-PMOXA nanoreactors possess high flexibility that allows for the insertion of channel proteins, such as OmpF, LamB, or Aquaporin Z without affecting their proper functionality. The incorporation of channel proteins within the vesicle membrane is essential to allow substances/products to penetrate through and support the nanoreactor functions. The chemical structure of the polymer used for preparing the nanoreactors has a major influence on both the shape and size of the nanoeactors and their ability to encapsulate molecules. For encapsulation of hemoglobin, nanoreactors with a radius of 100 nm were preferred. It is important that the polymer forms nanoreactors in higher numbers, high enough to encapsulate a reasonable amount of Hb molecules. The nanoreactors were formed by copolymer self-assembly in phosphate buffer. For the formation of nanoobjects with defined shapes such as micelles, rods,



vesicles or aggregates, the ratio between the length of the hydrophilic and the lengths of the hydrophobic blocks is crucial. The selection of a specific ratio defines the shape of the nanoobjects and their sizes. In order to determine the optimal ratio for vesicle formation, different PMOXA-*b*-PDMS-*b*-PMOXA copolymers with various ratios of hydrophilic to hydrophobic segments were tested. In addition to their ability to form vesicles, the polymer also has to fulfill other requirements. It is important that the polymer not interact with the molecules that will be encapsulated. An interaction of the polymer with the guest might interrupt vesicle formation. This kind of interaction usually occurs if the polymer and the substances are charged. As encapsulated molecules can be pH dependent, the encapsulation will work best at specific pH values.<sup>76</sup> The stability of the vesicles is important, because a nanoreactor is designed to circulate in the bloodstream for a long time. This is why it is crucial that the polymer form mainly vesicles and less so aggregates or rods. The polymer has to form nanoreactors with low size polydispersity. Several experiments have been conducted in order to decide which polymer to use for further experiments. All vesicle solutions obtained from the different PMOXA-*b*-PDMS-*b*-PMOXA copolymers were analyzed by TEM and FCS. TEM measurements give an overall image that shows whether a polymer forms vesicles, micelles, rods or aggregates, and also provides information about their size. In FCS, only nanoobjects that encapsulate fluorescent active molecules can be seen. Those nanoobjects, such as micelles or rods, that do not encapsulate fluorescent active molecules cannot be detected by FCS. FCS measurements indicate whether the produced nanoobjects can encapsulate Hb. These methods were used to analyze the vesicle solution formed by the different polymers and to choose the most suitable polymer. More detailed analyses were carried out with the chosen polymer.

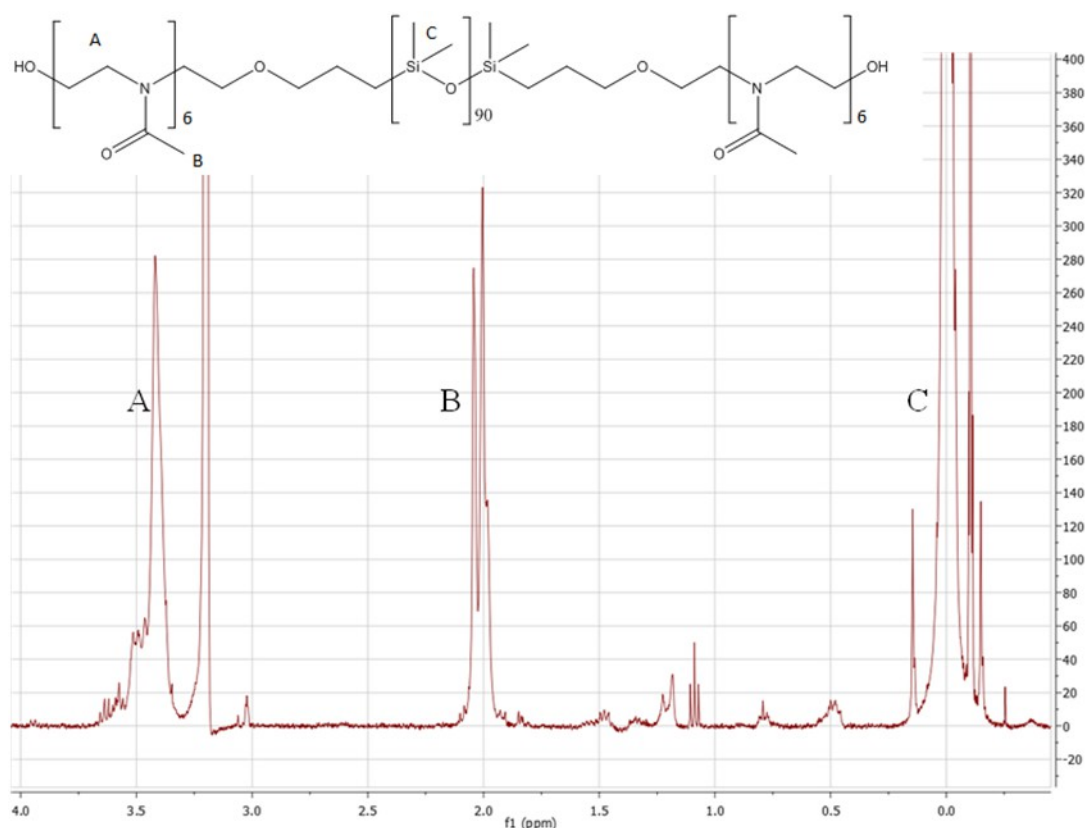


**Figure 16.** Chemical structure of PMOXA-*b*-PDMS-*b*-PMOXA consisting of the two hydrophilic PMOXA and one hydrophobic PDMS block. <sup>1</sup>H NMR spectra of the PMOXA-*b*-PDMS-*b*-PMOXA copolymer.

The shape and size distribution of polymer nanoreactors can be designed by choosing the optimal ratio of PMOXA to PDMS blocks. So even though the tested polymers only differ from the point of view of their lengths of the hydrophobic and hydrophilic blocks, their outcomes differ greatly. Every polymer has a specific tendency to form rods, micelles, vesicles or aggregates. This affects the encapsulation efficiency, because micelles or rods are not able to incorporate Hb.

The first polymer that was tested was an A<sub>10</sub>B<sub>87</sub>A<sub>10</sub> triblock copolymer. The vesicles were prepared using film rehydration. After the preparation and purification steps the polymer solutions were analyzed with TEM (**Figure 17**) and FCS. From the FCS measurements, information on the size of the vesicles and the encapsulation efficiency were obtained. The TEM images provided information on the shape and size of vesicles, micelles, rods or other aggregates. For the proper function of the nanoreactors, it is important to have a vesicle solution with specific, narrow size distribution,

because only vesicles with a certain diameter of a minimum of 50 nm have been shown to encapsulate hemoglobin. Because they are too small, micelles are not suitable for the encapsulation of hemoglobin and hence they reduce the encapsulation efficiency. For  $A_{10}B_{87}A_{10}$  copolymers, the obtained vesicle solution was not homogeneous, but contained fractions of vesicles, rods, micelles and aggregates. Only the vesicles fraction was able to incorporate labeled Hb, as the FCS data confirmed, while the fractions of micelles and rods formed do not encapsulate Hb.

This polymer could not be used further for the preparation of nanoreactors because of the high percentage of aggregates that were formed. The aggregates consist of small vesicles or micelles that stick together to form bigger structures. Aggregate formation can be caused by interactions between the polymers or polymer with hemoglobin. Therefore, it is difficult to analyze whether labeled Hb was successfully encapsulated into the polymer vesicles.

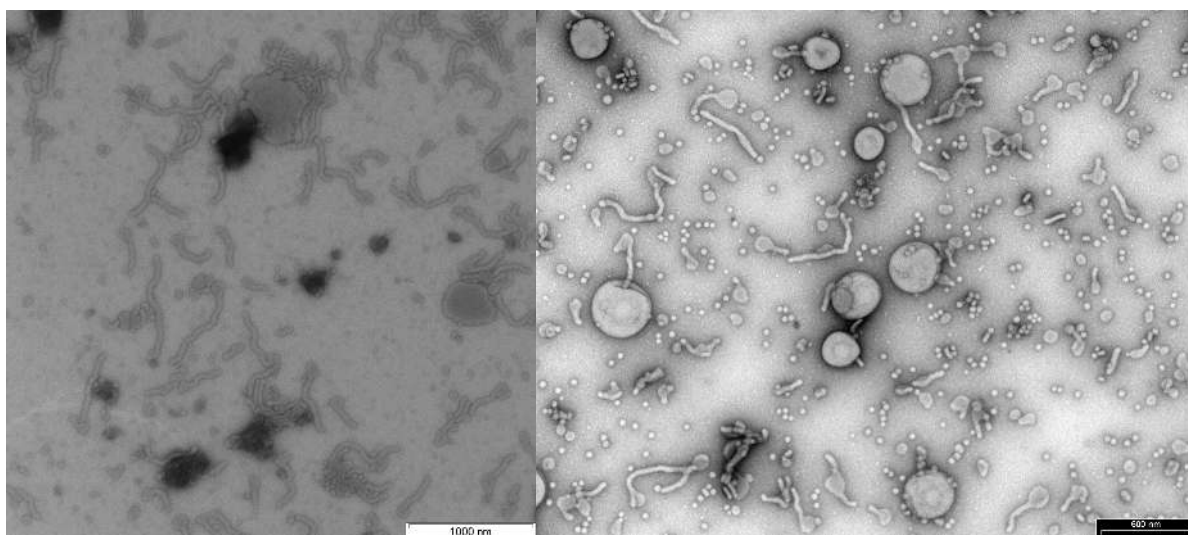


**Figure 17.** TEM images from the  $A_{10}B_{87}A_{10}$  copolymer showing vesicles, micelles and rods.

A second polymer tested was an  $A_{12}B_{55}A_{12}$  block copolymer. This was the first polymer that showed promise for nanoreactor preparation. TEM pictures indicated that mainly vesicles were formed by  $A_{12}B_{55}A_{12}$  self-assembly (**Figure 18**). The advantage of this polymer compared with those previous tested is that it did not form large aggregates and the formed vesicles were able to incorporate hemoglobin. In addition to the vesicles, the polymer also formed micelles and rods. Despite the formation of micelles and rods, the main reason why this polymer was not used for further studies

was that there was not enough polymer to proceed with the project.

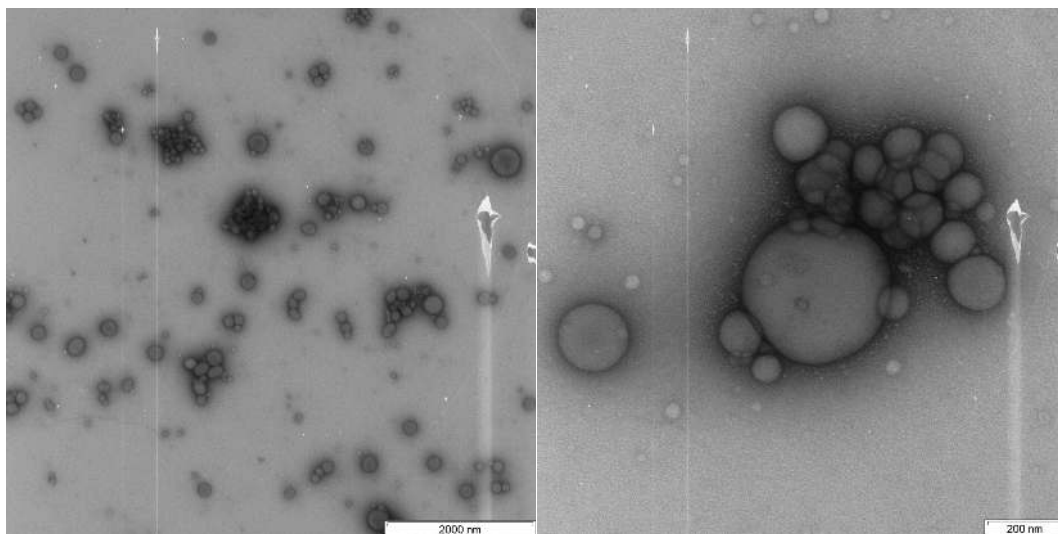


**Figure 18.** TEM images from the  $A_{12}B_{55}A_{12}$  copolymer showing vesicles and micelles.

The polymer tested finally was an  $A_6B_{90}A_6$  block copolymer. The polymer consists of two blocks of six repeating units of PMOXA and 90 repeating units of PDMS. The TEM images of the  $A_6B_{90}A_6$  copolymer showed the most promising results (**Figure 19**). The copolymer has a large hydrophobic block compared to the hydrophilic block. This polymer forms mainly vesicles and some micelles. No rods or aggregates were formed. The solution contained a good amount of vesicles that were large enough to encapsulate a reasonable amount of hemoglobin. The vesicles were larger than those generated by the other polymers. Although all of the polymers used were able to incorporate some quantity of Hb, some polymers, such as the  $A_{10}B_{87}A_{10}$ , could not be used because of the formation of large aggregates. The  $PMOXA_6$ - $PDMS_{90}$ - $PMOXA_6$  polymer has been shown to form a narrow size distribution population in solution. Because of its ability to form mainly vesicles, this polymer was chosen for further research. In addition to the composition of the polymer, the preparation method also has great influence on the formation of vesicles. For the chosen polymer, the vesicles were prepared using two different methods. The first was the film rehydration method. For this, 5 mg of triblock copolymer were dissolved in ethanol and the solution was then evaporated under reduced pressure. The polymer formed a thin film on the walls of a 25 ml round-bottom flask using a rotary evaporator. After the addition of 1 ml PBS buffer to the polymer film and stirring for

2 h, the solution was extruded through polycarbonate membranes (pore diameter = 400 nm) in order to generate vesicles with low size distribution. During the extrusion, the non-dissolved polymer was also removed. Both empty vesicles and protein-containing vesicles were prepared under similar conditions using 5 mg of polymer and PBS buffer. The vesicles were analysed by light scattering (dynamic light scattering, DLS, and static light scattering, SLS) and transmission electron microscopy, TEM. The other method that was used was the co-solvent method. In this method the polymer was dissolved in a small amount of ethanol and then it was added slowly into a buffer solution while stirring. The advantage of this approach is that it provides a more homogeneous vesicle solution than the film rehydration method, while nearly 100% of the polymer used forms vesicles or micelles. The problem with this method was that it only produced micelles and small vesicles with a radius of around 25 nm (**Figure 20**). The vesicles were thus too small to encapsulate Hb. This method was not used for any further experiments.

Not only does the method used have a great influence on the vesicle formation, but the conditions (temperature, stirring time and stirring intensity) during vesicle formation has a great influence on the final result. The different polymers behave differently and their ideal conditions depend strongly on their hydrophilic hydrophobic block ratio. Therefore, vesicle formation was performed under several different conditions in order to find the most suitable one for the requirements of the nanoreactors. For most of the polymers, a long stirring time of more than 8 h was optimal because this gave the polymer more time to self- assemble in order to form vesicles. However, extended stirring time is not always preferable because of the mechanical force that is applied during the stirring process. Therefore, a long stirring time is not ideal if the copolymer has a high hydrophobicity. The polymer used has both a high hydrophobicity and a tendency to clump together and precipitate after extended stirring. The ideal condition for nanoreactor formation was a stirring time of around 2 h at room temperature. One disadvantage of the short stirring time is that only 50% of the polymer forms vesicles or micelles, the rest of the polymer stays on the polymer film on the

bottom of the flask.

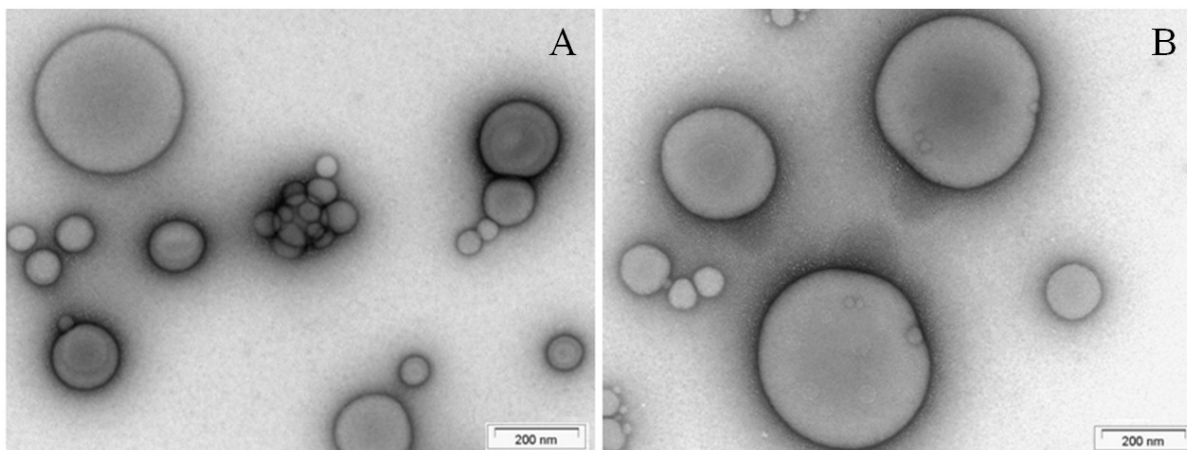


**Figure 19.** TEM images of  $A_6B_{90}A_6$  copolymer of empty vesicles (A), and vesicles with encapsulated methHb (B). Scale bar = 200 nm.

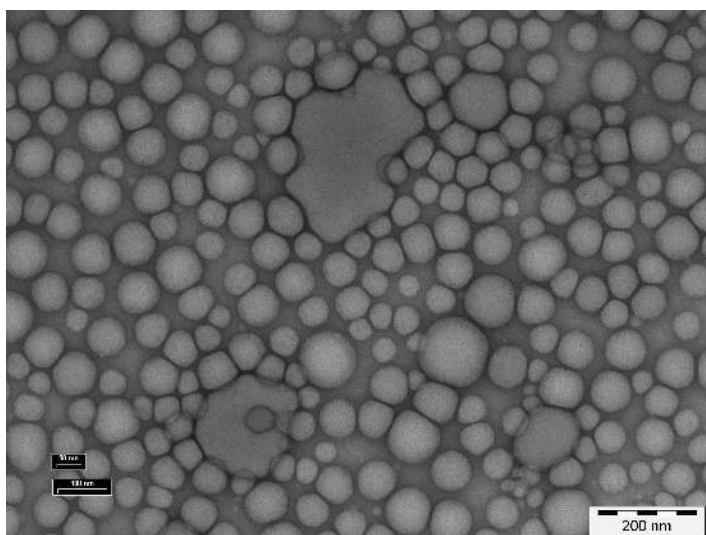


**Figure 20.** TEM images of  $A_6B_{90}A_6$  copolymer micelles that are produced by the co-solvent method.

The  $A_6B_{90}A_6$  copolymer behavior in solution was studied in more detail with DLS/SLS. The measurements were necessary because they provided additional data to characterize nanoreactors in solution.

**Static Light Scattering (SLS).** SLS is a technique that uses the intensities of scattered light at a number of angles to derive information on the nanoobjects in the solution. From light scattering, data on the radius of gyration  $R_g$  and the second virial coefficient  $A_2$  can be derived (**Figure 21**).

104-107

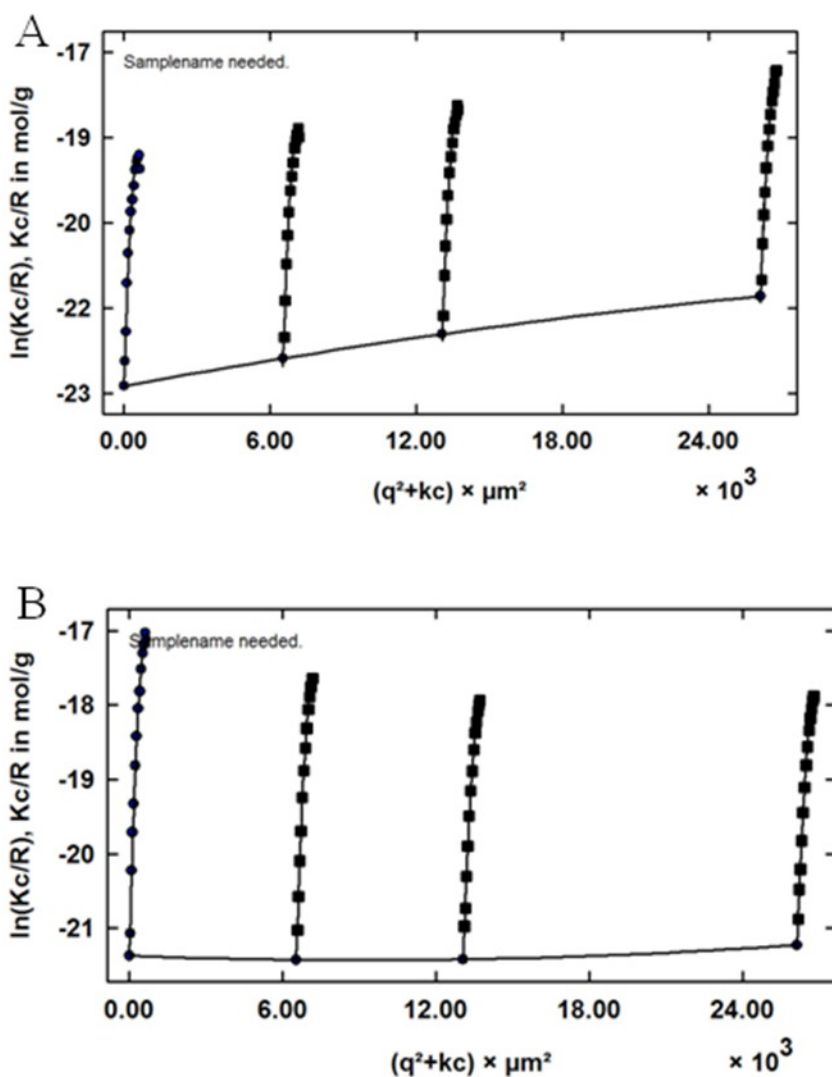


**Figure 21.** Second order fits of SLS data in a Guinier plot of nanoreactors (A) and empty vesicles (B).

**Dynamic Light Scattering (DLS).** Dynamic light scattering uses the concept of small particles moving randomly in solution. Fluctuations in the scattering arise from the fact that small molecules in solution undergo Brownian motion. Brownian motion causes a change in the distance between the scattering objects in the solution. The change in the distance leads to either constructive or destructive interference by the surrounding particles. The information on the nanoobjects is derived from an autocorrelation function of the intensity trace recorded during the experiment (**Figure 22**).

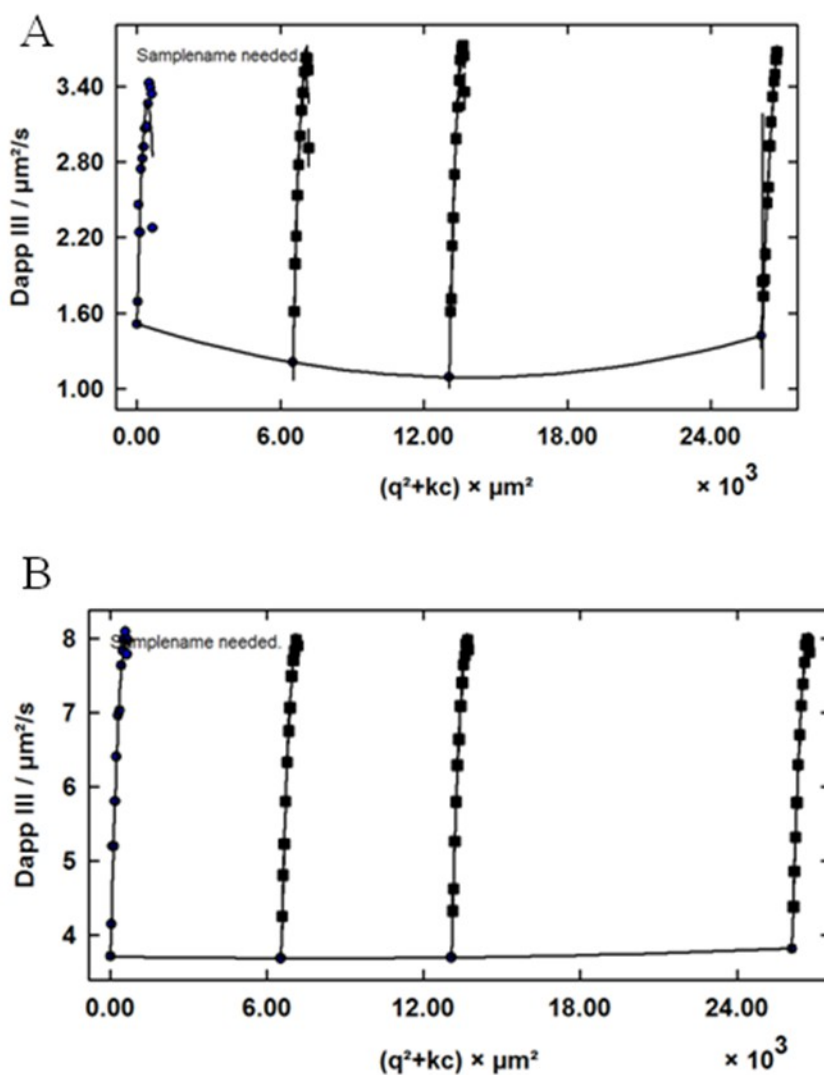


**Figure 22.** Second order fits of DLS by nanoreactors (A) and empty vesicles (B).

The analysis of the samples by DLS and SLS indicates the presence of two different populations of nanoobjects: a small fraction of spherical objects with a hydrodynamic radius ( $R_H$ ) of around 45 nm, and a larger fraction of spherical objects with a hydrodynamic radius of  $R_H = 164 \pm 15.4$  nm. The small  $R_H$  of around 45 nm of the first fraction indicates micelles. The light scattering from the micelles fraction was not as dominant, and the influence of the scattering was therefore not significant. The majority of the scattering occurs from the fraction with the larger  $R_H$  of 164 nm. The analysis of the samples by SLS showed that the fraction of the larger spherical objects has a radius of gyration  $R_g$  of  $194 \pm 8.2$  nm. In order to analyze whether this population consists of vesicles, the ratios of the hydrodynamic radius  $R_H$  and the radius of gyration  $R_g$  were compared as



$R_H/R_g = 0.84$ . A value of 0.84 indicates that the major population consists of spherical vesicles. In order to analyze whether the encapsulation of metHb has an influence on vesicle formation, the DLS and SLS data of empty vesicles and vesicles that contain metHb were compared. A comparison of the DLS data shows that the presence of metHb does not influence vesicle formation. Therefore, there is no interaction between the polymer and the metHb. The samples were also analyzed by Transmission Electron Microscopy, TEM. The TEM micrographs indicate the presence of circular objects with a mean radius of around  $28 \pm 8.5$  nm and spherical objects with a mean radius of  $120 \pm 20$  nm. From the small radius of  $28 \pm 8.5$  nm of the first fraction, we assume them to be micelles. The fraction of spherical objects with a mean radius of  $120 \pm 20$  nm was expected to be vesicles. The higher value  $R_H$  obtained by LS experiments as compared to the size of the vesicles estimated from the TEM micrographs was expected. The higher value from DLS experiments represents the sum of the particle radii and the contribution of the particle's surrounding hydration sphere, whereby the TEM micrographs only show the size of the actual vesicle. The influence of the encapsulation of metHb and the incorporation of OmpF into the polymer membrane were also studied by TEM. TEM micrographs of metHb-containing vesicles or metHb-containing vesicles with OmpF incorporated in the polymer membrane were compared to a solution of empty vesicles and did not show any significant morphological change. This is in good agreement with other protein-polymer nanoreactors based on this type of amphiphilic copolymer.<sup>74</sup> The stability of the vesicles was analyzed by measuring the sample again after storage for more than three weeks at 4 °C. The TEM micrographs revealed no significant changes. This suggests that the vesicles prepared from PMOXA<sub>6</sub>-PDMS<sub>90</sub>-PMOXA<sub>6</sub> polymers are mechanically stable.

### **3.2.2 Protein encapsulation efficiency**

The activity of the nanoreactor is affected by the encapsulation efficiency. It is important to have a reasonable number of Hb molecules inside the nanoreactors in order to obtain reasonable reaction efficiency. It is therefore important to know how many Hb molecules are encapsulated inside the

nanoreactors.

In order to quantify the actual amount of Hb that is encapsulated inside the nanoreactors and the remaining free Hb, the sample was further analyzed.

FCS was used to determine whether metHb was encapsulated inside the vesicles or if it was only outside the vesicle. In addition FCS measurements performed after sample purification allowed us to quantify the free Hb ratio and the efficiency of separation. For these measurements, metHb was labeled with the Alexa488 fluorescent dye. The labeling was necessary because the FCS measurements are based on the laser-induced fluorescence of excited fluorescent molecules. The fluorescent labeled Hb molecules are measured when they pass through the confocal volume. The signal is then auto-correlated in time and allows the calculation of the diffusion times. From the diffusion times the size of the vesicle can be calculated, because the encapsulated fluorescent molecule has the same diffusion time as the vesicle. The hydrodynamic radius of the vesicle can be obtained from the diffusion time by the use of the Stokes-Einstein equation. This method has been used for the analysis of fluorescently-labeled proteins in nanovesicles. The labeled Hb was analyzed under free conditions and encapsulated in the nanoreactors. The diffusion time of the Alexa488 dye, the Alexa488 labeled Hb, and the encapsulated Alexa488-labeled metHb in polymer vesicles were measured. The diffusion times of the Alexa488-labeled metHb encapsulated in polymer vesicles was compared to the diffusion time of the free Alexa488-labeled protein.<sup>110</sup> The free Alexa488 dye had a diffusion time of around 26  $\mu\text{s}$ , while the Alexa488-labeled metHb featured a diffusion time of 95  $\mu\text{s}$  (**Figure 23 a and b**). From the diffusion time of 95  $\mu\text{s}$ , the hydrodynamic radius of 2.5 nm for the Alexa488-labeled metHb was calculated. The calculated hydrodynamic radius of Alexa488-metHb was in good agreement with the reported value of 3.1 nm.<sup>111</sup> The analyzed solution contained vesicles and Alexa488-labeled metHb. The obtained data was fitted for several different populations. The best fit that was obtained (**Figure 23 c**), indicating the presence of two fractions with different diffusing times. There is a smaller fraction (2%) with a diffusing time of 95  $\mu\text{s}$  and a

major fraction with an average diffusion time of around 6930  $\mu\text{s}$  (98%). The diffusion time of 95  $\mu\text{s}$  for the smaller fraction indicates that it is the free Alexa488-labeled metHb. The major fraction with a diffusion time of 6930  $\mu\text{s}$  corresponds to vesicles with a calculated hydrodynamic radius of around 170 nm  $\pm$  15 nm. The hydrodynamic radius obtained by the FCS measurements is in good agreement with the LS results. To analyze whether the Hb was encapsulated in the vesicles or whether the Hb was attached to the outside of the vesicle, Hb was added in the same concentration as used for the nanoreactor preparation, to a vesicle solution that contained no Hb. The diffusion time of the free Alexa488-metHb was not modified by the addition of empty vesicles. This indicates that metHb was not attached to the outside of the polymeric membrane of the vesicles.

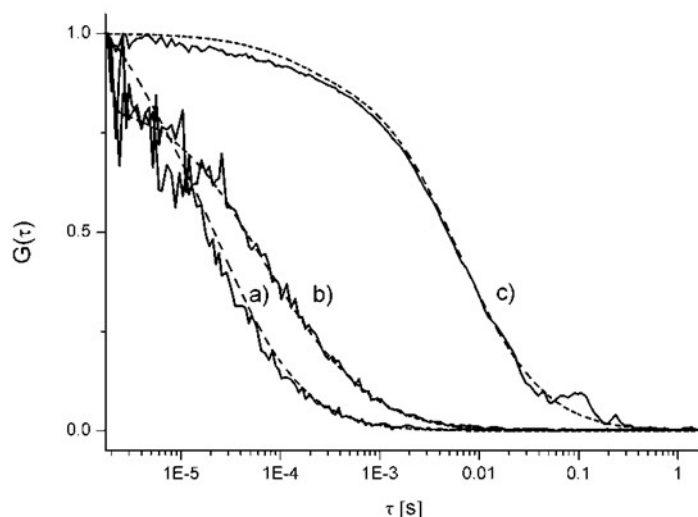


**Figure 23.** Autocorrelation function of free Alexa488 (a), Alexa488- metHb (b), and Alexa488-metHb-containing vesicles (c)

To determine the encapsulation efficiency, we first evaluated the average number of Alexa488 molecules connected to one metHb molecule. The average number was estimated by the UV spectra. For this, the absorption spectra of the Alexa488-labeled Hb in solution was analyzed. The absorption of the Alexa488 was compared to the absorption of the Soret band of metHb. On average, 2.3 dye molecules were attached per metHb molecule. The number of molecules that were encapsulated in the nanoreactor was calculated accordingly.

The number of Alexa488-metHb molecules per vesicle was estimated via brightness measurements.

In this respect, we compared the count rates per molecule (cpm, in kHz) of Alexa488, Alexa488-metHb, and encapsulated Alexa488-metHb.

The free Alexa488 dye has a count rate of around 22.81CPM. It decreases to 14.59 CPM when the dye is attached to Hb molecules. The nanoreactors have an average count rate of 829.45 CPM. The count rate of the nanoreactors depends on the number of encapsulated Hb molecules. The count rate corresponded to an average of 55 molecules of Alexa488 labeled Hb. The number of Alexa488-metHb molecules per vesicle, obtained from brightness experiments (for an initial concentration of metHb of 0.47  $\mu\text{M}/\text{mL}$ ) was then compared to the theoretical number of metHb/vesicle (120 molecules/vesicles), and resulted in an encapsulation efficiency of around 20.6 %.

### **3.2.3 Conclusion: Nanoreactors**

Finding a good polymer that forms vesicles that are able to function as a nanoreactor is difficult. In order to be used for biomedical applications, nanoreactors must fulfill some crucial requirements. The nanoreactor has to be stable for storage; the vesicle solution has to be homogenous and the vesicles should not form large aggregates; the vesicles must be able to encapsulate a reasonable amount of guest, in our case modified Hb; the purification methods must be efficient enough to remove the majority of the non-encapsulated Hb. In this study we showed that nanoreactors made of  $\text{A}_6\text{B}_{90}\text{A}_6$  copolymer could easily be produced using the film re-hydration method. Such nanoreactors are mechanically stable and can be stored for several weeks. The nanoreactors and the empty vesicles did not differ by size or shape, as indicated by TEM or DLS/SLS. That shows that Hb does not interfere with vesicle formation. The polymer mainly forms vesicles and a smaller fraction of micelles, with the vesicles being the dominant species. The polymer did not form aggregates. The obtained vesicles have an average radius of the 120 nm. A well defined vesicle solution was obtained. The FCS data show that the purification method removes nearly all of the non-encapsulated Hb. A good encapsulation efficiency of around 20.6 %, with hardly any free Hb in the solution, was determined.

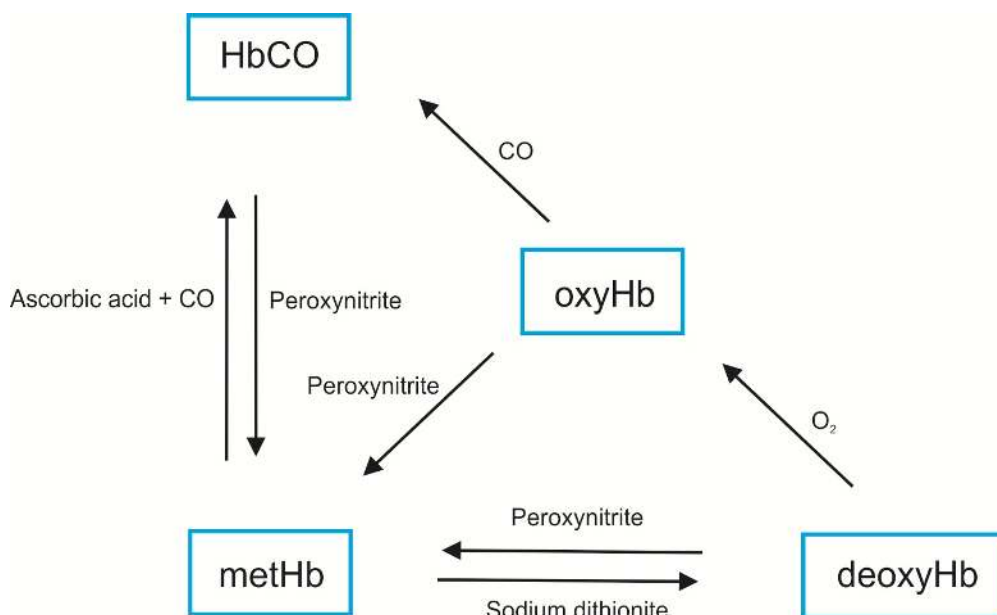
### 3.2.4 Activity studies

For the preparation of nanoreactors it is not only important that the polymer be able to produce stable vesicles, but also that they incorporate Hb. Moreover, the encapsulated, active guest should maintain its function inside the nanoreactor. Therefore, the functionality of the nanoreactor needs to be demonstrated. Thus, one of the key steps in this project was to investigate the activity of the nanoreactor. The activity of the nanoreactor strongly depends on the activity of the encapsulated molecules. One of the major differences between a nanocarrier and a nanoreactor is that the encapsulated molecules must retain their activity inside the nanoreactor, whereas nanocarriers require activity upon release. On the other hand, nanoreactors do not need controlled release of the encapsulated molecule. For every nanoreactor, it is important to investigate the activity of its encapsulated molecules. This study is important in demonstrating that the encapsulation procedure does not damage the hemoglobin. The encapsulation could force a change in the conformation of the hemoglobin that would cause a significant decrease in the activity when encapsulated. Another problem could arise from strong, unspecific interactions with the polymer membrane that could also lead to a decrease in the activity of the hemoglobin inside the nanoreactor. And yet another problem might be that, in order to be functional, the heme pockets of the hemoglobin must still be accessible to the chemicals that have to be detoxified. In our case, peroxynitrite must be able to enter the nanoreactor; otherwise, no detoxification could occur.

The activity was measured by changing the oxidation state of Hb ( **Scheme 2** ). The structural information on the oxidation state was achieved using UV-Vis absorption spectroscopy. The Soret absorption band was examined for metHb, HbCO, HbO<sub>2</sub>, and deoxyHb (**Figure 25 A, right**). The other bands were used only to verify the reactions in the case of protein solution (**Figure 24**). We did not consider the other bands (between 450 nm and 600 nm) because, even if they appear in bulk conditions, they cannot be observed in the conditions of the nanoreactors due to the low concentration of the protein inside nanoreactors. The transition from metHb to deoxyHb was

observed by a shift in the maximum of the Soret absorption band from 405 – to 430 nm (**Figure 25 A right**), while, for metHb to HbCO, the shift was from 405 – to 419 nm. The conversion of deoxyHb to HbO<sub>2</sub> after removal of sodium dithionite excess in the presence of oxygen has been demonstrated by a shift of the maximum of the Soret absorption band from 430 – to 415 nm.<sup>76</sup>

A study of the different oxidation states was not only important to show the activity of the encapsulated hemoglobin, but also to understand what happens on a molecular level. Because the different oxidation states have different activities, it is vital to change the oxidation state in a controlled way. Not all oxidation states have the same activity and therefore it is problematic when hemoglobin transforms into a less active state. MetHb is one of the most stable oxidation states, but it cannot be used for the nanoreactors. MetHb cannot carry oxygen and it is not able to react with peroxynitrite and cannot detoxify it. In the bloodstream there are many substances that prevent HbO<sub>2</sub> and deoxyHb from forming metHb. Without these substances, the HbO<sub>2</sub> and the deoxyHb will transform into the nonreactive metHb state.



**Scheme 2.** Conversion of Hb to different oxidation states in solution and *in situ* inside nanoreactors.

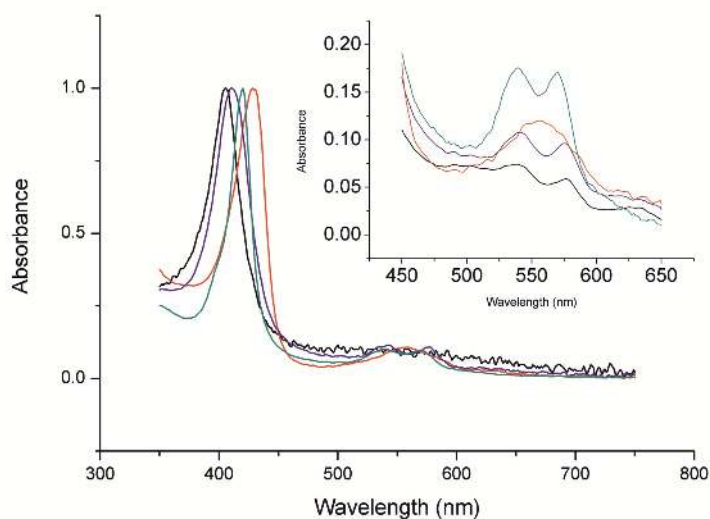


**Figure 24.** UV spectra of metHb (black), HbO<sub>2</sub> (blue), HbCO (green) and deoxyHb (red) at wavelengths between 350 – 750 nm

### 3.2.5 Free Hemoglobin

One major problem in studying the activity of hemoglobin inside nanoreactors is the fact that the hemoglobin concentration inside the nanoreactor is very low. This limits the possibilities for spectroscopic measurements. Another difficulty is that the vesicles scatter light in the area where hemoglobin has the highest absorption, thereby affecting the final results. The redox-reaction of Hb can be best studied in solution. The concentrations of Hb that can be analyzed are much higher and

therefore the signals obtained by the analytic methods, UV/Vis and Raman, are much more reliable. It is possible to observe changes in the spectra that could not be observed with a nanoreactor solution because the signal is too weak. Another advantage is that reaction conditions can be changed. The optimization of the reaction conditions was therefore achieved in bulk solution. The measurements of the redox-reaction with the Hb inside the nanoreactors were carried out in the same condition as in solution. The advantage of the activity measurements in solution is also that the results can be compared with results that are obtained by measuring the activity of hemoglobin inside the nanoreactors. The comparison of the data is also important because it allows predicting the influence of the polymer membrane. The permeability of the polymer membrane also has an influence, because it can act like a barrier to entering molecules which, in turn, react with the molecules inside the nanoreactor.

### **3.2.6 Hemoglobin in nanoreactors.**

After the preparation the nanoreactors were purified. The purification was necessary because most of the Hb present in the solution is not encapsulated in the nanoreactor. It is essential to have a good purification procedure in order to get rid of the majority of the free hemoglobin. The non-encapsulated Hb interferes with the measurements and provides incorrect readings, because the activity measurements show the activity of the whole system and not simply that of the encapsulated hemoglobin. Therefore, it is important to reduce the amount of nonencapsulated Hb to a level where it does not have a significant impact. The nonencapsulated Hb was removed by SEC as mentioned previously. The amount of nonencapsulated Hb was estimated using FCS measurements. The remaining, nonencapsulated Hb was minimal (2%), so it had no impact on the next measurements. Moreover, the purification method did not decrease the amount of nanoreactors obtained.



### 3.2.7 Characterisation of nanoreactors reactivity

In contrast to the characterisation of the nanoreactors performed by TEM, DLS, and FCS, the estimation of the activity of the encapsulated Hb is more difficult. A major drawback to the investigation of nanoreactor activity was their low concentration and the limited amount of encapsulated Hb that was available. The limited amount of Hb significantly reduced the variety of analytical methods that could be used to investigate the activity of the nanoreactor. Therefore, Raman spectroscopy could not be used for the analysis of the oxidation state of Hb in nanoreactors. (The main analysis methods are based on absorption measurements in the UV region.)

The ability to change the oxidation state is crucial for the two key functions of the nanoreactor.

We chose to start with metHb, due to its stability and availability, and to convert it *in situ*, inside the nanoreactors, to deoxyhemoglobin (deoxyHb) and carbonmonoxyhemoglobin (HbCO), respectively, followed by the inverse reaction in the presence of peroxynitrites. Previous studies have shown that peroxynitrite is degraded by the conversion reaction of HbO<sub>2</sub> to metHb. The conversion to different oxidation states of hemoglobin was studied with spectroscopic techniques, both in bulk and inside nanoreactors. The conversion reactions in bulk served to optimize the reaction conditions previous to the encapsulation.

In order to obtain different oxidation states of hemoglobin, several different methods to convert metHb to HbO<sub>2</sub>, and to deoxyHb, and to HbCO(**Figure 24**) have been used.

### 3.2.8 Reducing agents

Because metHb has the highest oxidation state, there is always the need to use a reducing agent to convert metHb to a different oxidation state. The first reducing agent used was ascorbic acid. Ascorbic acid is present in the blood stream and is one of the natural reducing agents for Hb. The problems with ascorbic acid are that it is not ideal for reducing metHb, because it is not strong enough to reduce metHb by itself. Ascorbic acid has to be used in combination with other

substances to reduce metHb. It is also not possible to achieve every oxidation state of Hb with ascorbic acid as the reducing agent. In order to achieve the more relevant oxidation states such as HbO<sub>2</sub> and deoxyHb, another reducing agent has to be used. The second problem with ascorbic acid is that ascorbic acid is too big to penetrate the polymer membrane of the nanoreactor. It therefore needs tunnel proteins such as OmpF to enter the nanoreactor. Because of these problems with ascorbic acid, sodium dithionite was used as a reducing agent. Sodium dithionite is a stronger reducing agent than ascorbic acid. Another advantage of sodium dithionite is that it can penetrate the polymer membrane without the help of tunnel proteins. Sodium dithionite is strong enough to reduce metHb to deoxyHb when sodium dithionite is added.

The problem with sodium dithionite is that it is not stable in aqueous solution. Thus, an excess of sodium dithionite had to be added to the metHb solution to completely reduce it to deoxyHb. Sodium dithionite is also a reactive species that can interact with the Hb. Therefore, if excess sodium dithionite was not removed, a precipitate was observed after 10 min.

### **3.2.9 Reduction of free Hb**

#### **3.2.9.1 Reduction of metHb to HbCO**

The first experiment was to test the activity of the Hb. It was converted from metHb to HbCO. This experiment showed the activity of the Hb in terms of the redox-reaction and in terms of the ability to bind carbon monoxide in order to investigate the binding affinity of HbCO. That showed the ability of Hb to form complexes. The ability to form complexes is also important for gas transportation.

The first oxidation of metHb was performed by adding ascorbic acid to the metHb solution and then flushing it with carbon monoxide in order to produce HbCO. Previous experiments have shown that the reduction only occurs when both ascorbic acid and carbon monoxide are present. Ascorbic acid alone is not strong enough to completely reduce the metHb. And carbon monoxide is not able to

bind to metHb. In experiments where only one of these substances was present, no change in the UV spectra was observed. The Soret band was shifted from 405 nm to 418 nm. In this reaction, two things happened. The metHb was reduced by ascorbic acid and a complex with carbon monoxide was formed. When the solution was flushed for a long time, the formation of precipitate was observed. MetHb can also be converted to HbCO by adding sodium dithionite and then flushing the solution with carbon monoxide.

### **3.2.9.2 Reduction of metHb to deoxyHb**

The reduction of metHb to HbCO showed the activity of the Hb. But HbCO is not a reactive species that can be used for the transport of oxygen. In order to reduce metHb to an oxidation state that can bind oxygen, metHb was reduced to deoxyHb. DeoxyHb was obtained by adding an excess of sodium dithionite to a metHb solution. The reduction was observed by a change in the UV spectra; the Soret band was shifted from 405 nm to 430 nm.

### **3.2.9.3 Reduction of metHb to HbO<sub>2</sub>**

An oxygen carrier has to be able to bind oxygen. The oxygen binding can be shown by the formation of HbO<sub>2</sub>. HbO<sub>2</sub> is the oxidation state of Hb in which oxygen is bound to the heme group. The oxidation of metHb to HbO<sub>2</sub> was more difficult, because there was no direct way to reduce metHb to HbO<sub>2</sub>. MetHb was first reduced to deoxyHb by addition of sodium dithionite. The excess of dithionite was then removed by SEC. The solution was then exposed to air. The oxygen from the air binds to the deoxyHb to form HbO<sub>2</sub>. The formation of HbO<sub>2</sub> was confirmed via UV spectroscopy by a peak shift from 430 nm to 415 nm. The oxidation from deoxyHb to HbO<sub>2</sub> was not observed when the excess of dithionite was not removed. In a second experiment the procedure was repeated in the absence of oxygen. The buffer solution was flushed with argon to remove the oxygen. In this experiment no HbO<sub>2</sub> formation was observed.

#### 3.2.9.4 Reduction from HbO<sub>2</sub> to deoxyHb

For an oxygen carrier, not only is the uptake of oxygen important, it is also important to release oxygen. HbO<sub>2</sub> can be reduced to deoxyHb by releasing the oxygen. In HbO<sub>2</sub> the oxygen is bound to the heme group by a complex bond. The oxygen binding to the Hb is reversible. HbO<sub>2</sub> can be converted to deoxyHb by removing the oxygen. The oxygen was removed from the Hb with a vacuum. The formation of deoxyHb was confirmed via UV spectroscopy by a peak shift from 415 nm to 430 nm. By exposing the deoxyHb solution to air the deoxyHb was converted back to HbO<sub>2</sub>. HbO<sub>2</sub> can also be reduced to deoxyHb by adding sodium dithionite.

#### 3.2.9.5 Conversion of HbO<sub>2</sub> to HbCO

In addition to the reduction of HbO<sub>2</sub> to deoxyHb, the release of oxygen can also be shown by the conversion from HbO<sub>2</sub> to HbCO. HbO<sub>2</sub> was converted to HbCO by flushing with carbon monoxide. The oxygen was replaced by carbon monoxide, which forms more stable complexes with Hb than oxygen. This experiment demonstrates that the oxygen of the HbO<sub>2</sub> can be removed and be replaced with carbon monoxide. This is important because it shows that oxygen can be released in a controlled way. The formation of HbCO was confirmed via UV spectroscopy; by a peak shift from 415 nm to 430 nm.

#### 3.2.9.6 Raman spectra

In addition to UV-Vis spectroscopy, complementary structural information was obtained using Raman absorption spectroscopy. The samples for the Raman measurement were prepared in the same way as the samples for UV-Vis measurements.

Raman spectra of the different oxidation states of Hb within the frequency range 1300 – 1900 cm<sup>-1</sup> were recorded (**Figure 25 A left**). The Raman spectra agree with the spectra already reported in the literature, and the main peaks have been indexed accordingly.<sup>112-115</sup> The changes in the Raman spectra are associated with conformational changes of Hb. These changes are caused by the binding

of ligands such as oxygen, carbon monoxide or by electron transfer. We focused on the bands between 1300 and 1400  $\text{cm}^{-1}$  and the region within 1500 and 1650  $\text{cm}^{-1}$ . The bands between 1300 and 1400  $\text{cm}^{-1}$  are named oxidation state marker bands, and the bands between 1500 and 1650  $\text{cm}^{-1}$  are named spin state marker bands.<sup>113</sup> These bands are described in literature as the best suited to identify the different oxidation states. The change in the oxidation states of Hb can be observed by a unique spectral shift of the relative intensities and positions of the peaks.<sup>115</sup> When metHb is converted to deoxyHb or HbCO, a change in the Raman peak intensity occurs in the spin state marker band region. In both spectra of deoxyHb and HbCO the intensity of the peaks at 1555 and 1610  $\text{cm}^{-1}$  increased. Therefore, the major peaks in the Raman spectrum of HbCO are largely similar to the major peaks of the deoxyHb spectra.<sup>116</sup> The formation of HbO<sub>2</sub> could not be observed by Raman spectroscopy. The samples that showed HbO<sub>2</sub> in UV measurements showed deoxyHb in the Raman spectra. This is due to the rapid dissociation of HbO<sub>2</sub> to deoxyHb, as already reported.<sup>117</sup> The Raman spectra were used to confirm the oxidation state of the Hb in bulk conditions. But the Raman spectra could not be used for the analysis of Hb inside nanoreactors, because of the low concentration of Hb.

Although the total Hb concentration used for nanoreactor preparation was close to 30  $\mu\text{M}$ , the overall protein concentration in solution after purification was only 100 nM. That concentration was far below the Raman detection limit of 10  $\mu\text{M}$ . In addition to the limited concentration of Hb, Rayleigh scattering from the 200 – 300 nm-size vesicles interfered greatly with spectra acquisition. Several efforts were made to overcome the concentration limitations, such as vesicle solution concentration by centrifugation. The signal can also be increased by the co-encapsulation of silver nanoparticles. This allows the detection of single hemoglobin molecules in the presence of silver nanoparticles, which have the role of enhancing the weak Raman scattering signal of the molecules absorbed on the metal surface, and this enhancement has previously been reported.<sup>118</sup> The problem with this method is that silver nanoparticles perturb the conformation of hemoglobin's heme pocket.

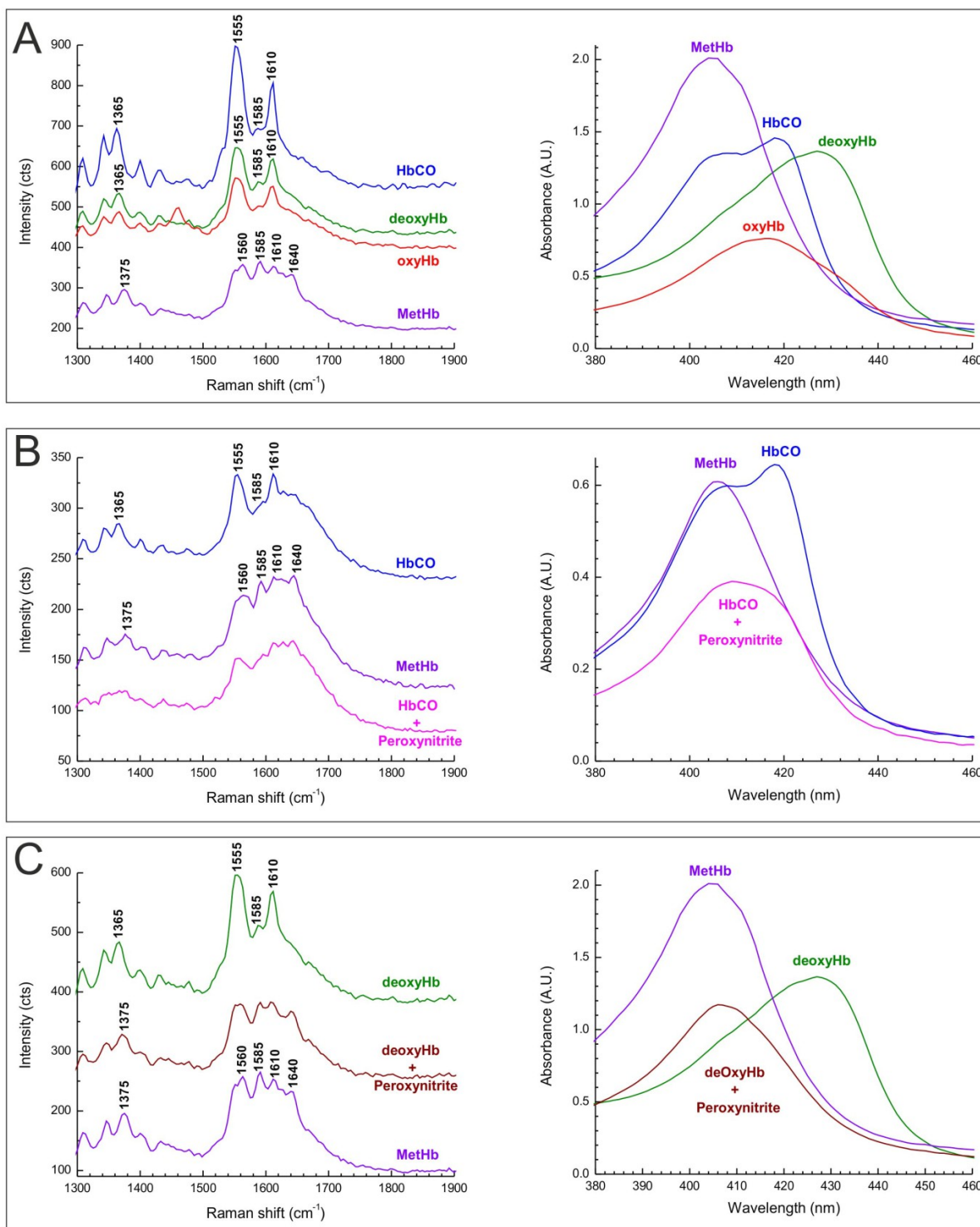


**Figure 25.** A) Raman spectra (left) for 50  $\mu\text{M}$  metHb, deoxyHb and HbCO excited at 532 nm and the corresponding UV-Vis absorption spectra (right). B) Raman spectra and corresponding UV-Vis absorbance for 20  $\mu\text{M}$  metHb, HbCO and HbCO in the presence of 40  $\mu\text{M}$  peroxynitrite, and C) 50  $\mu\text{M}$  metHb, deoxyHb and deoxyHb in the presence of 540  $\mu\text{M}$  peroxynitrite.

### **3.2.10 Reduction of Hb in Nanoreactors.**

After the studies of Hb in solution, the redox-reactions were repeated with a nanoreactor solution. The reactions were done in the same manner and under the same conditions as the experiments in bulk conditions. Only the amount of reducing agents was lowered, in order to have the same ratio as under bulk conditions. The results were compared with the results from the redox-reactions in solution.

#### **3.2.10.1 Reduction of metHb to HbCO**

The oxidation of metHb was performed by addition of ascorbic acid to the nanoreactor solution and it was then flushed with carbon monoxide in order to produce HbCO. The experiment was done with nanoreactors that contain OmpF in their membranes, and with nanoreactors without OmpF incorporated in their membranes. UV measurements showed that, for nanoreactors without OmpF, no reaction occurred; the Hb encapsulated in nanoreactors remained unchanged as MetHb. The reason for this is that ascorbic acid is not able to penetrate the polymer membrane of the nanoreactor. When the nanoreactor contains OmpF, the ascorbic acid can enter the nanoreactor through the OmpF tunnel protein. In the experiment with the OmpF-containing nanoreactors the formation of HbCO was observed, due to the presence of ascorbic acid. This proves that OmpF is incorporated in the polymer membrane (**Figure 26**). The experiment also showed that all of the Hb is encapsulated in the nanoreactor. Otherwise, the ascorbic acid would have reacted with the free Hb, and the formation of HbCO would have been observed in both experiments. HbCO could also be obtained by using sodium dithionite instead of ascorbic acid. The difference is that sodium dithionite is able to penetrate the polymeric membrane of the nanoreactor. In that case it makes no difference if the hemoglobin is encapsulated or not.

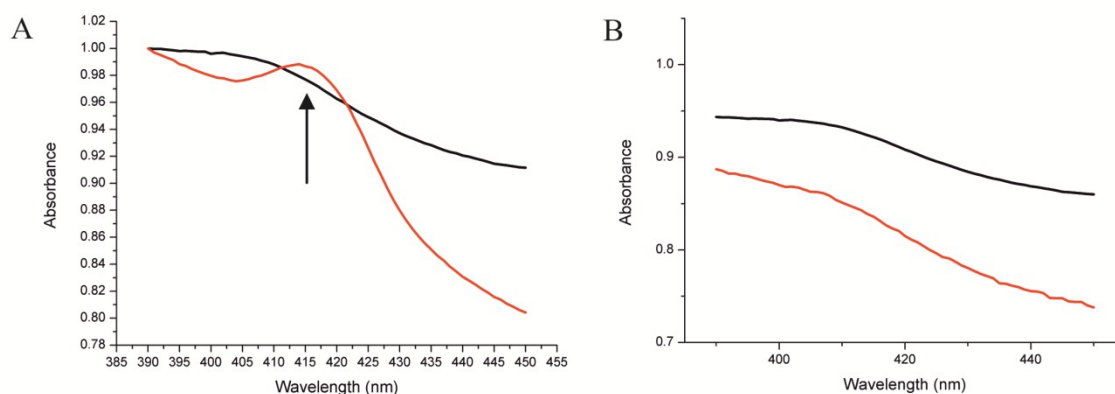


**Figure 26.** A. Normalized UV-Vis spectra of metHb-containing nanoreactors with OmpF inserted in the membrane: before (black), and after flushing the solution with carbon monoxide (red). B. UV-Vis spectra of metHb-containing nanoreactors without OmpF inserted in the membrane: before (black), and after flushing with carbon monoxide (red).

### 3.2.10.2 Reduction of metHb to deoxyHb

The reduction of metHb to deoxyHb can be performed in the same manner as under free conditions by addition of sodium dithionite. This reaction is fast and leads to a complete reduction of the metHb. The conversion can be observed by a peak shift from 405 to 430 nm. Since sodium dithionite is used for this reaction, there is no need to incorporate OmpF in the polymeric membrane. The same problem that occurs in free solution also occurs in nanoreactors. The problem is that an excess of sodium dithionite has to be used in order to convert metHb to deoxyHb. If the excess of sodium dithionite is not removed from the solution, the nanoreactors precipitate.

### 3.2.10.3 Conversion of metHb to HbO<sub>2</sub>

For the conversion of metHb to HbO<sub>2</sub>, metHb had to be reduced to deoxyHb first. This was done in the same way as in the previous reactions. Therefore, an excess of sodium dithionite was also added to the metHb solution. For the oxidation from deoxyHb to HbO<sub>2</sub> the excess of sodium dithionite had to be removed. The removal of the sodium dithionite from a nanoreactor solution was difficult. The problem was that, after the purification step, where the free Hb is removed, the Hb concentration in the nanoreactor solution is very low. A second purification where the excess of



sodium dithionite is removed would even further decrease the Hb concentration. Therefore, the sodium dithionite was added to the nanoreactor solution before the purification. The excess of sodium dithionite and the non-encapsulated Hb were removed at the same time. After the removal of the excess of dithionite the deoxyHb reacted with the oxygen present in the buffer to form HbO<sub>2</sub> (**Figure 27**). If a degassed buffer was used for the purification, deoxyHb did not convert to HbO<sub>2</sub>.

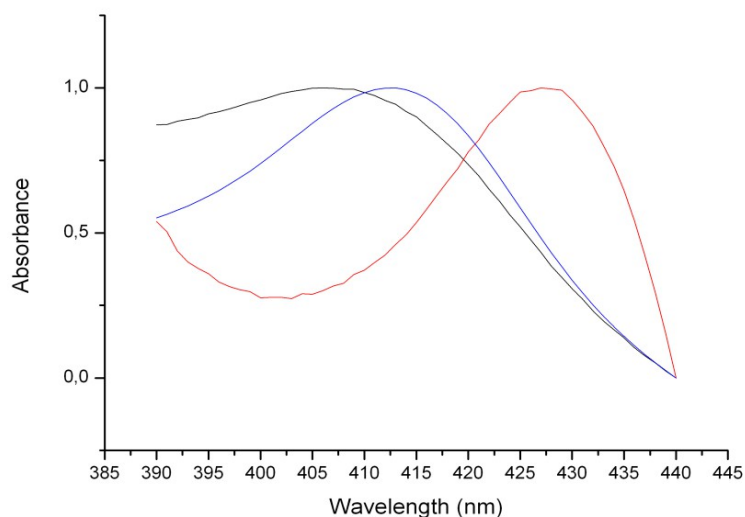


**Figure 27.** UV spectra of metHb-containing nanoreactors: before addition of sodium dithionite (black), after addition of sodium dithionite in excess (red), and after removal of sodium dithionite excess (blue).

### 3.2.10.4 Conversion of HbO<sub>2</sub> to HbCO

One requirement for oxygen carriers is that the oxygen can be released from the nanoreactor in a controlled way. In order to prove that oxygen is released from the nanoreactor, the oxygen bound to the encapsulated HbO<sub>2</sub> was removed. The oxygen was removed by flushing the nanoreactor solution with carbon monoxide. Carbon monoxide binds to the Hb and replaces the oxygen. The prepared HbO<sub>2</sub> solution was converted to HbCO by flushing with carbon monoxide for 10 min. The oxygen was replaced by carbon monoxide that forms more stable complexes with Hb than oxygen. The reaction was observed by a peak shift from 415 nm to 419 nm.

### **3.2.10.5 Reduction from HbO<sub>2</sub> to deoxyHb**

The reduction from HbO<sub>2</sub> to deoxyHb was another experiment that was conducted in order to show that oxygen can be removed from the encapsulated Hb in a controlled way. The aim was to reduce HbO<sub>2</sub> to deoxyHb by removing the oxygen with a vacuum. This was successfully done under bulk conditions. But the concentration of Hb in the nanoreactor solution is extremely low; therefore, it was not possible to remove enough oxygen from the solution to convert a significant amount of HbO<sub>2</sub> to deoxyHb.

### **3.2.11 Conclusion: metHb Reduction**

The reduction of metHb to the different oxidation states can be achieved in nanoreactors in a similar way as under free conditions. The reduction of metHb with ascorbic acid and carbon monoxide is different from the other reducing procedures. This reaction requires that OmpF be incorporated in the polymeric membrane of the nanoreactor. If sodium dithionite is used instead of ascorbic acid, the conversion can be done without the incorporation of OmpF in the polymer membrane, because sodium dithionite is able to penetrate the polymer membrane. Sodium dithionite also reacts fast with the encapsulated Hb and reduces it to deoxyHb. The metHb can be easily converted to deoxyHb and HbCO. Having it convert to HbO<sub>2</sub> was a bit more difficult, because of the low concentration of the Hb in the nanoreactor solution. The low concentration of the nanoreactor solution made it more difficult to remove the excess of sodium dithionite by SEC. It was shown that the hemoglobin inside the nanoreactor can be reduced to an active oxidation state. Therefore, encapsulated Hb retained its functionality unaffected.

The biggest problem in converting Hb in nanoreactors to the different oxidation states is the low concentration of the Hb in the nanoreactor solution. That reduces the stability with regard to reactive species such as sodium dithionite. That could reduce the amount of intact Hb to a level at which it cannot be detected. That also happened when the nanoreactor solution was flushed

extensively with carbon monoxide or oxygen. Thus, the reaction conditions have to be chosen carefully to get a complete conversion without destroying the Hb inside the nanoreactors. Another problem was the limited amount of nanoreactor solution that was available. This makes a concentration of the nanoreactors through centrifugation nearly impossible. Even the concentrated nanoreactor solution contained so little Hb that it was not suitable for most of the experiments.

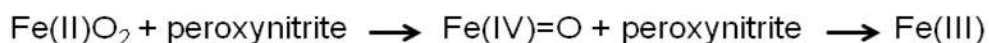
With the right reaction conditions the encapsulated Hb was able to be reduced to every oxidation state with only minimal losses.

### 3.2.12 Peroxynitrite degradation

One of the main functions of the nanoreactors is the degradation of peroxynitrite. The degradation of peroxynitrite occurs when the peroxynitrite reacts with the encapsulated Hb. Therefore, the reaction between the peroxynitrite and the different oxidation states of Hb were studied.

In this reaction the Hb is oxidized and the peroxynitrite is then degraded. The previous studies on the reduction of metHb to an active oxidation state are important for the study of the reaction with peroxynitrite. The reaction of peroxynitrite with different oxidation states was studied extensively.

We chose to start with metHb because of its stability and availability, and its ability to be converted *in situ*, inside the nanoreactors, to deoxyHb and HbO<sub>2</sub>. Previous studies showed that peroxynitrite is degraded by the conversion reaction of HbO<sub>2</sub> to metHb via the corresponding oxoiron(IV) of the hemoglobin protein (**Scheme 3**).



**Scheme 3.** Peroxynitrite degradation by the conversion reaction of oxyHb (Fe(II)O<sub>2</sub>) to metHb (Fe(III)).

We studied the reaction of peroxynitrite with the different oxidation states of hemoglobin. The experiments were performed in solution, and inside nanoreactors (**Figure 28**). The conversion reactions of free hemoglobin in solution served to optimize the conditions previous to the encapsulation.

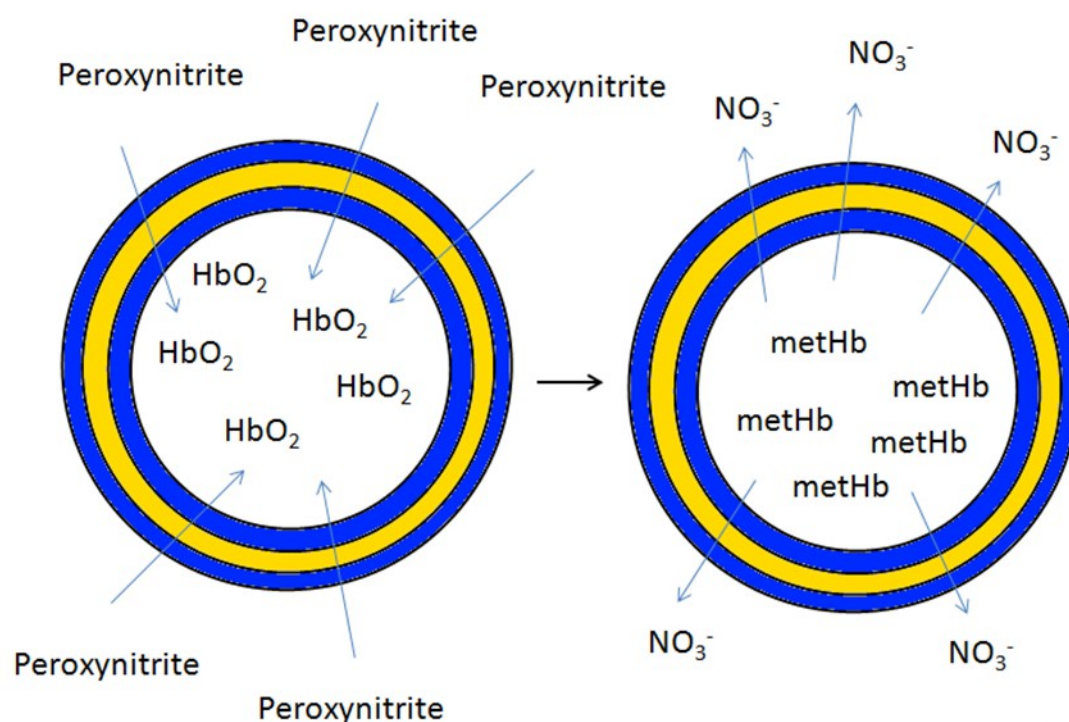


**Figure 28.** Schematic representation of the degradation of peroxyntirite with the use of nanoreactors.

### 3.2.13 Oxidation of deoxyHb, HbO<sub>2</sub> and HbCO

In free solution the previously prepared deoxyHb was converted back to metHb by adding an excess of peroxyntirite to the deoxyHb solution. The conversion was observed by a peak shift in the UV spectra from 430 nm to 405 nm as well as by a change in the Raman spectrum. For a complete conversion, an excess of peroxyntirite was required. The reaction of HbO<sub>2</sub> with peroxyntirite was similar to the reaction of peroxyntirite with deoxyHb. There was also a peak shift in the UV spectra from 415 nm to 405 nm and a change in the Raman spectrum was observed. In addition to the two oxidation states that were important for the function of the nanoreactor, HbCO was also oxidized with peroxyntirite. This conversion was observed by a peak shift in the UV spectra from 419 nm to 405 nm and by a change in the Raman spectrum. All of the different oxidation states were able to be converted to metHb by adding peroxyntirite.

After the experiments had been done under free conditions, they were also been done in

nanoreactors.

In nanoreactors, deoxyHb was converted back to metHb by adding an excess of peroxynitrite. DeoxyHb was oxidized rapidly by the addition of peroxynitrite. Experiments with nanoreactors that did not contain OmpF showed that peroxynitrite is able to pass through the polymeric membrane without the need for tunnel proteins. In addition to deoxyHb, HbO<sub>2</sub> was also converted back to metHb by addition of an excess of peroxynitrite (**Figure 29**). HbO<sub>2</sub> was oxidized rapidly after the addition of peroxynitrite. HbCO was also converted back to metHb by the addition of an excess of peroxynitrite. The reaction between peroxynitrite and the different oxidation states of Hb is a redox-reaction, where the peroxynitrite is reduced and the different oxidation states of Hb are oxidized. Hb is oxidized to metHb because it is the highest oxidation state. The oxidation to metHb was observed by a peak shift in the Soret band to 405 nm under free conditions and 408 nm in nanoreactors. The slight shift of the maximum of the absorption band of metHb from 405- to 408 nm was already observed when metHb was encapsulated in a silica matrix<sup>123</sup> or immobilized on a glass surface.<sup>124</sup> The degradation of peroxynitrite can be observed by a reduction of the peak at 302 nm. The problem with the observation of the peroxynitrite degradation is that peroxynitrite degrades fast. This happens especially under acidic or neutral conditions, and peroxynitrite is also unstable at higher temperatures. Because the concentration of Hb in the nanoreactor solution is really small, it is best to not monitor the change at 302 nm; instead, the change in the absorption peak characteristic for deoxy-Hb should be quantified.

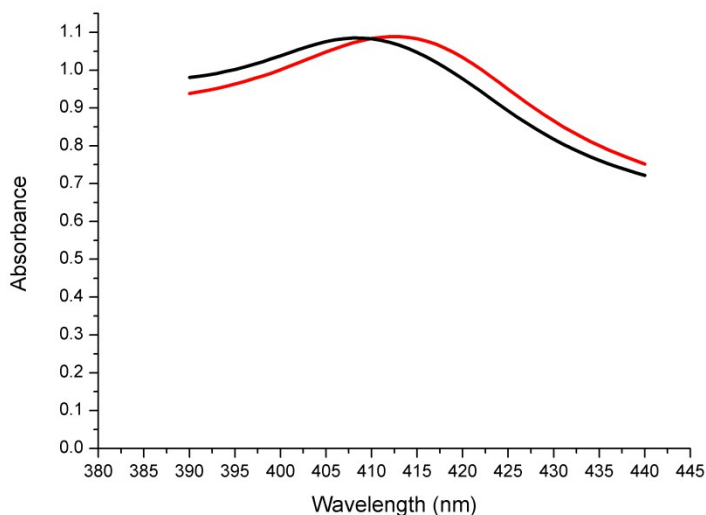


**Figure 29.** UV spectra of HbO<sub>2</sub>-containing nanoreactors before (black), and after addition of peroxynitrite (red).

### 3.2.14 Hb extracted from fresh blood

In our experiments, commercially available lyophilized blood was used to form nanoreactors.

In order to analyze the activity of the commercially available lyophilized blood, the commercial Hb was compared to a sample of freshly extracted blood. The main oxidation state of the Hb in fresh blood is HbO<sub>2</sub>. This was compared with the HbO<sub>2</sub> that was produced by oxidation of metHb. The fresh Hb was also converted to deoxyHb by the addition of sodium dithionite as well as converted to metHb by the addition of peroxynitrite. The freshly extracted Hb reacted similarly to the commercially available lyophilized blood sample.

### 3.2.15 Conclusion: Peroxynitrite degradation

The reactions of the encapsulated Hb with the peroxynitrite in nanoreactors were in good agreement with the experiments that were conducted under bulk condition. The peak shifts of the Soret band that were observed under bulk conditions were also observed in the nanoreactors, while the peak shifts in the other regions could not be observed because of the low Hb concentration. All of the oxidation states except for metHb showed a reaction with the peroxynitrite – under free conditions

as well as in nanoreactors. It was shown that peroxynitrite reacts with the encapsulated Hb and is therefore degraded. In this reaction, Hb is oxidized and the peroxynitrite is degraded. These reactions were important to verify the function of the nanoreactors. Peroxynitrite is also able to pass through the polymeric membrane without the need for tunnel proteins. Peroxynitrite reacts fast with the encapsulated Hb and oxidizes it to metHb. All oxidation forms were able to be completely oxidized to metHb, which shows that all of the encapsulated Hb was active. It was shown that the behavior of Hb encapsulated in nanoreactors was not different to the Hb in free solution. That proves that the nanoreactors have the ability to degrade peroxynitrite. These experiments also showed that the previous reduction methods are reversible.

### **3.2.16 Kinetics of peroxynitrite degradation**

Using UV and Raman spectroscopy, the change in the Hb oxidation state could be shown both under free conditions and inside the nanoreactors. That is why the two spectroscopic methods can be employed to study how the polymeric membrane of the nanoreactor influences the Hb reaction kinetics. The UV spectra are not adequate to prove that an Hb encapsulating nanoreactor degrades peroxynitrite fast enough. Kinetic data were required to show how fast peroxynitrite was degraded inside the nanoreactors. If the encapsulation of Hb in nanoreactors reduces the activity of the encapsulated Hb too much, then it does not fulfill the purpose of peroxynitrite degradation. In order to distinguish the mechanism of the peroxynitrite degradation, various kinetics studies on hemoglobin, peroxynitrite, and the intermediate species that are involved have been performed.<sup>121</sup> The low concentration of Hb in the nanoreactor solution allowed only the study of the characteristic heme Soret band. Because of this limitation and considering the requirements of the project-related peroxynitrite degradation, we focused on a different approach. This study allowed us to characterize and quantify the activity of hemoglobin-containing nanoreactors, and the overall influence of the polymeric membrane. The study was mainly focused on the formation and degradation of deoxyHb.

In order to follow the reaction inside nanoreactors, we used the wavelength of the absorption maximum of deoxyHb at 430 nm, and not the absorption bands at 586 nm or 609 nm, because of their low extinction coefficients. This limitation prevented us from demonstrating the presence of the ferryl intermediate already proposed by Exner.<sup>121</sup> Despite this limitation, we were able to obtain a rate constant value that fully characterizes the degradation process of peroxyxynitrite mediated by the nanoreactor. Because of the very small difference between the rate constants for the two steps of the reaction, the kinetic studies were performed both with Hb in solution and in nanoreactors. The reaction kinetics was then compared in order to estimate the influence of the polymeric membrane. The first kinetic study was related to the formation of deoxyHb from metHb. By the addition of sodium dithionite to both free metHb and to a solution with nanoreactors containing metHb, the metHb was reduced to deoxyHb.

The absorption from the nanoreactor solution was higher than from the solution containing free Hb, because of light scattering from the nanoreactors. The obtained  $k_{on}$  value for the conversion reaction of metHb to deoxyHb in the case of free Hb ( $4.42 \cdot 10^6 \text{ M}^{-1} \text{ s}^{-1}$ ) was similar to that of encapsulated Hb in the nanoreactors ( $k_{on}$  of  $4.19 \cdot 10^6 \text{ M}^{-1} \text{ s}^{-1}$ ) (**Figure 30 A**). This similarity leads to the assumption that the polymeric membrane does not influence the reaction kinetics. This result was expected because of the permeability of the polymer membrane. In a second experiment, deoxyHb was converted to metHb by the reaction with peroxyxynitrite. This experiment was done by the addition of peroxyxynitrite to free deoxyHb, and to deoxyHb-containing nanoreactors. In this reaction, a decrease in the absorption at the absorption maximum for deoxyHb of 430 nm was observed.

The decrease was observed under free conditions and inside nanoreactors. This indicates that deoxyHb was converted to a different oxidation state. The obtained  $k_{on}$  value of  $2.75 \cdot 10^4 \text{ M}^{-1} \text{ s}^{-1}$  for free Hb in solution was also similar to the  $k_{on}$  value of  $2.28 \cdot 10^4 \text{ M}^{-1} \text{ s}^{-1}$  (**Figure 30 B**) for Hb inside nanoreactors. The values were also in good agreement with the values previously reported for this reaction in free human Hb solution ( $2.9 \times 10^4 \text{ M}^{-1} \text{ s}^{-1}$  for an Hb concentration of  $3.0 \text{ } \mu\text{M}$ ).<sup>122</sup> In



addition, the peroxynitrite degradation inside red blood cells (RBC), mediated by oxyHb present at a 5 mM concentration, has a rate constant  $k_{on}$  of  $1.7 \times 10^4 \text{ M}^{-1} \text{ s}^{-1}$  at  $37^\circ\text{C}$  and pH 7.4,<sup>127</sup> which is on the same order of magnitude as the rate constant that we obtained both for free Hb and for the nanoreactors. Peroxynitrite degradation was also followed at 302 nm, the maximum of the absorbance band for peroxynitrite (**Figure 31**).<sup>75</sup> The kinetic measurements show that Hb is still active inside the nanoreactors.

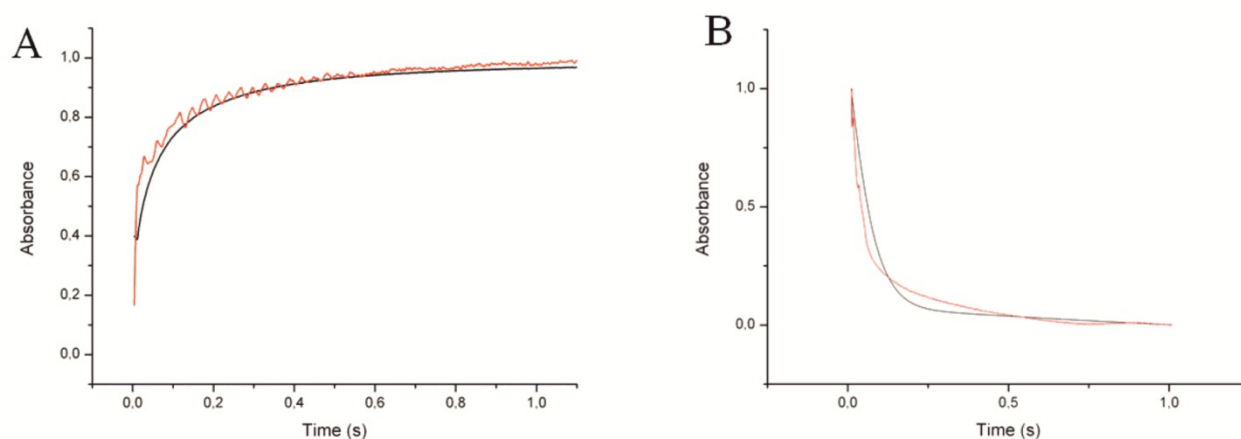


**Figure 30.** A. Normalized trace of the conversion of encapsulated metHb (red) and free metHb (black) with 1 mmol/L sodium dithionite solution. B. Normalized trace of the conversion of encapsulated deoxyHb (red) and free deoxyHb (black) with 10 mmol/L peroxynitrite solution.

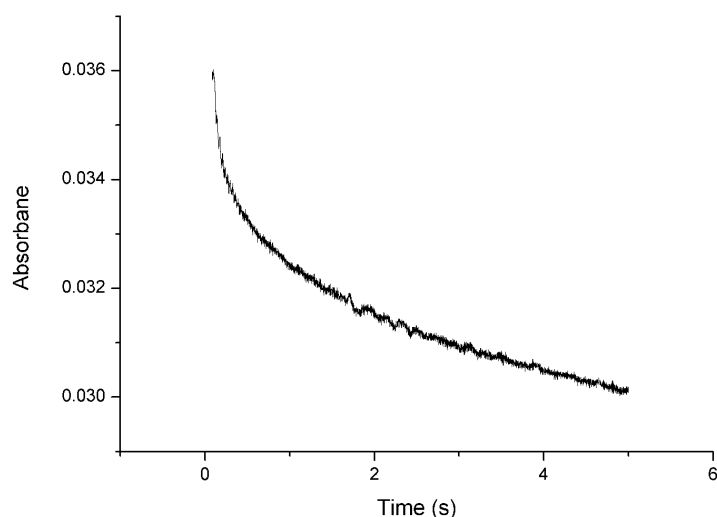


**Figure 31.** The degradation of peroxynitrite was analyzed with stopped flow at a wavelength of 302 nm. The peroxynitrite solution showed a strong degradation with a  $k_{on}$  of  $3.18 \times 10^4 \text{ M}^{-1} \text{ s}^{-1}$  after addition of a deoxyHb solution. These measurements were done with unencapsulated Hb.

### 3.2.17 Oxygen transport

The main advantage of using Hb for detoxification of peroxynitrite is that Hb is well known for its ability to carry oxygen. Therefore, as hemoglobin is the active part of our nanoreactors, we also tested them as oxygen carriers. But there are specific conditions that have to be fulfilled in order to prove that Hb has the ability to carry oxygen. One important condition is the selected oxidation state of the Hb. In the blood stream, HbO<sub>2</sub> and deoxyHb are both present, and deoxyHb is able to take up oxygen while HbO<sub>2</sub> releases oxygen. MetHb is not able to bind oxygen. One of the main problems with hemoglobin-based oxygen carriers is that HbO<sub>2</sub> is rapidly oxidized to metHb when outside of physiological conditions. In the bloodstream, reducing agents such as ascorbic acid are present, preventing Hb from being oxidized to metHb. To avoid metHb formation inside the nanoreactors, previous studies show that various enzymes, such as carbonic anhydrase, catalase, and superoxide dismutase, were co-encapsulated together with hemoglobin.<sup>56</sup> The problem with this approach is that it increases the complexity of the system. This is problematic because the control of the necessary enzyme amount inside the carrier is limited. Therefore, this system is extremely difficult to optimize, especially for medical applications.

The advantage of our system is that it does not require co encapsulation of other enzymes. Our nanoreactors feature the advantage that OmpF can be inserted in the polymer membrane. This allows the free passage for molecules with a mass up to 600 Da into the nanoreactor. Therefore, reducing agents such as ascorbic acid or glutathione, which are present in the plasma,<sup>128</sup> can penetrate through the polymer membrane. These reducing agents support the conversion of metHb to deoxyHb. Therefore, the presence of a co encapsulated enzyme is not required in case the concentration of the reducing agent *in vivo* is sufficient. The nanoreactors can be modified by co-encapsulation of a second biomolecule, for example NADH-cytochrome b<sub>5</sub>, known to reduce metHb in red blood cells.<sup>129</sup>

To establish the oxygen transport ability of Hb, the uptake and release of oxygen was studied in

solution and in nanoreactors. The oxygen uptake was proven by the conversion of deoxyHb to oxyHb. This was demonstrated when a solution of deoxyHb-containing nanoreactors was passed through a column to remove the excess sodium dithionite. This experiment was done under argon and in the presence of oxygen. The sample was then analyzed by UV-Vis. In the experiment that was done in the presence of oxygen, the maximum of the Soret absorption band shifted to 415nm. In the experiment done without oxygen, no peak shift was detected. The peak shift indicated the formation of HbO<sub>2</sub>, and therefore proved that oxygen is binding to the heme pocket of the Hb inside nanoreactors.

The release of oxygen from the Hb-containing nanoreactors was shown by flushing the nanoreactors solution with carbon monoxide. This is a slightly modified approach as compared to that reported by Sakai et al.<sup>130</sup> The carbon monoxide replaces the oxygen that is bound to the heme pocket. After the flushing, a shift in the maximum Soret absorption band was observed. That proves that HbCO was formed both under free protein conditions, and when encapsulated in the nanoreactors (**Figure 32**).

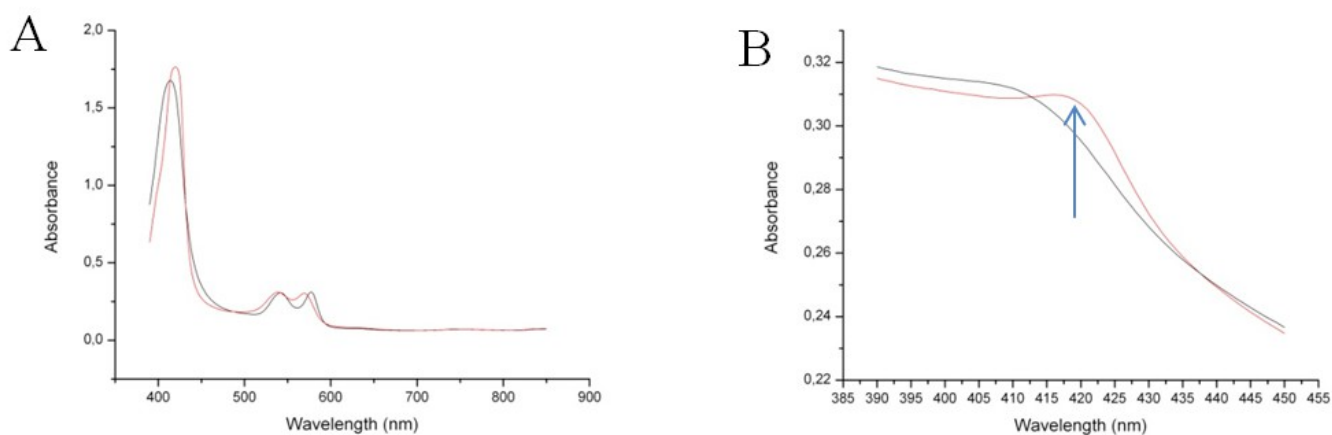


**Figure 32.** A. UV spectra of HbO<sub>2</sub> solution before flushing with carbon monoxide (black), and after flushing with carbon monoxide (red). B. UV spectra in the domain of Soret absorption band of HbO<sub>2</sub> containing nanoreactors, with OmpF inserted into the polymer membrane before flushing with carbon monoxide (black), and after flushing with carbon monoxide (red).

These experiments also showed that oxygen binding is not affected by the width of the polymeric membrane. This is due to the chemical nature of the PMOXA-*b*-PDMS-*b*-PMOXA copolymers, which do not interact with Hb, and to their intrinsic permeability to oxygen species, which does not

limit the penetration of oxygen.

We have proven the functionality of our nanoreactors separately in both the degradation of peroxynitrites and in the transport of oxygen. These processes run inversely in terms of oxygenated Hb species, one inducing their consumption, the other requiring them to be at a stable concentration. Therefore, co-encapsulation of a reducing biomolecule in tandem with Hb favors the oxygen carrier function. The co-encapsulation should be carefully optimized (so as not to obstruct the peroxynitrite degradation function.) Depending on the intended medical application, one or the other of the nanoreactors functions is expected to play the major role.

## 4 General Conclusion

In this thesis, we have introduced the results gathered in two different principal projects. The first project required producing a responsive polymer brush that provides dual-functionality: surface passivation and selective binding sites for specific molecules. In order to create a polymer brush with specific functions, we used a polymer with branched architecture. The advantage of that architecture is the potential for further modification and copolymerization, which allows for the incorporation of specific binding sites for various molecules.

The polymer was successfully synthesized with ARGET ATRP. The polymer was deposited on the surface via the “grafting to” method. The polymer was shown to be efficient in passivation. The surface passivation abilities were confirmed with SPR and QCM. In addition to the passivation, the system also provides many possible binding sites. Antibody binding was demonstrated with SPR. Using this technique, high selectivity was achieved with interesting results in terms of low unspecific binding and high specific binding. In the second project, functional nanoreactors were developed. The nanoreactors have dual-functionality: the detoxification of peroxynitrites and oxygen transport.

The degradation of peroxynitrite and oxygen transport are relevant for medical applications. The peroxynitrite degradation is important, because peroxynitrite is a reactive oxidative species that is involved in various pathologic conditions. In addition, the nanoreactors have the ability to carrier oxygen and to serve as artificial blood. Nanoreactors were formed by the self-assembly of PMOXA-*b*-PDMS-*b*-PMOXA copolymers. Hb was encapsulated in the nanoreactors. Hemoglobin was used as a model protein, because of its ability to provide the dual functionality of transporting oxygen and degrading peroxinitrites. It was shown that the encapsulated Hb preserved its functionality inside the nanoreactor. The preservation of functionality is based on the mild encapsulation procedure. The self-assembly process used for vesicle formation was done under

physiological conditions for hemoglobin and does not affect this protein's activity.

The activity of the encapsulated Hb was shown by the conversion reactions involving various oxidation states of hemoglobin, such as HbO<sub>2</sub>, HbCO and deoxyHb. The changes in oxidation states were reversible. The high activity of the nanoreactor is not only due to the activity of the encapsulated Hb. It was also demonstrated that channel porins can be inserted into the polymer membrane and these channel porins serve as gates for molecules such as peroxynitrite or oxygen.

We demonstrated that encapsulated HbO<sub>2</sub> and deoxyHb react with environmental peroxynitrite, resulting in the degradation of peroxynitrite. The data obtained from the kinetic measurements are in good agreement with the literature. The data also allowed a comparison of the reaction kinetics of encapsulated Hb and free Hb. The reaction kinetics of the free Hb is not significantly different from the reaction kinetics of the encapsulated Hb. This proves that the Hb inside the nanoreactor is active and the reaction kinetics of the encapsulated Hb is not decreased. In addition, the ability to function as an oxygen carrier has been proven by demonstrating that oxygen can be taken up and released inside nanoreactors. Because of the stability of the of PMOXA-*b*-PDMS-*b*-PMOXA vesicles, the nanoreactors maintain their function for an extended period of time.

## 5 References

1. Hagemann, R., [The Watson-Crick model of the DNA doublehelix. The history of the discovery and the role of the protein paradigm]. *Acta Hist Leopoldina* **2007**, 48, 113-58.
2. Labrude, P.; Becq, C., [Pharmacist and chemist Henri Braconnot]. *Rev Hist Pharm* **2003**, 51, (337), 61-78.
3. Crespy, D.; Bozonnet, M.; Meier, M., 100 Years of Bakelite, the Material of a 1000 Uses. *Angewandte Chemie International Edition* **2008**, 47, (18), 3322-3328.
4. Aoshima, S.; Kanaoka, S., A Renaissance in Living Cationic Polymerization. *Chemical Reviews* **2009**, 109, (11), 5245-5287.
5. Khanna, K.; Varshney, S.; Kakkar, A., Miktoarm star polymers: advances in synthesis, self-assembly, and applications. *Polymer Chemistry* **2010**, 1, (8), 1171-1185.
6. Inoue, K., Functional dendrimers, hyperbranched and star polymers. *Progress in Polymer Science* **2000**, 25, (4), 453-571.
7. Yokota, K., Periodic copolymers. *Progress in Polymer Science* **1999**, 24, (4), 517-563.
8. Jain, P.; Baker, G. L.; Bruening, M. L., Applications of polymer brushes in protein analysis and purification. *Annu Rev Anal Chem* **2009**, 2, 387-408.
9. Segawa, Y.; Higashihara, T.; Ueda, M., Hyperbranched Polymers with Controlled Degree of Branching from 0 to 100%. *Journal of the American Chemical Society* **2010**, 132, (32), 11000-11001.
10. Lee, C. C.; MacKay, J. A.; Frechet, J. M. J.; Szoka, F. C., Designing dendrimers for biological applications. *Nat Biotech* **2005**, 23, (12), 1517-1526.
11. Zhao, B.; Brittain, W. J., Polymer brushes: surface-immobilized macromolecules. *Progress in Polymer Science* **2000**, 25, (5), 677-710.
12. Kritikos, G.; Terzis, A. F., Theoretical study of polymer brushes by a new numerical mean field theory. *Polymer* **2007**, 48, (2), 638-651.
13. Brittain, W. J.; Minko, S., A structural definition of polymer brushes. *Journal of Polymer Science Part A: Polymer Chemistry* **2007**, 45, (16), 3505-3512.
14. Decher, G., Fuzzy Nanoassemblies: Toward Layered Polymeric Multicomposites. *Science* **1997**, 277, (5330), 1232-1237.
15. Kruk, M.; Dufour, B.; Celer, E. B.; Kowalewski, T.; Jaroniec, M.; Matyjaszewski, K., Grafting Monodisperse Polymer Chains from Concave Surfaces of Ordered Mesoporous Silicas. *Macromolecules* **2008**, 41, (22), 8584-8591.
16. Sofia, S. J.; Premnath, V.; Merrill, E. W., Poly(ethylene oxide) Grafted to Silicon Surfaces: Grafting Density and Protein Adsorption. *Macromolecules* **1998**, 31, (15), 5059-5070.
17. Carlmark, A.; Malmström, E. E., ATRP Grafting from Cellulose Fibers to Create Block-Copolymer Grafts. *Biomacromolecules* **2003**, 4, (6), 1740-1745.
18. Razumovitch, J.; Meier, W.; Vebert, C., A microcontact printing approach to the immobilization of oligonucleotide brushes. *Biophysical Chemistry* **2009**, 139, (1), 70-74.
19. Ionov, L.; Zdyrko, B.; Sidorenko, A.; Minko, S.; Klep, V.; Luzinov, I.; Stamm, M., Gradient Polymer Layers by "Grafting To" Approach. *Macromolecular Rapid Communications* **2004**, 25, (1), 360-365.
20. Rakhmatullina, E.; Braun, T.; Kaufmann, T.; Spillmann, H.; Malinova, V.; Meier, W., Functionalization of Gold and Silicon Surfaces by Copolymer Brushes Using Surface-Initiated ATRP. *Macromolecular Chemistry and Physics* **2007**, 208, (12), 1283-1293.
21. Pyun, J.; Kowalewski, T.; Matyjaszewski, K., Synthesis of Polymer Brushes Using Atom Transfer Radical Polymerization. *Macromolecular Rapid Communications* **2003**, 24, (18), 1043-1059.

22. Rakhmatullina, E.; Manton, A.; Bürgi, T.; Malinova, V.; Meier, W., Solid-supported amphiphilic triblock copolymer membranes grafted from gold surface. *Journal of Polymer Science Part A: Polymer Chemistry* **2009**, 47, (1), 1-13.
23. Wu, T.; Efimenko, K.; Vlček, P.; Šubr, V.; Genzer, J., Formation and Properties of Anchored Polymers with a Gradual Variation of Grafting Densities on Flat Substrates. *Macromolecules* **2003**, 36, (7), 2448-2453.
24. Ruckenstein, E.; Li, Z. F., Surface modification and functionalization through the self-assembled monolayer and graft polymerization. *Advances in Colloid and Interface Science* **2005**, 113, (1), 43-63.
25. Yim, H.; Kent, M. S.; Mendez, S.; Lopez, G. P.; Satija, S.; Seo, Y., Effects of Grafting Density and Molecular Weight on the Temperature-Dependent Conformational Change of Poly(N-isopropylacrylamide) Grafted Chains in Water. *Macromolecules* **2006**, 39, (9), 3420-3426.
26. Lee, H.-i.; Pietrasik, J.; Sheiko, S. S.; Matyjaszewski, K., Stimuli-responsive molecular brushes. *Progress in Polymer Science* **2010**, 35, (1-2), 24-44.
27. Discher, D. E.; Eisenberg, A., Polymer Vesicles. *Science* **2002**, 297, (5583), 967-973.
28. Kita-Tokarczyk, K.; Grumelard, J.; Haefele, T.; Meier, W., Block copolymer vesicles—using concepts from polymer chemistry to mimic biomembranes. *Polymer* **2005**, 46, (11), 3540-3563.
29. López-Dávila, V.; Seifalian, A. M.; Loizidou, M., Organic nanocarriers for cancer drug delivery. *Current Opinion in Pharmacology* **2012**, 12, (4), 414-419.
30. Tomalia, D. A.; Naylor, A. M.; Goddard, W. A., Starburst Dendrimers: Molecular-Level Control of Size, Shape, Surface Chemistry, Topology, and Flexibility from Atoms to Macroscopic Matter. *Angewandte Chemie International Edition in English* **1990**, 29, (2), 138-175.
31. Twyman, L. J.; Beezer, A. E.; Esfand, R.; Hardy, M. J.; Mitchell, J. C., The synthesis of water soluble dendrimers, and their application as possible drug delivery systems. *Tetrahedron Letters* **1999**, 40, (9), 1743-1746.
32. Liu, M.; Kono, K.; Fréchet, J. M. J., Water-soluble dendritic unimolecular micelles:: Their potential as drug delivery agents. *Journal of Controlled Release* **2000**, 65, (1-2), 121-131.
33. Li, S.; Nickels, J.; Palmer, A. F., Liposome-encapsulated actin-hemoglobin (LEAcHb) artificial blood substitutes. *Biomaterials* **2005**, 26, (17), 3759-3769.
34. Arifin, D. R.; Palmer, A. F., Polymersome Encapsulated Hemoglobin: A Novel Type of Oxygen Carrier. *Biomacromolecules* **2005**, 6, (4), 2172-2181.
35. Arifin, D. R.; Palmer, A. F., Stability of Liposome Encapsulated Hemoglobin Dispersions. *Artificial Cells, Blood Substitutes and Biotechnology* **2005**, 33, (2), 113-136.
36. Yechezkel, B., Liposome application: problems and prospects. *Current Opinion in Colloid & Interface Science* **2001**, 6, (1), 66-77.
37. Sakai, H.; Tomiyama, K.-i.; Sou, K.; Takeoka, S.; Tsuchida, E., Poly(ethylene glycol)-Conjugation and Deoxygenation Enable Long-Term Preservation of Hemoglobin-Vesicles as Oxygen Carriers in a Liquid State. *Bioconjugate Chemistry* **2000**, 11, (3), 425-432.
38. Bermudez, H.; Brannan, A. K.; Hammer, D. A.; Bates, F. S.; Discher, D. E., Molecular Weight Dependence of Polymersome Membrane Structure, Elasticity, and Stability. *Macromolecules* **2002**, 35, (21), 8203-8208.
39. T. M. S. Chang, D. P., W. P. Yu, *Artif. Cells, Blood, Artif. Cells, Blood Substitutes. Immobilization Biotechnol* **2003**, 31, 231.
40. Rameez, S.; Alost, H.; Palmer, A. F., Biocompatible and Biodegradable Polymersome Encapsulated Hemoglobin: A Potential Oxygen Carrier. *Bioconjugate Chemistry* **2008**, 19, (5), 1025-1032.
41. Zhao, J.; Liu, C.-S.; Yuan, Y.; Tao, X.-Y.; Shan, X.-Q.; Sheng, Y.; Wu, F., Preparation of hemoglobin-loaded nano-sized particles with porous structure as oxygen carriers. *Biomaterials* **2007**, 28, (7), 1414-1422.
42. Graff, A.; Fraysse-Ailhas, C.; Palivan, C. G.; Grzelakowski, M.; Friedrich, T.; Vebert, C.;



Gescheidt, G.; Meier, W., Amphiphilic Copolymer Membranes Promote NADH:Ubiquinone Oxidoreductase Activity: Towards an Electron-Transfer Nanodevice. *Macromolecular Chemistry and Physics* **2010**, 211, (2), 229-238.

43. Trujillo, M.; Ferrer-Sueta, G.; Radi, R., Peroxynitrite detoxification and its biologic implications. *Antioxid Redox Signal* **2008**, 10, (9), 1607-20.

44. Burns, J.; Cooper, W.; Ferry, J.; King, D. W.; DiMento, B.; McNeill, K.; Miller, C.; Miller, W.; Peake, B.; Rusak, S.; Rose, A.; Waite, T. D., Methods for reactive oxygen species (ROS) detection in aqueous environments. *Aquatic Sciences* **2012**, 74, (4), 683-734.

45. Pillai, S.; Oresajo, C.; Hayward, J., Ultraviolet radiation and skin aging: roles of reactive oxygen species, inflammation and protease activation, and strategies for prevention of inflammation-induced matrix degradation - a review. *Int J Cosmet Sci* **2005**, 27, (1), 17-34.

46. Dandan, C.; Tingfei, X.; Jing, B., Biological effects induced by nanosilver particles: in vivo study. *Biomedical Materials* **2007**, 2, (3), S126.

47. Slemmer, J. E.; Shacka, J. J.; Sweeney, M. I.; Weber, J. T., Antioxidants and Free Radical Scavengers for the Treatment Of Stroke, Traumatic Brain Injury and Aging. *Current Medicinal Chemistry* **2008**, 15, (4), 404-414.

48. Droege, W., Oxidative Stress, Disease and Cancer. *Imperial College Press* **2006**, 885.

49. Torreilles, F.; Salman-Tabcheh, S. d.; Guérin, M.-C.; Torreilles, J., Neurodegenerative disorders: the role of peroxynitrite. *Brain Research Reviews* **1999**, 30, (2), 153-163.

50. Li, J.; Su, J.; Li, W.; Liu, W.; Altura, B. T.; Altura, B. M., Peroxynitrite induces apoptosis in canine cerebral vascular muscle cells: possible relation to neurodegenerative diseases and strokes. *Neuroscience Letters* **2003**, 350, (3), 173-177.

51. Bouloumié, A.; Bauersachs, J.; Linz, W.; Schölkens, B. A.; Wiemer, G.; Fleming, I.; Busse, R., Endothelial Dysfunction Coincides With an Enhanced Nitric Oxide Synthase Expression and Superoxide Anion Production. *Hypertension* **1997**, 30, (4), 934-941.

52. Pacher, P.; Beckman, J. S.; Liaudet, L., Nitric Oxide and Peroxynitrite in Health and Disease. *Physiological Reviews* **2007**, 87, (1), 315-424.

53. Nauser, T.; Koppenol, W. H., The Rate Constant of the Reaction of Superoxide with Nitrogen Monoxide: Approaching the Diffusion Limit. *The Journal of Physical Chemistry A* **2002**, 106, (16), 4084-4086.

54. Radi, R.; Peluffo, G.; Alvarez, M. a. N.; Naviliat, M.; Cayota, A., Unraveling peroxynitrite formation in biological systems. *Free Radical Biology and Medicine* **2001**, 30, (5), 463-488.

55. Lakshminrusimha, S.; Wiseman, D.; Black, S. M.; Russell, J. A.; Gugino, S. F.; Oishi, P.; Steinhorn, R. H.; Fineman, J. R., The role of nitric oxide synthase-derived reactive oxygen species in the altered relaxation of pulmonary arteries from lambs with increased pulmonary blood flow. *Am J Physiol Heart Circ Physiol* **2007**, 293, (3), 18.

56. Fridovich, I., Superoxide Radical and Superoxide Dismutases. *Annual Review of Biochemistry* **1995**, 64, (1), 97-112.

57. Denicola, A.; Souza, J. M.; Radi, R.; Lissi, E., Nitric Oxide Diffusion in Membranes Determined by Fluorescence Quenching. *Archives of Biochemistry and Biophysics* **1996**, 328, (1), 208-212.

58. Mihm, Michael J.; Bauer, John A., Peroxynitrite-induced inhibition and nitration of cardiac myofibrillar creatine kinase. *Biochimie* **2002**, 84, (10), 1013-1019.

59. Stachowiak, O.; Dolder, M.; Wallimann, T.; Richter, C., Mitochondrial Creatine Kinase Is a Prime Target of Peroxynitrite-induced Modification and Inactivation. *Journal of Biological Chemistry* **1998**, 273, (27), 16694-16699.

60. Szabo, C.; Ischiropoulos, H.; Radi, R., Peroxynitrite: biochemistry, pathophysiology and development of therapeutics. *Nat Rev Drug Discov* **2007**, 6, (8), 662-680.

61. Arteel, G. E.; Briviba, K.; Sies, H., Protection against peroxynitrite. *FEBS letters* **1999**, 445, (2), 226-230.

62. Rhee, S. G.; Chae, H. Z.; Kim, K., Peroxiredoxins: A historical overview and speculative preview of novel mechanisms and emerging concepts in cell signaling. *Free Radical Biology and Medicine* **2005**, 38, (12), 1543-1552.
63. Wood, Z. A.; Schröder, E.; Robin Harris, J.; Poole, L. B., Structure, mechanism and regulation of peroxiredoxins. *Trends in Biochemical Sciences* **2003**, 28, (1), 32-40.
64. Romero, N.; Radi, R.; Linares, E.; Augusto, O.; Detweiler, C. D.; Mason, R. P.; Denicola, A., Reaction of Human Hemoglobin with Peroxynitrite. *Journal of Biological Chemistry* **2003**, 278, (45), 44049-44057.
65. Cohn, S. M., The Current Status of Haemoglobin-based Blood Substitutes. *Annals of Medicine* **1997**, 29, (5), 371-376.
66. Schreiber, G. B.; Busch, M. P.; Kleinman, S. H.; Korelitz, J. J., The Risk of Transfusion-Transmitted Viral Infections. *New England Journal of Medicine* **1996**, 334, (26), 1685-1690.
67. Bunn, H. F.; Esham, W. T.; Bull, R. W., THE RENAL HANDLING OF HEMOGLOBIN. *The Journal of Experimental Medicine* **1969**, 129, (5), 909-924.
68. Chan, W. L.; Tang, N. L. S.; Yim, C. C. W.; Mac-Moune Lai, F.; Tam, M. S. C., New Features of Renal Lesion Induced by Stroma Free Hemoglobin. *Toxicologic Pathology* **2000**, 28, (5), 635-642.
69. Sanders, K. E.; Lo, J.; Sligar, S. G., Intersubunit circular permutation of human hemoglobin. *Blood* **2002**, 100, (1), 299-305.
70. Yu, B.; Liu, Z.; Chang, T. M. S., Polyhemoglobin with Different Percentage of Tetrameric Hemoglobin and Effects on Vasoactivity and Electrocardiogram. *Artificial Cells, Blood Substitutes and Biotechnology* **2006**, 34, (2), 159-173.
71. Graff, A.; Sauer, M.; Van Gelder, P.; Meier, W., Virus-assisted loading of polymer nanocontainer. *Proceedings of the National Academy of Sciences* **2002**, 99, (8), 5064-5068.
72. Tremper, K. K.; Anderson, S. T., Perfluorochemical Emulsion Oxygen Transport Fluids: A Clinical Review. *Annual Review of Medicine* **1985**, 36, (1), 309-313.
73. A. Prilipov, P. S. P., P. Van Gelder, J. P. Rosenbusch, R. Koebnik, *FEMS Microbiol Lett* **1998**, 163, 65-72.
74. Grzelakowski, M.; Onaca, O.; Rigler, P.; Kumar, M.; Meier, W., Immobilized Protein-Polymer Nanoreactors. *Small* **2009**, 5, (22), 2545-2548.
75. Uppu, R. M.; Pryor, W. A., Synthesis of Peroxynitrite in a Two-Phase System Using Isoamyl Nitrite and Hydrogen Peroxide. *ANALYTICAL BIOCHEMISTRY* **1996**, 236, (2), 242-249.
76. Sun, J.; Huang, Y.; Shi, Q.; Chen, X.; Jing, X., Oxygen Carrier Based on Hemoglobin/Poly(l-lysine)-block-poly(l-phenylalanine) Vesicles†. *Langmuir* **2009**, 25, (24), 13726-13729.
77. J.K.G, D., An introduction to Dynamics of Colloids. *Elsevier* **1996**, 147-149.
78. Dalsin, J. L.; Hu, B.-H.; Lee, B. P.; Messersmith, P. B., Mussel Adhesive Protein Mimetic Polymers for the Preparation of Nonfouling Surfaces. *Journal of the American Chemical Society* **2003**, 125, (14), 4253-4258.
79. Asatekin, A.; Kang, S.; Elimelech, M.; Mayes, A. M., Anti-fouling ultrafiltration membranes containing polyacrylonitrile-graft-poly(ethylene oxide) comb copolymer additives. *Journal of Membrane Science* **2007**, 298, (1-2), 136-146.
80. Knop, K.; Hoogenboom, R.; Fischer, D.; Schubert, U. S., Poly(ethylene glycol) in Drug Delivery: Pros and Cons as Well as Potential Alternatives. *Angewandte Chemie International Edition* **2010**, 49, (36), 6288-6308.
81. Su, Y.-C.; Chen, B.-M.; Chuang, K.-H.; Cheng, T.-L.; Roffler, S. R., Sensitive Quantification of PEGylated Compounds by Second-Generation Anti-Poly(ethylene glycol) Monoclonal Antibodies. *Bioconjugate Chemistry* **2010**, 21, (7), 1264-1270.
82. Cheng, T.-L.; Cheng, C.-M.; Chen, B.-M.; Tsao, D.-A.; Chuang, K.-H.; Hsiao, S.-W.; Lin, Y.-H.; Roffler, S. R., Monoclonal Antibody-Based Quantitation of Poly(ethylene glycol)-

- Derivatized Proteins, Liposomes, and Nanoparticles. *Bioconjugate Chemistry* **2005**, 16, (5), 1225-1231.
83. Controlled/Living Radical Polymerization, Copyright, Foreword. In *Controlled/Living Radical Polymerization*, American Chemical Society: 2000; Vol. 768, pp i-v.
84. Patten, T. E.; Matyjaszewski, K., Atom Transfer Radical Polymerization and the Synthesis of Polymeric Materials. *Advanced Materials* **1998**, 10, (12), 901-915.
85. Wang, J.-S.; Matyjaszewski, K., Controlled/"living" radical polymerization. atom transfer radical polymerization in the presence of transition-metal complexes. *Journal of the American Chemical Society* **1995**, 117, (20), 5614-5615.
86. Coessens, V.; Pintauer, T.; Matyjaszewski, K., Functional polymers by atom transfer radical polymerization. *Progress in Polymer Science* **2001**, 26, (3), 337-377.
87. Matyjaszewski, K.; Ziegler, M. J.; Arehart, S. V.; Greszta, D.; Pakula, T., Gradient copolymers by atom transfer radical copolymerization. *Journal of Physical Organic Chemistry* **2000**, 13, (12), 775-786.
88. Beers, K. L.; Gaynor, S. G.; Matyjaszewski, K.; Sheiko, S. S.; Möller, M., The Synthesis of Densely Grafted Copolymers by Atom Transfer Radical Polymerization. *Macromolecules* **1998**, 31, (26), 9413-9415.
89. Matyjaszewski, K., The synthesis of functional star copolymers as an illustration of the importance of controlling polymer structures in the design of new materials. *Polymer International* **2003**, 52, (10), 1559-1565.
90. Matyjaszewski, K.; Nakagawa, Y.; Jasieczek, C. B., Polymerization of n-Butyl Acrylate by Atom Transfer Radical Polymerization. Remarkable Effect of Ethylene Carbonate and Other Solvents. *Macromolecules* **1998**, 31, (5), 1535-1541.
91. Dong, H.; Matyjaszewski, K., Thermally Responsive P(M(EO)<sub>2</sub>MA-co-OEOMA) Copolymers via AGET ATRP in Miniemulsion. *Macromolecules* **2010**, 43, (10), 4623-4628.
92. Neugebauer, D., Graft copolymers with poly(ethylene oxide) segments. *Polymer International* **2007**, 56, (12), 1469-1498.
93. Neugebauer, D.; Zhang, Y.; Pakula, T.; Sheiko, S. S.; Matyjaszewski, K., Densely-Grafted and Double-Grafted PEO Brushes via ATRP. A Route to Soft Elastomers. *Macromolecules* **2003**, 36, (18), 6746-6755.
94. Hyotyła, J. T.; Deng, J.; Lim, R. Y. H., Synthetic Protein Targeting by the Intrinsic Biorecognition Functionality of Poly(ethylene glycol) Using PEG Antibodies as Biohybrid Molecular Adaptors. *ACS Nano* **2011**, 5, (6), 5180-5187.
95. Mol, N. J.; Fischer, M. J., Surface Plasmon Resonance: A General Introduction. In 2010; Vol. 627, pp 1-14.
96. Sauerbrey, G., The use of quartz oscillators for weighing thin layers and for microweighing. *Zeitschrift fuer Physik* **1959**, (206-22), 206-22.
97. Broz, P.; Ben-Haim, N.; Grzelakowski, M.; Marsch, S.; Meier, W.; Hunziker, P., Inhibition of macrophage phagocytotic activity by a receptor-targeted polymer vesicle-based drug delivery formulation of pravastatin. *J Cardiovasc Pharmacol* **2008**, 51, (3), 246-52.
98. Brož, P.; Benito, S. M.; Saw, C.; Burger, P.; Heider, H.; Pfisterer, M.; Marsch, S.; Meier, W.; Hunziker, P., Cell targeting by a generic receptor-targeted polymer nanocontainer platform. *Journal of Controlled Release* **2005**, 102, (2), 475-488.
99. Litvinchuk, S.; Lu, Z.; Rigler, P.; Hirt, T. D.; Meier, W., Calcein release from polymeric vesicles in blood plasma and PVA hydrogel. *Pharm Res* **2009**, 26, (7), 1711-7.
100. Onaca, O.; Hughes, D. W.; Balasubramanian, V.; Grzelakowski, M.; Meier, W.; Palivan, C. G., SOD Antioxidant Nanoreactors: Influence of Block Copolymer Composition on the Nanoreactor Efficiency. *Macromolecular Bioscience* **2010**, 10, (5), 531-538.
101. Baines, F. L.; Billingham, N. C.; Armes, S. P., Synthesis and Solution Properties of Water-Soluble Hydrophilic-Hydrophobic Block Copolymers. *Macromolecules* **1996**, 29, (10), 3416-3420.

102. Kumar, M.; Grzelakowski, M.; Zilles, J.; Clark, M.; Meier, W., Highly permeable polymeric membranes based on the incorporation of the functional water channel protein Aquaporin Z. *Proceedings of the National Academy of Sciences* **2007**, 104, (52), 20719-20724.
103. Nardin, C.; Thoeni, S.; Widmer, J.; Winterhalter, M.; Meier, W., Nanoreactors based on (polymerized) ABA-triblock copolymer vesicles. *Chemical Communications* **2000**, (15), 1433-1434.
104. Zimm, B. H., Molecular theory of the scattering of light in fluids. *Journal of Chemical Physics* **1945**, 13, 141-5.
105. Zimm, B. H., The scattering of light and the radial distribution function of high-polymer solutions. *Journal of Chemical Physics* **1948**, 16, 1093-9.
106. Debye, P., Light scattering in solutions. *Journal of Applied Physics* **1944**, 15, 338-42.
107. Einstein, A., Opalescence theory of homogeneous liquids and liquid mixtures in the vicinity of the critical state. *Annalen der Physik (Weinheim, Germany)* **1910**, 33, 1275-1298.
108. Rigler, P.; Meier, W., Encapsulation of Fluorescent Molecules by Functionalized Polymeric Nanocontainers: Investigation by Confocal Fluorescence Imaging and Fluorescence Correlation Spectroscopy. *Journal of the American Chemical Society* **2005**, 128, (1), 367-373.
109. Axthelm, F.; Casse, O.; Koppenol, W. H.; Nauser, T.; Meier, W.; Palivan, C. G., Antioxidant Nanoreactor Based on Superoxide Dismutase Encapsulated in Superoxide-Permeable Vesicles. *The Journal of Physical Chemistry B* **2008**, 112, (28), 8211-8217.
110. Wohland, T.; Rigler, R.; Vogel, H., The Standard Deviation in Fluorescence Correlation Spectroscopy. *Biophysical Journal* **2001**, 80, (6), 2987-2999.
111. Arosio, D.; Kwansa, H. E.; Gering, H.; Piszczek, G.; Bucci, E., Static and dynamic light scattering approach to the hydration of hemoglobin and its supertetramers in the presence of osmolites. *Biopolymers* **2002**, 63, (1), 1-11.
112. Torres Filho, I. P.; Terner, J.; Pittman, R. N.; Proffitt, E.; Ward, K. R., Measurement of hemoglobin oxygen saturation using Raman microspectroscopy and 532-nm excitation. *Journal of Applied Physiology* **2008**, 104, (6), 1809-1817.
113. Gaoshan Shen Gaoshan, S.; Tiarrxiu Yan Tiarrxiu, Y.; Huaimin Gu Huaimin, G.; Huajian Wei Huajian, W., Micro-Raman Spectroscopy Monitor Methemoglobin Induced by Sodium Nitrite in Whole Blood. *CORD Conference Proceedings* **2008**, 1476-1479.
114. Spiro, T. G., Biological Applications of Resonance Raman Spectroscopy: Haem Proteins. *Proceedings of the Royal Society of London. Series A, Mathematical and Physical Sciences* **1975**, 345, (1640), 89-105.
115. Spiro, T. G.; Streckas, T. C., Resonance Raman Spectra of Hemoglobin and Cytochrome c: Inverse Polarization and Vibronic Scattering. *Proceedings of the National Academy of Sciences* **1972**, 69, (9), 2622-2626.
116. Nagatomo, S.; Nagai, M.; Kitagawa, T., A New Way To Understand Quaternary Structure Changes of Hemoglobin upon Ligand Binding On the Basis of UV-Resonance Raman Evaluation of Intersubunit Interactions. *Journal of the American Chemical Society* **2011**, 133, (26), 10101-10110.
117. Yamamoto, T.; Palmer, G.; Gill, D.; Salmeen, I. T.; Rimai, L., The Valence and Spin State of Iron in Oxyhemoglobin as Inferred from Resonance Raman Spectroscopy. *Journal of Biological Chemistry* **1973**, 248, (14), 5211-5213.
118. Xu, H.; Bjerneld, E. J.; Käll, M.; Börjesson, L., Spectroscopy of Single Hemoglobin Molecules by Surface Enhanced Raman Scattering. *Physical Review Letters* **1999**, 83, (21), 4357-4360.
119. Tsuruga, M.; Matsuoka, A.; Hachimori, A.; Sugawara, Y.; Shikama, K., The Molecular Mechanism of Autoxidation for Human Oxyhemoglobin. *Journal of Biological Chemistry* **1998**, 273, (15), 8607-8615.
120. Zhang, X.; Liu, C.; Yuan, Y.; Shan, X.; Sheng, Y.; Xu, F., Reduction and suppression of methemoglobin loaded in the polymeric nanoparticles intended for blood substitutes. *Journal of*

- Biomedical Materials Research Part B: Applied Biomaterials* **2008**, 87B, (2), 354-363.
121. Exner, M.; Herold, S., Kinetic and Mechanistic Studies of the Peroxynitrite-Mediated Oxidation of Oxymyoglobin and Oxyhemoglobin. *Chemical Research in Toxicology* **2000**, 13, (4), 287-293.
122. Ascenzi, P.; Marinis, E. D.; Masi, A. d.; Ciaccio, C.; Coletta, M., Peroxynitrite scavenging by ferryl sperm whale myoglobin and human hemoglobin. *Biochemical and Biophysical Research Communications* **2009**, 390, (1), 27-31.
123. McCool, B. A.; Cashon, R.; Karles, G.; DeSisto, W. J., Silica encapsulated hemoglobin and myoglobin powders prepared by an aqueous fast-freezing technique. *Journal of Non-Crystalline Solids* **2004**, 333, (2), 143-149.
124. Masayoshi Matsui, A. N., Akiko Takatsu, Kenji Kato, Naoki Matsuda, In Situ Observation of Reduction Behavior of Hemoglobin Molecules Adsorbed on Glass Surface. *IEICE Transactions 89-C* **2006**, 12, 1741 - 1745.
125. Herold, S., Kinetic and spectroscopic characterization of an intermediate peroxynitrite complex in the nitrogen monoxide induced oxidation of oxyhemoglobin1 Reprinted in its entirety from vol. 439 (1998) 85–88 because of errors explained on p. 80.1. *FEBS letters* **1999**, 443, (1), 81-84.
126. Li, D.-J.; Luo, H.; Wang, L.-L.; Zou, G.-L., Potential of Peroxynitrite to Promote the Conversion of Oxyhemoglobin to Methemoglobin. *Acta Biochimica et Biophysica Sinica* **2004**, 36, (2), 87-92.
127. Romero, N.; Denicola, A.; Radi, R., Red blood cells in the metabolism of nitric oxide-derived peroxynitrite. *IUBMB Life* **2006**, 58, (10), 572-580.
128. Faivre B, M. P., Labrude P, Vigneron C., Hemoglobin autooxidation/oxidation mechanisms and methemoglobin prevention or reduction processes in the bloodstream. Literature review and outline of autooxidation reaction. *Artif Cells Blood Substit Immobil Biotechnol.* **1998**, 26, 17-26.
129. Abe, K.; Sugita, Y., Properties of Cytochrome b5, and Methemoglobin Reduction in Human Erythrocytes. *European Journal of Biochemistry* **1979**, 101, (2), 423-428.
130. Sakai, H.; Sato, A.; Masuda, K.; Takeoka, S.; Tsuchida, E., Encapsulation of Concentrated Hemoglobin Solution in Phospholipid Vesicles Retards the Reaction with NO, but Not CO, by Intracellular Diffusion Barrier. *Journal of Biological Chemistry* **2008**, 283, (3), 1508-1517.

## 6 Abbreviations and symbols

%	percent
°C	degree celsius
ARGET	activators regenerated by electron transfer
ATRP	atom transfer radical polymerization
ATR-IR	attenuated total reflection infrared (spectroscopy)
DLS	Dynamic light scattering
DMF	dimethylformamide
DNA	deoxyribonucleic acid
FCS	fluorescence correlation spectroscopy
GPC	gel permeation chromatography
Hb	Hemoglobin
HEA	2-hydroxyethyl acrylate
<sup>1</sup> HNMR	nuclear magnetic resonance
k	reaktionskonstante
k <sub>D</sub>	dissoziationskonstante
kDa	kilo Dalton
LbL	Layer by Layer
<i>M<sub>n</sub></i>	number average molecular weight
<i>M<sub>w</sub></i>	weight average molecular weight
OmpF	Outer membrane protein F
PBS	phosphate buffered saline
PDI	polydispersity index
PDMS	Polydimethylsiloxan
PEG	poly(ethylene glycol)
PEGA	poly(ethylene glycol)methyl ether acrylate

PFCs	perfluorochemicals
PMOXA	poly(2-methyl-2-oxazoline)
QCM	Quartz crystal microbalance
R <sub>g</sub>	radius of gyration
RH	hydrodynamic radius
ROS	reactive oxygen species
SEC	Size-exclusion chromatography
SLS	Static light scattering
SOD	Superoxide dismutase
SPR	surface plasmon resonance (spectroscopy)
TEM	transmission electron microscopy
UV	UV/VIS-Spektroskopie

## 7 Curriculum vitae

### Personal Data

Name	Dominik Dobrunz
Date and place of birth	26.12.1983 in Lörrach (Germany)
Nationality	German

### Education

*05/2008 -* PhD studies supervised by Prof. Dr. Wolfgang Meier  
*03/2013* (University of Basel, Switzerland)

*04/2007 -* master studies in chemistry  
*04/2008* (University of Basel, Switzerland)  
master thesis supervised by Prof. Dr. Angelo Vedani

*10/2003 -* bachelor studies  
*03/2007* (University of Basel, Switzerland)

*08/2003* A-levels (“Abitur”)  
(Freie Evangelische Schule Lörrach , Germany)

The following lecturers participated in the educational training during the PhD studies:

Edwin Constable, Katarzyna Kita-Tokarczyk, Wolfgang Meier, Markus Meuwly, Cornelia Palivan,



Thomas Pfohl, Stefan Willitsch, Peter Hauser.

## 8 Impact of the work

### Publications

Dobrunz, D.; Toma, A. C.; Tanner, P.; Pfohl, T.; Palivan, C. G., Polymer Nanoreactors with Dual Functionality: Simultaneous Detoxification of Peroxynitrite and Oxygen Transport. *Langmuir* **2012**.

Belegriou, S.; Menon, S.; Dobrunz, D.; Meier, W., Solid-supported polymeric membranes. *Soft Matter* **2011**, 7, (6), 2202-2210.